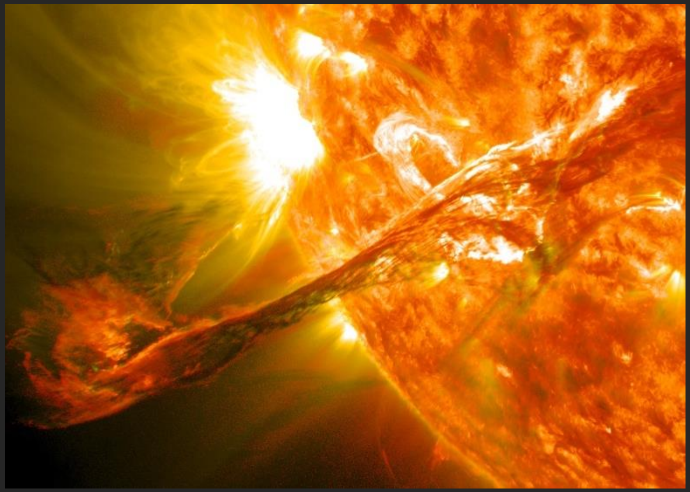

Solar Flares and Eruptions

Jaroslav Dudík

Astronomical Institute of the Czech Academy of Sciences

Lecture 2

Selected Chapters in Astrophysics

Faculty of Mathematics and Physics, Charles University, 2018-10-23

Outline

I. The CSHKP Standard Solar Flare Model in 2D

Observations of Inflow: Imaging, Spectroscopy and Stereoscopy
DEM Temperature Maps from Atmospheric Imaging Assembly
Chromospheric Evaporation: Role of spatial resolution

II. Intrinsically 3D Processes

Filament Eruption observed by SDO/AIA + Hinode/EIS
Magnetic “Implosion”: Loop Contractions & Oscillations

III. 3D Reconnection and Magnetic Topology

Magnetic Null-points and Null-Point Reconnection
Nature of the EUV Late Phase of Solar Flares

IV. The Standard Solar Flare Model in 3D

Torus-Unstable Flux rope and Its Signatures
Slipping Reconnection; connection to precursors and evaporation
New types of reconnection in 3D

What is a Solar Flare?

- Short (usually) and very bright manifestation of the solar magnetic activity
- **Consequence of magnetic reconnection: Free magnetic energy converted to thermal and kinetic energies**
- Thermal energy leads to increase in thermal radiation: plasma at $T > 10$ MK
- Kinetic energy: particle acceleration and associated non-thermal emission

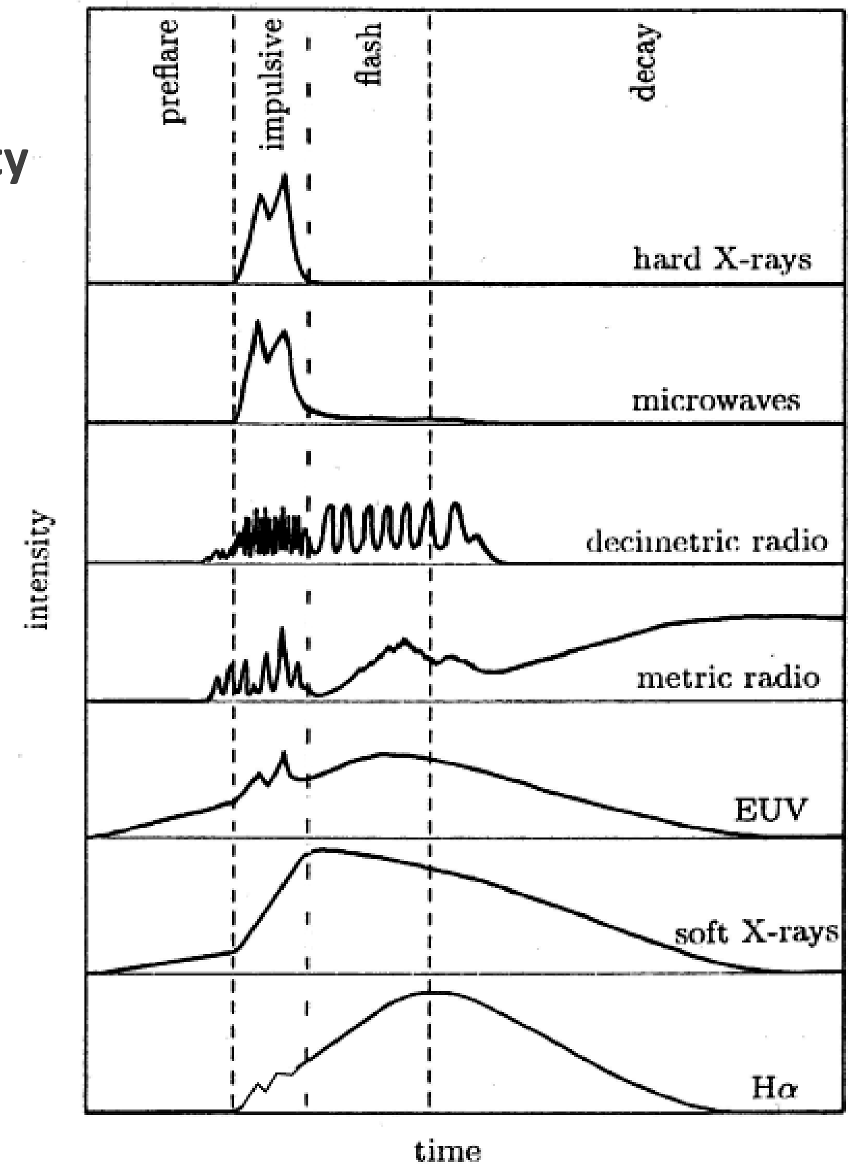

Benz (2002)

Atmospheric Imaging Assembly

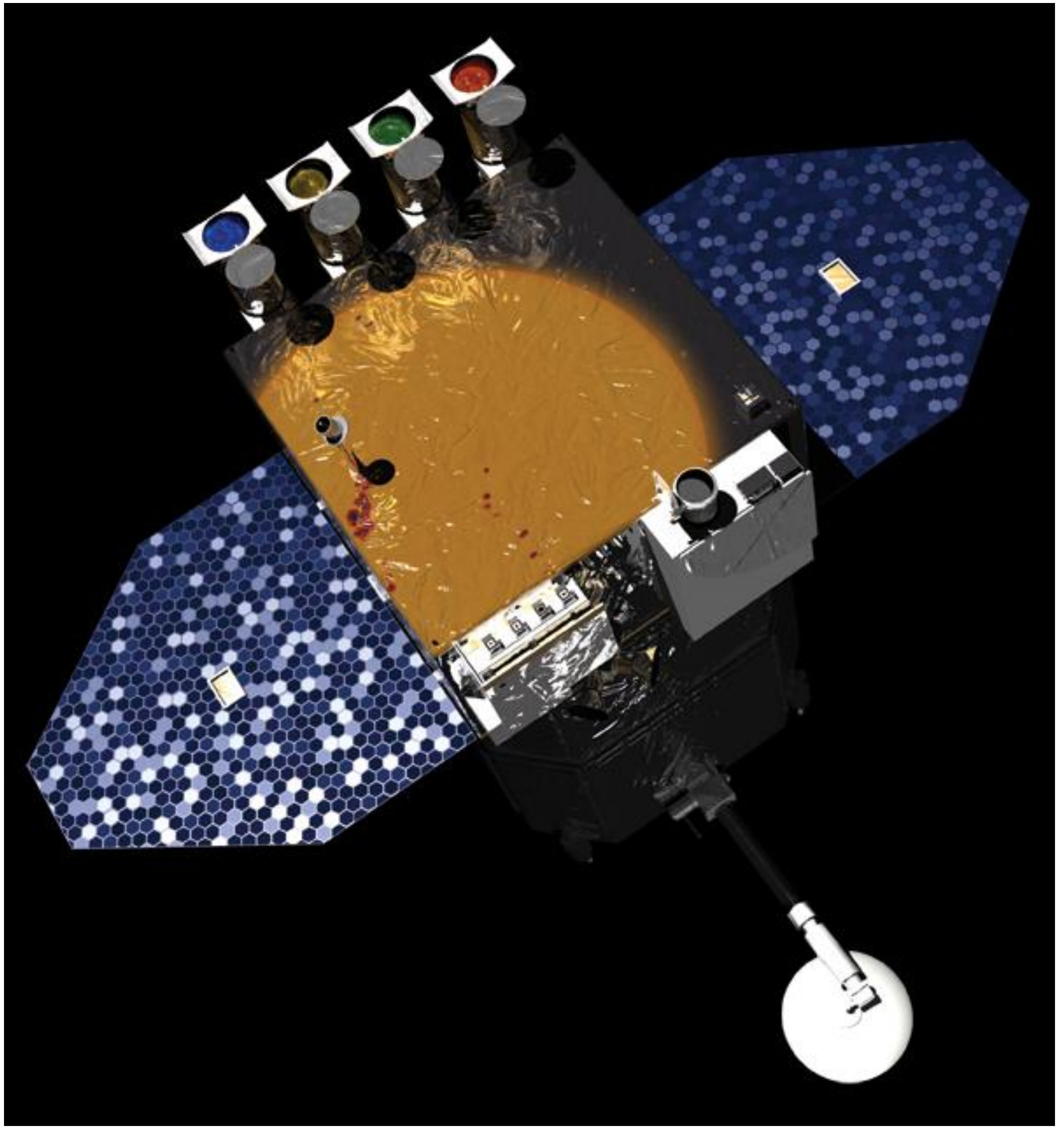

Solar Dynamics Observatory:

- NASA, launched 2010
- current workhorse for Solar Physics

Atmospheric Imaging Assembly (AIA):

- four identical EUV full-disc telescopes, state-of-the-art
- cadence of 12 seconds
- 0.6” px size, 1.5” resolution
- broad temperature coverage to study coronal and flare physics

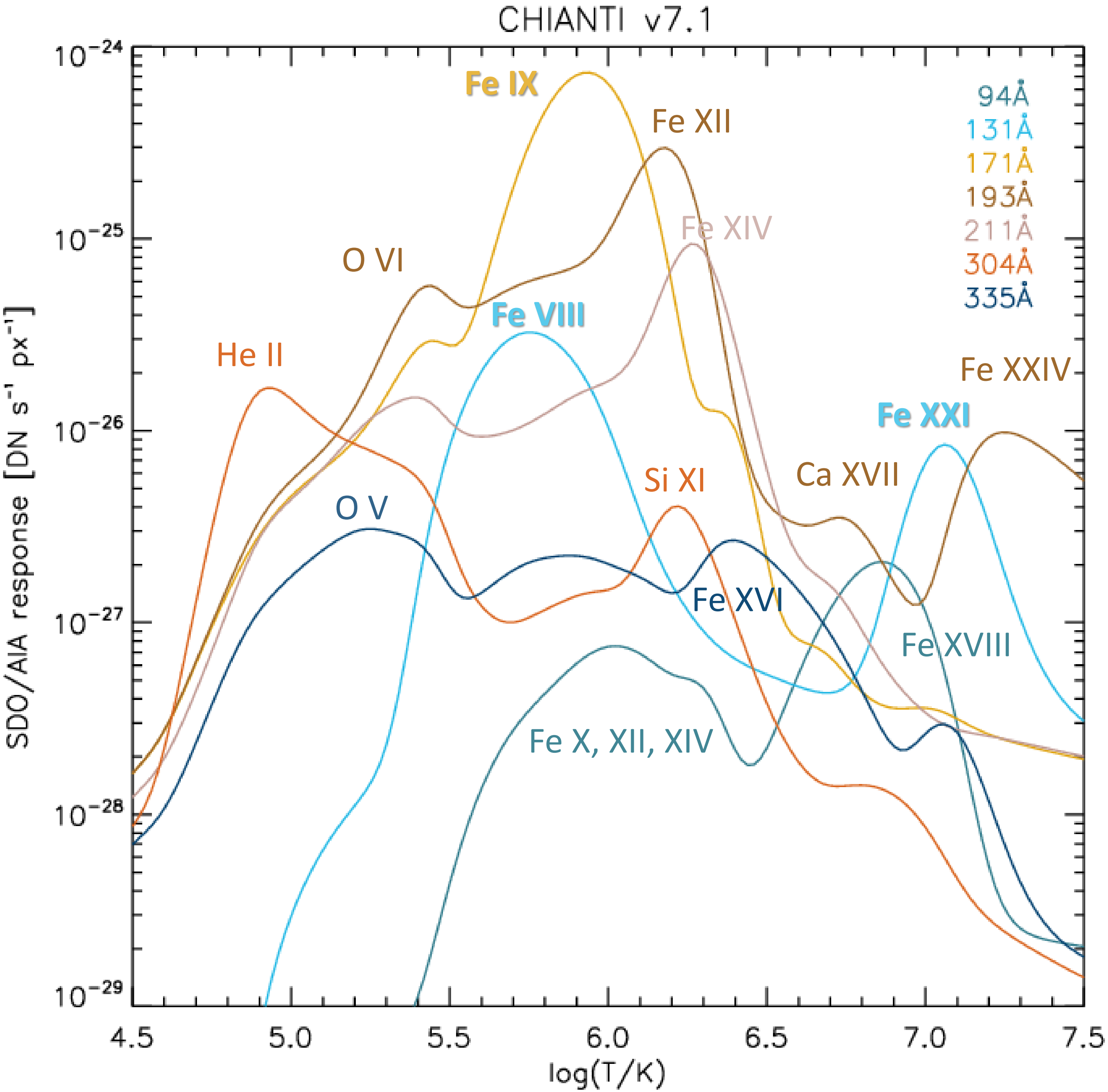
CHIANTI v7.1
94Å
131Å
171Å
193Å
211Å
304Å
335Å
Fe IX
Fe XII
Fe XIV
O VI
Fe VIII
He II
Fe XXIV
Fe XXI
Ca XVII
Si XI
O V
Fe XVI
Fe XVIII
Fe X, XII, XIV
SDO/AIA response [DN s^-1 px^-1]
log(T/K)
10^-24
10^-25
10^-26
10^-27
10^-28
10^-29
4.5
5.0
5.5
6.0
6.5
7.0
7.5

I. The Standard Model... in 2D

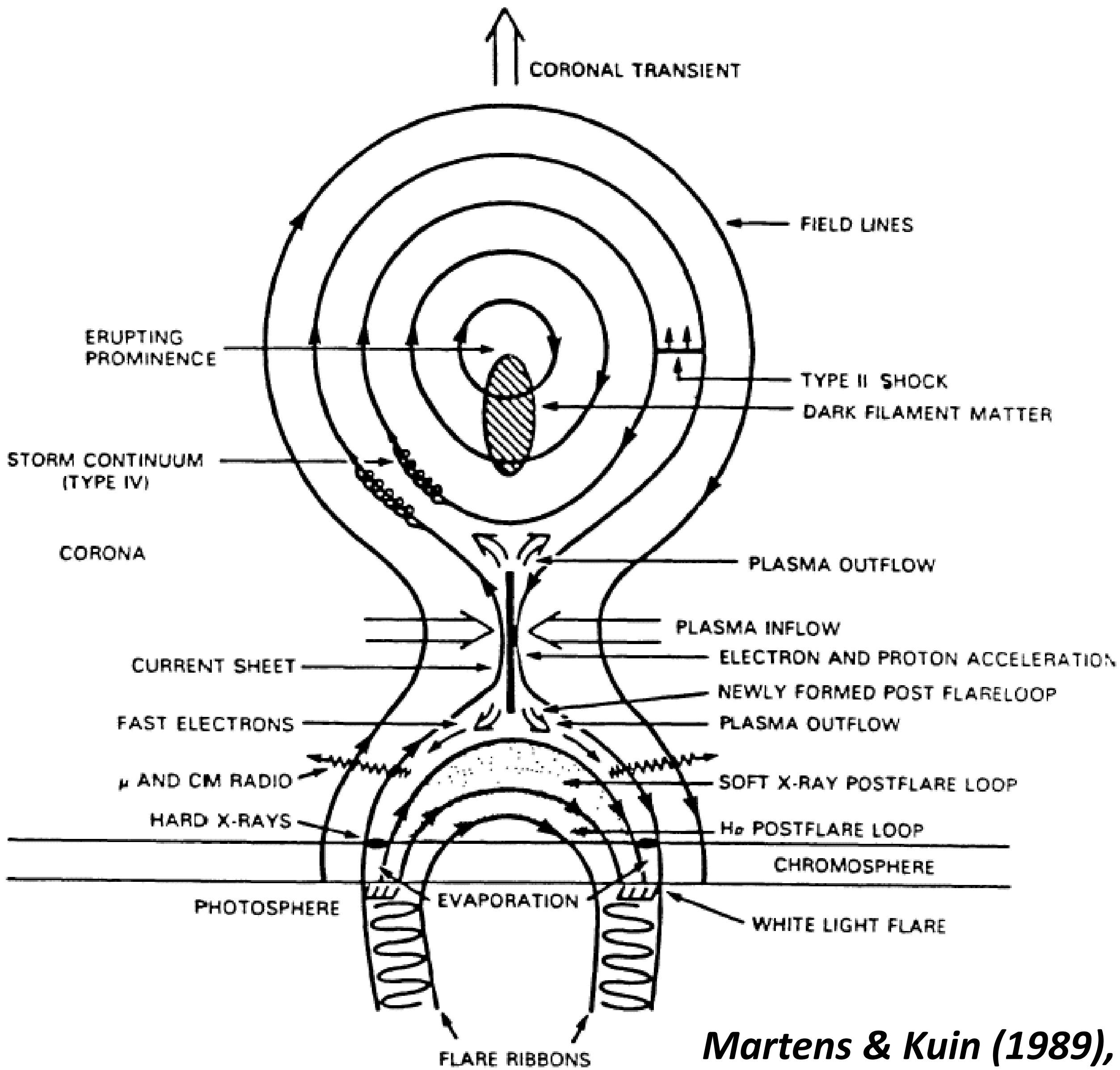

Martens & Kuin (1989), SoPh, 122, 263

Solar Flare of 2013 Dec 10

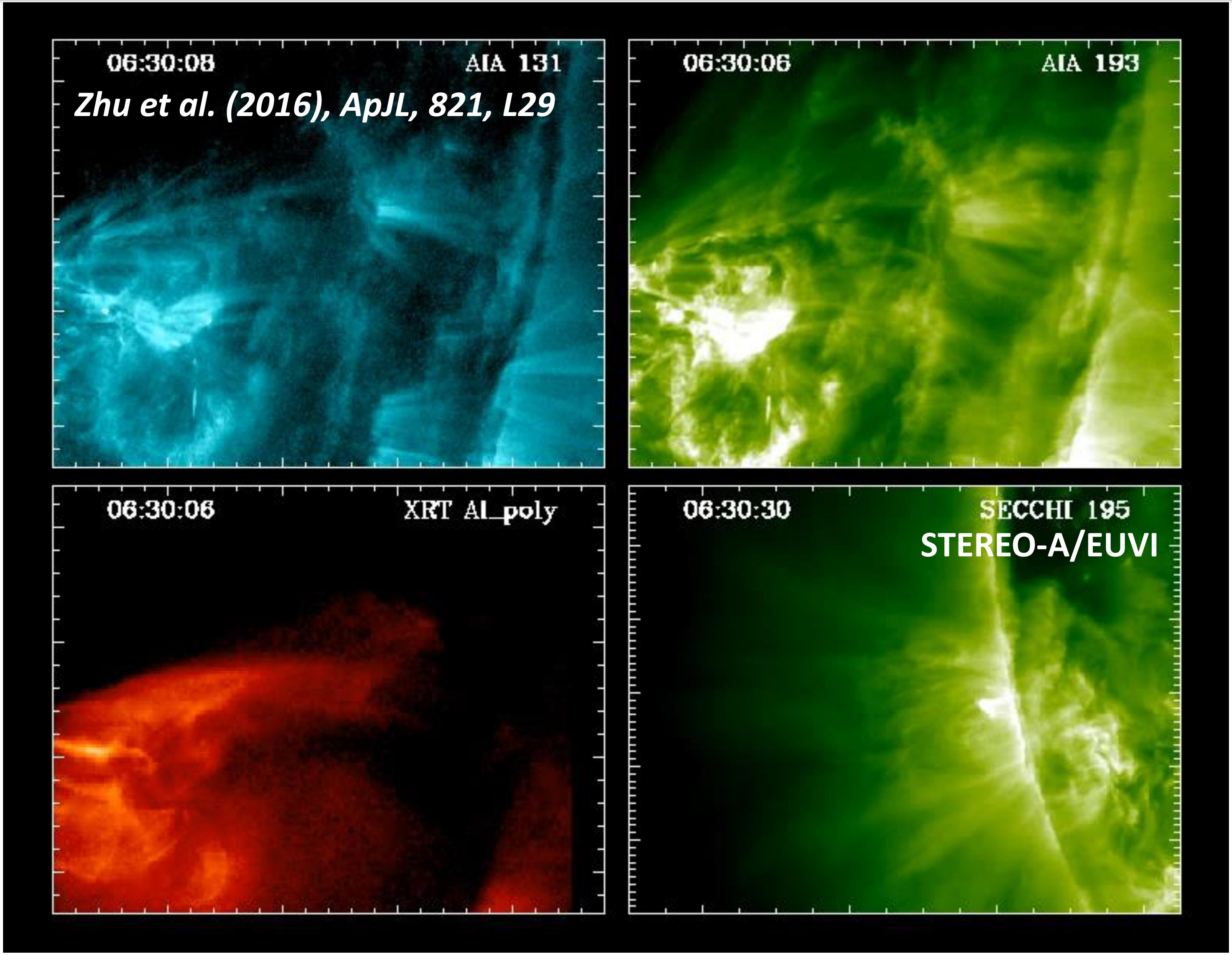

Inflows and Flare Loops

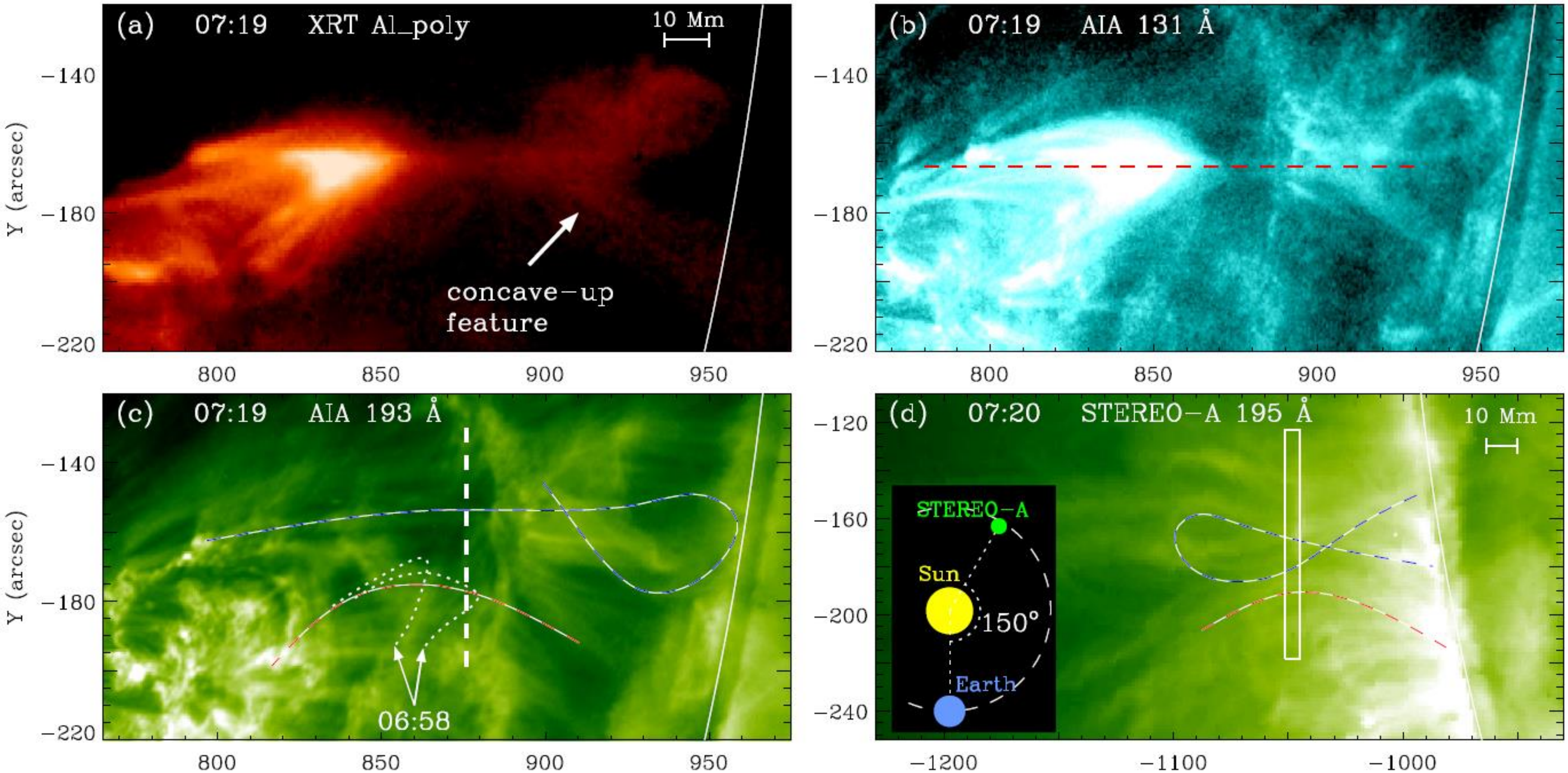

Zhu et al. (2016), ApJL, 821, L29

- **Cuts along the dashed lines: inflows in AIA 171 Å and 193 Å**
- **Outflows in 131 Å: flare plasma**

Inflows and Outflows

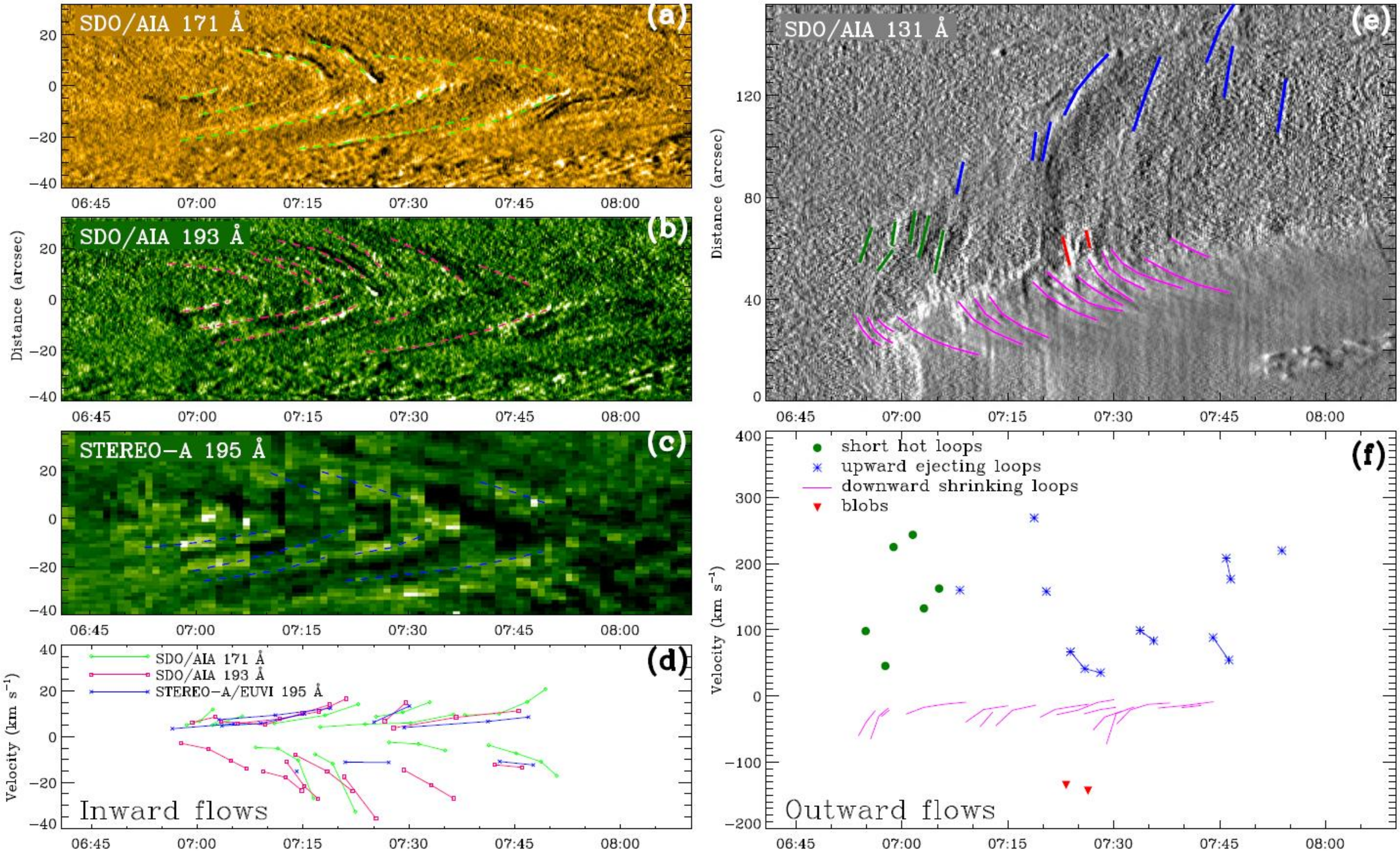

“Current Sheet”

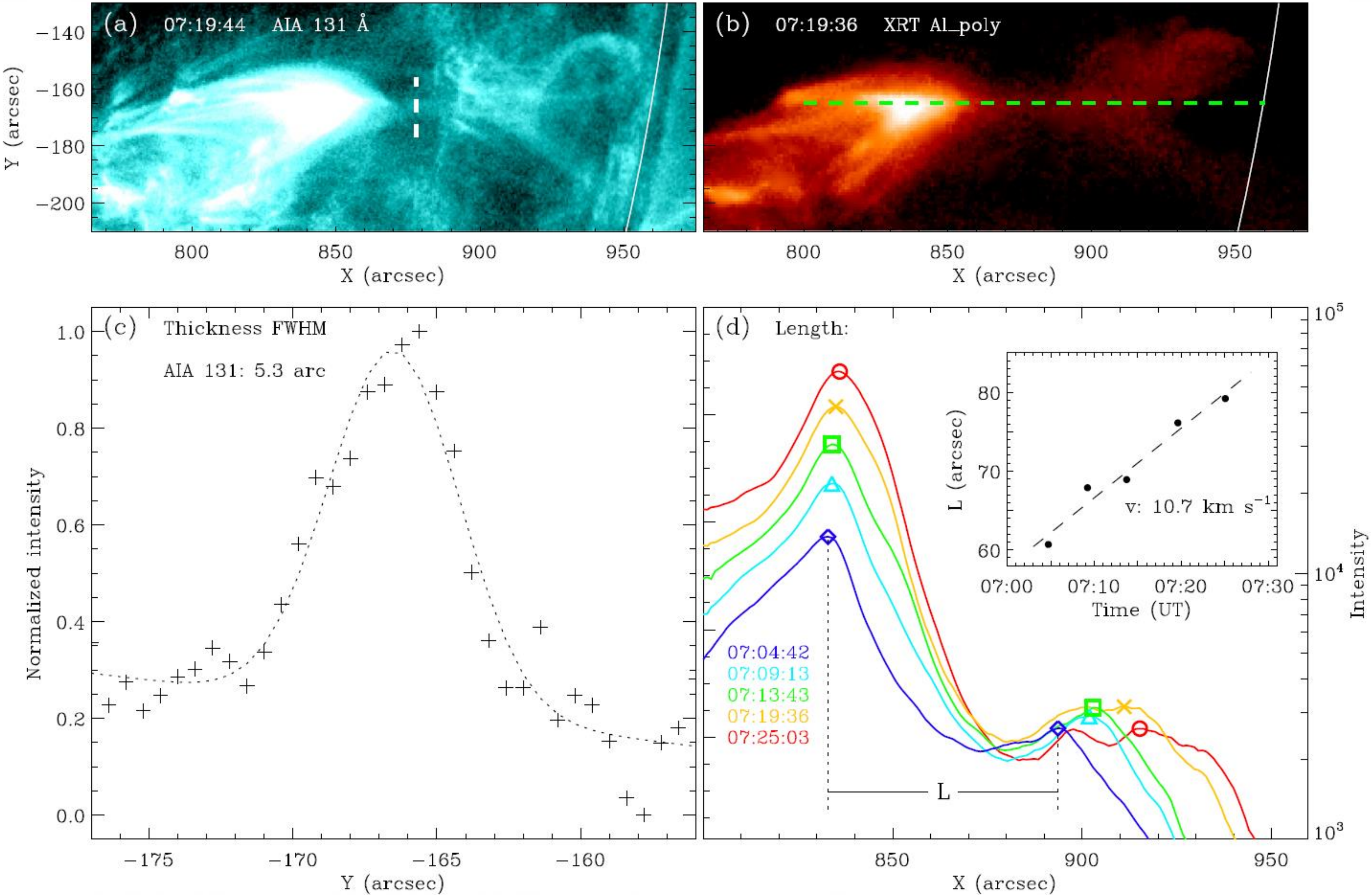

Ejection observed by SDO/AIA

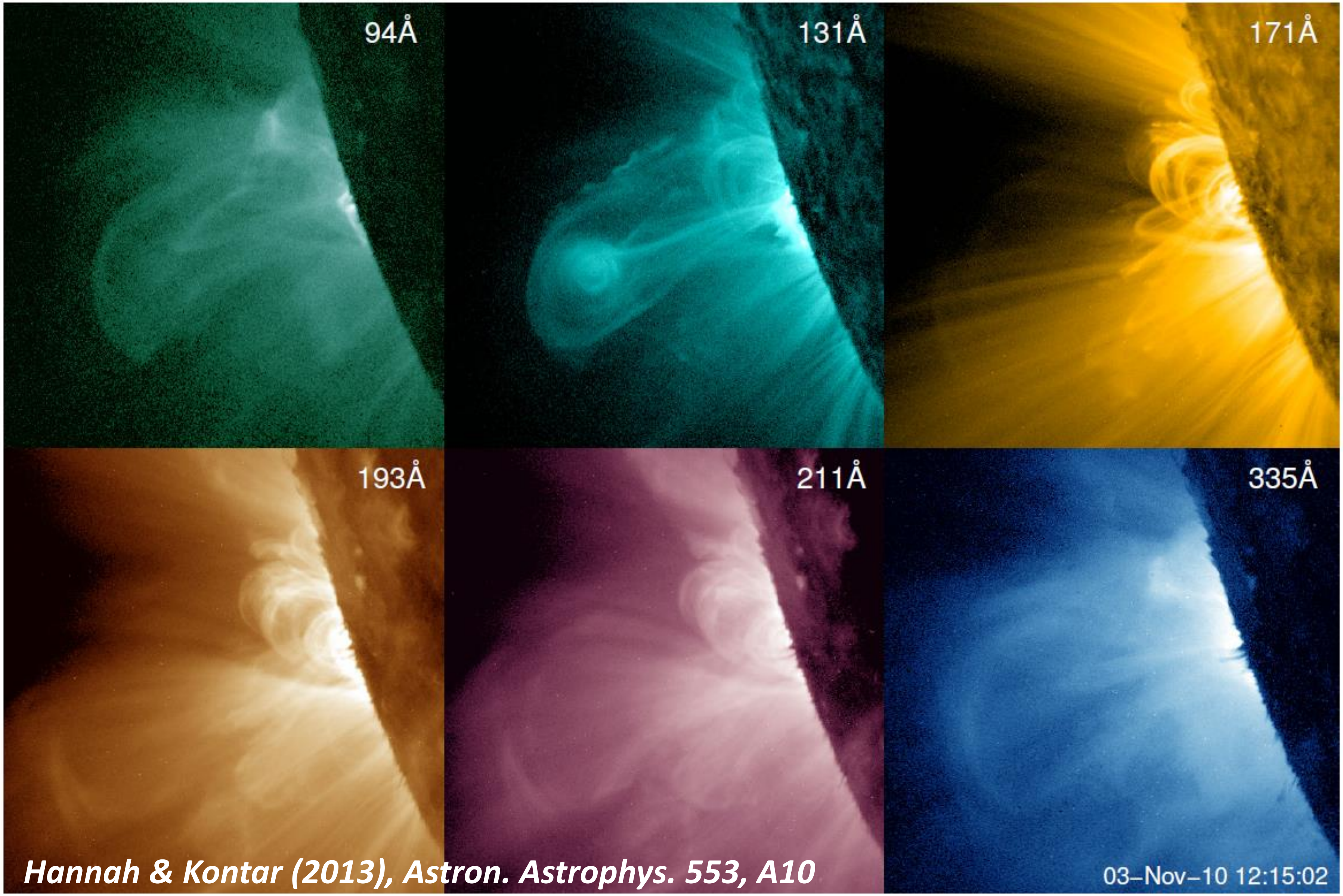

Hannah & Kontar (2013), Astron. Astrophys. 553, A10

AIA DEMs – Regularized Inversion

$$I_{\mathrm{AIA}} = \int A_X\left(\int G(\lambda, T, n_{\mathrm{e}}) R(\lambda) \mathrm{d}\lambda\right) n_{\mathrm{e}} n_{\mathrm{H}} \frac{dV}{dT} dT$$

$$= \int C(T, n_{\mathrm{e}})\, DEM(T) dT$$

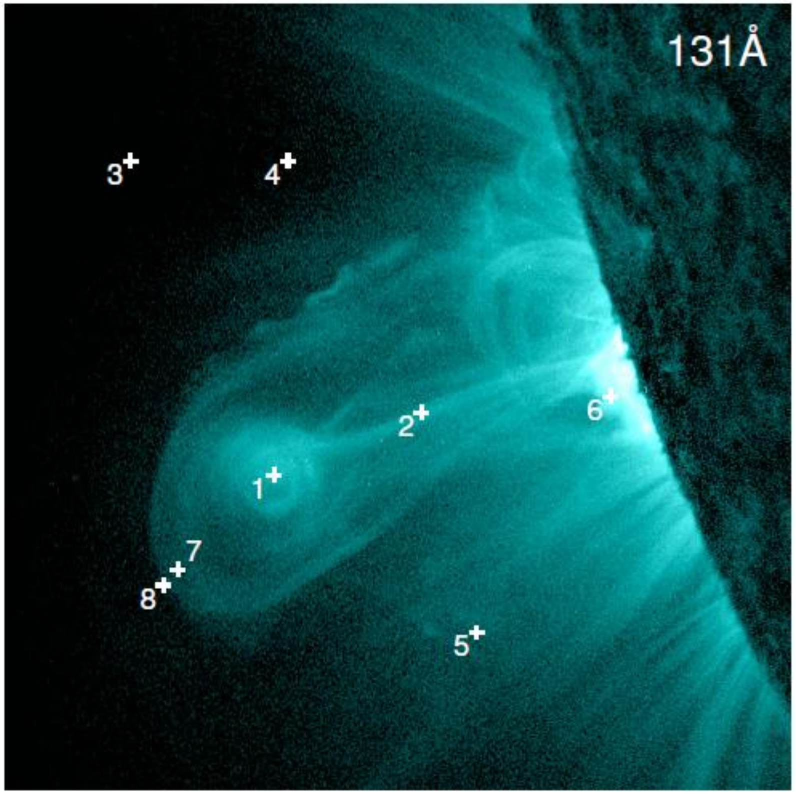

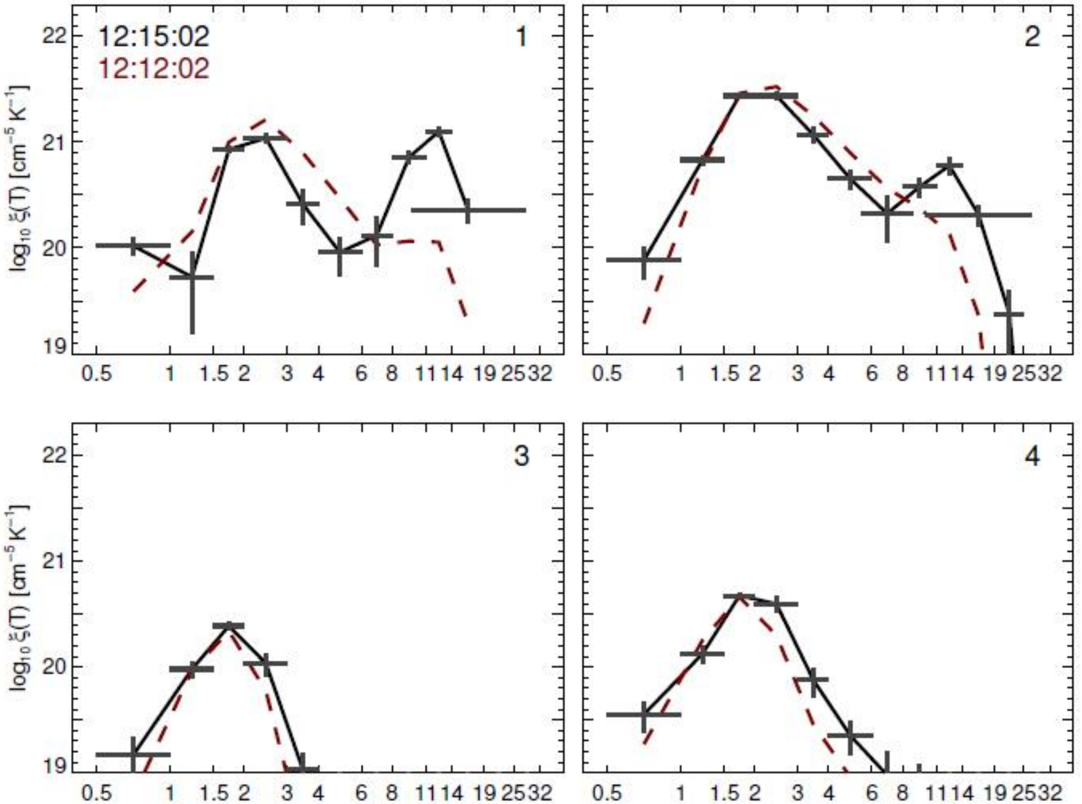

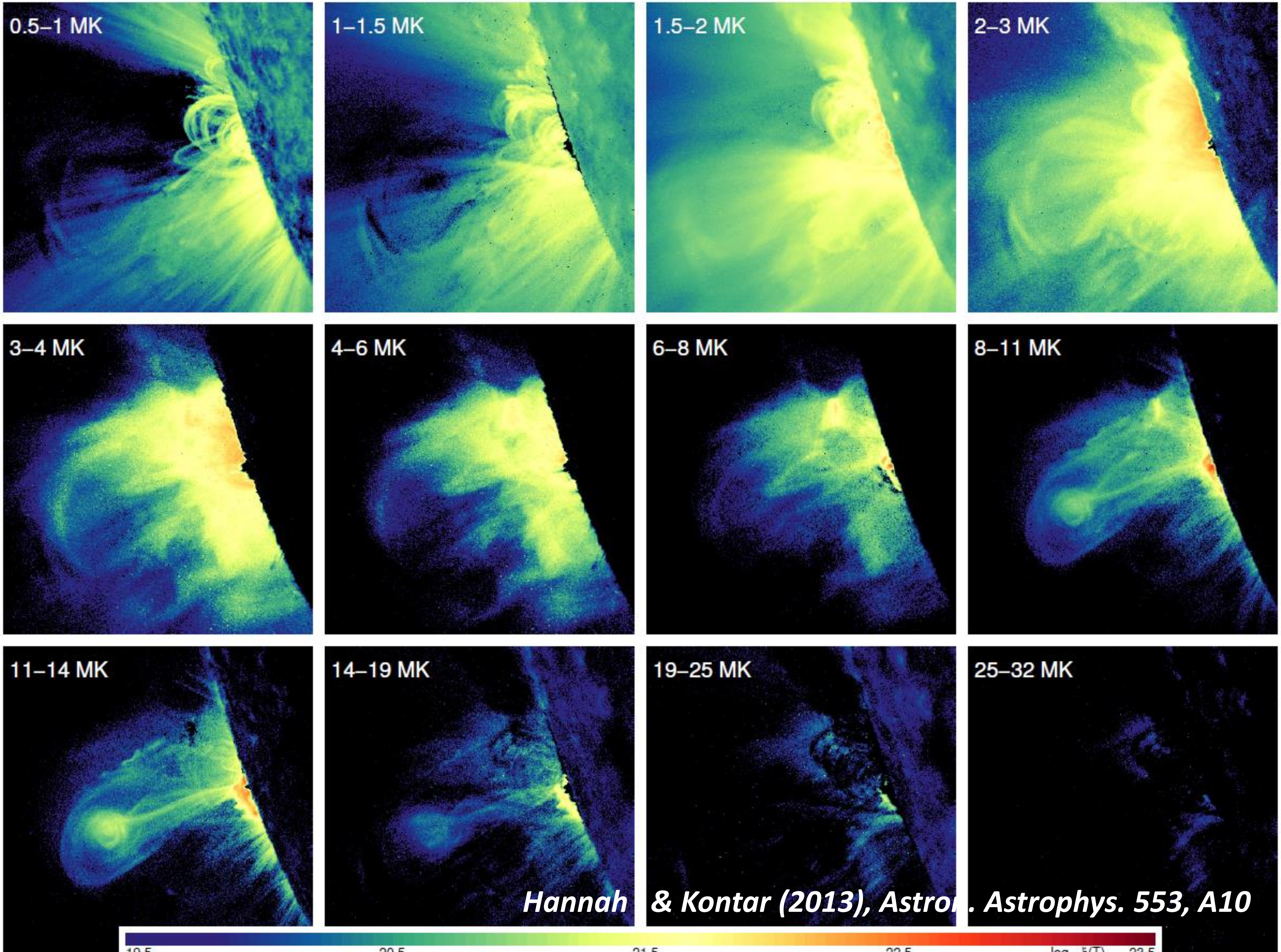
0.5–1 MK
1–1.5 MK
1.5–2 MK
2–3 MK
3–4 MK
4–6 MK
6–8 MK
8–11 MK
11–14 MK
14–19 MK
19–25 MK
25–32 MK
Hannah & Kontar (2013), Astro. Astrophys. 553, A10
19.5
20.5
21.5
22.5
$\log_{10} \xi(T)$
23.5

A Recent Example of a 2D-ish Flare

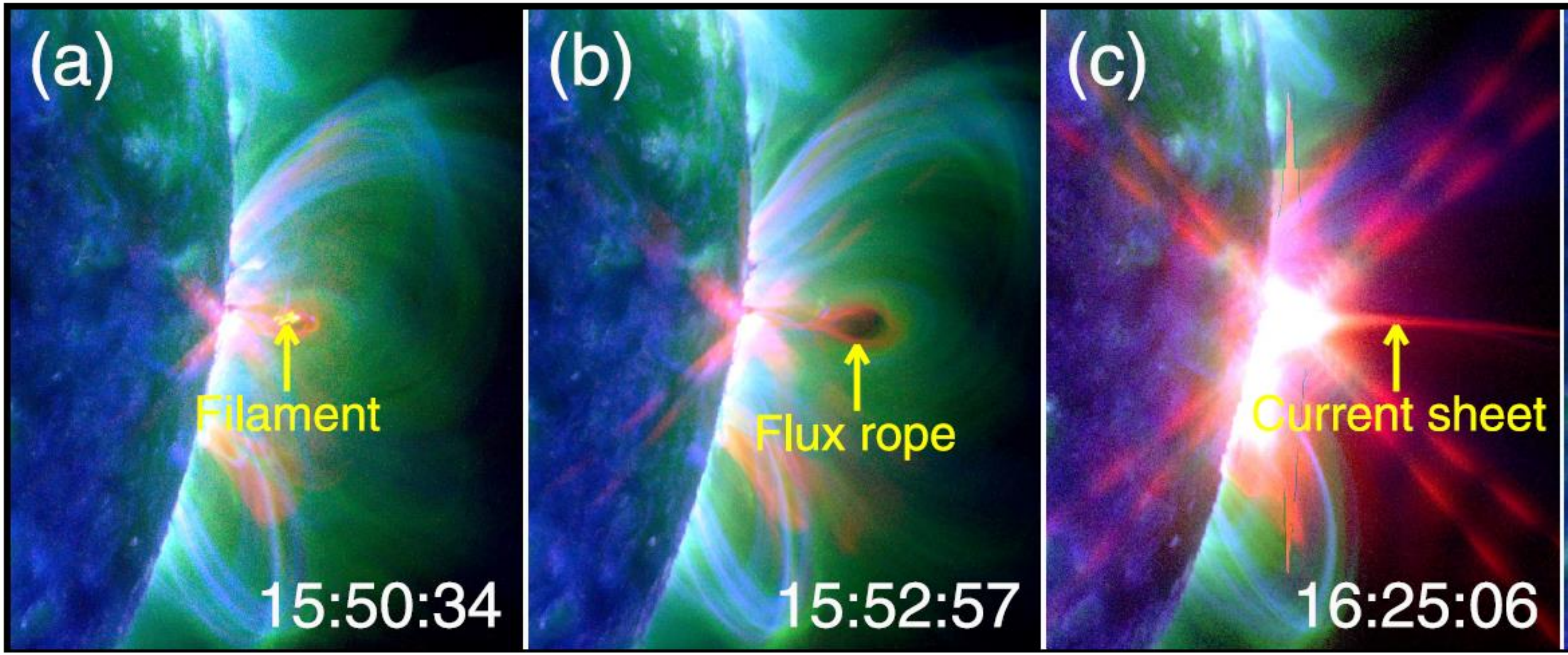

Yan et al. (2018), ApJ, 853, L18

- Major X8.2 limb flare of 2017-09-10
- Observations of an erupting filament / hot flux rope
- After eruption: Long, protruding “current sheet” structure
- Properties of the current sheet in *Warren et al. (2018, ApJ, 854, 122)*

A Recent Example of a 2D-ish Flare

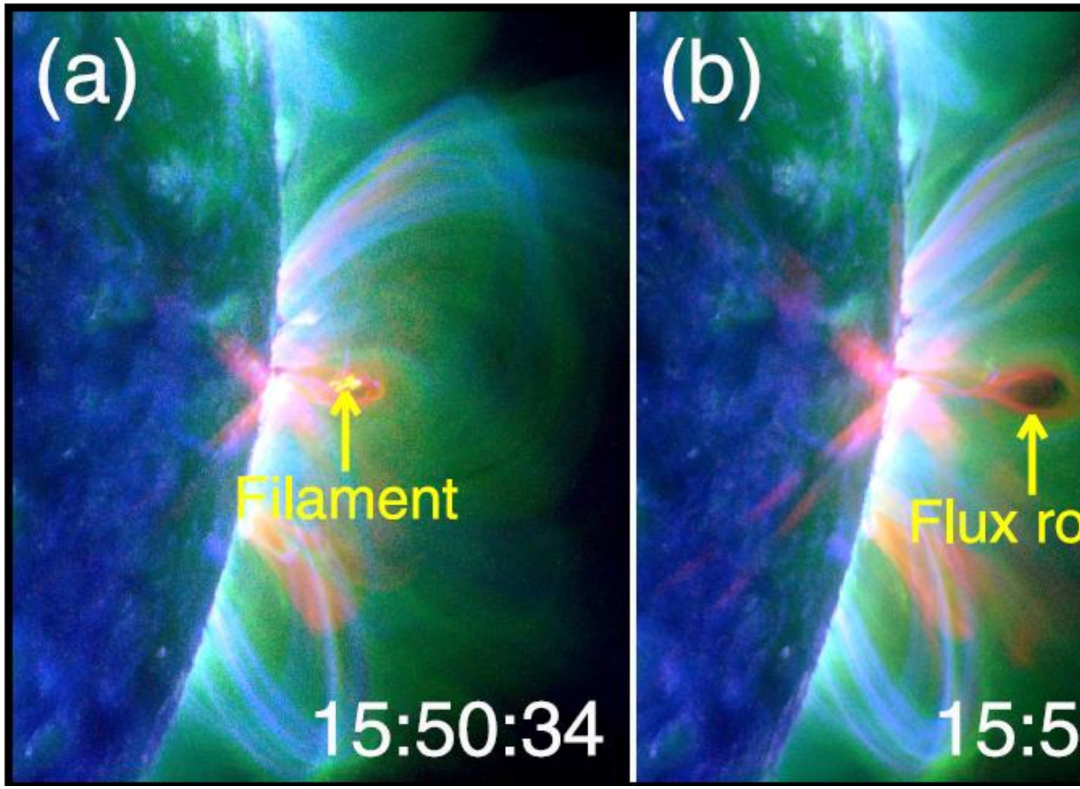

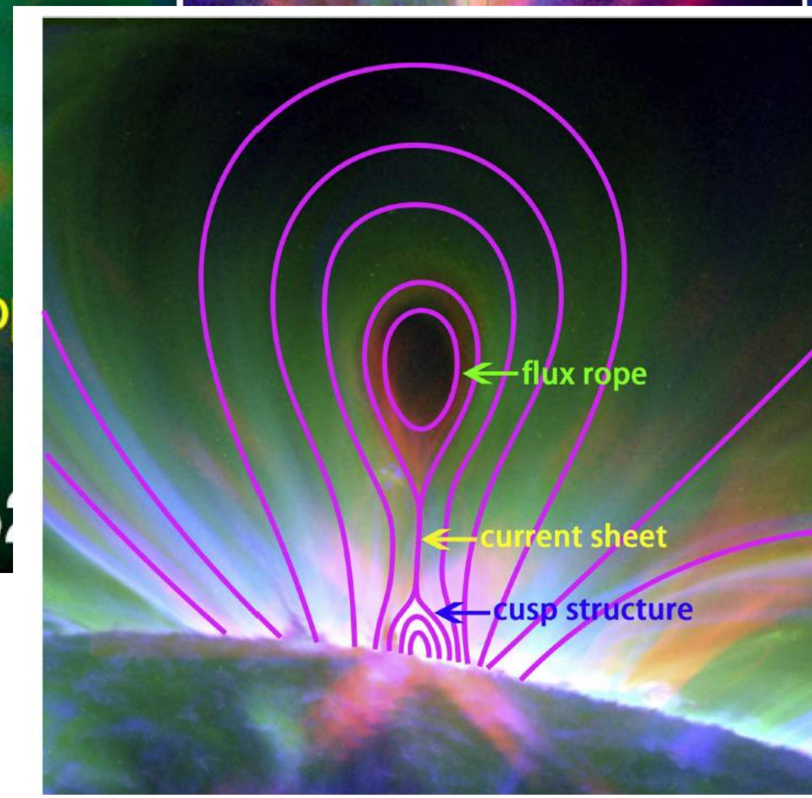

Yan et al. (2018), ApJ, 853, L18

- **Major X8.2 limb flare of 2017-09-10**
- **Observations of an erupting filament / hot flux rope**
- **After eruption: Long, protruding "current sheet" structure**
- **Properties of the current sheet in *Warren et al. (2018, ApJ, 854, 122)***

Precursors & Tether-cutting

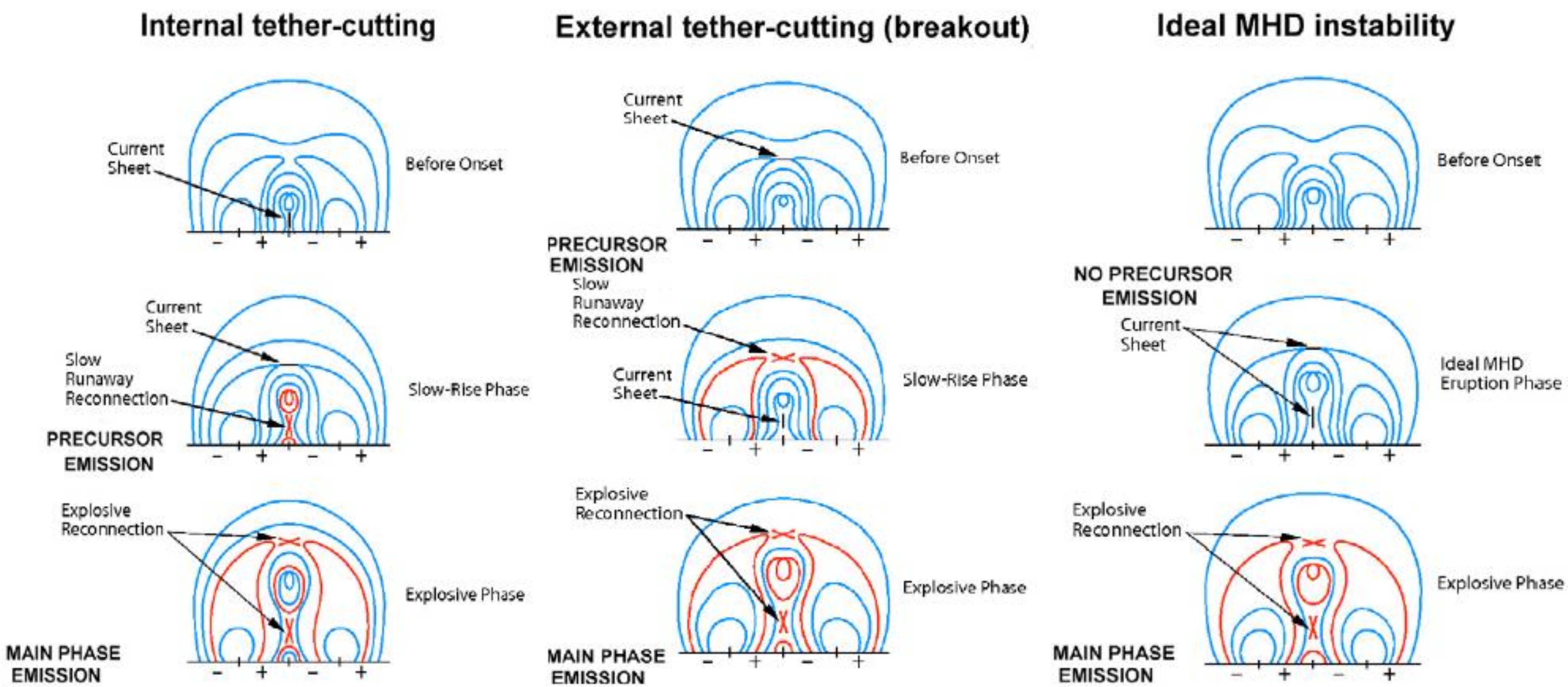

Chifor et al. (2007), A&A, 472, 967, after *Moore & Sterling (2006), AGU Conf.*

- **Analyzed 8 major flares**
- **Precursors in 5-out-of-8 flares:**
  - UV and X-ray brightenings 2-50 min prior to impulsive phase
  - located 10" from the PIL; with eruption from the location of the precursor

Tether-cutting Reconnection

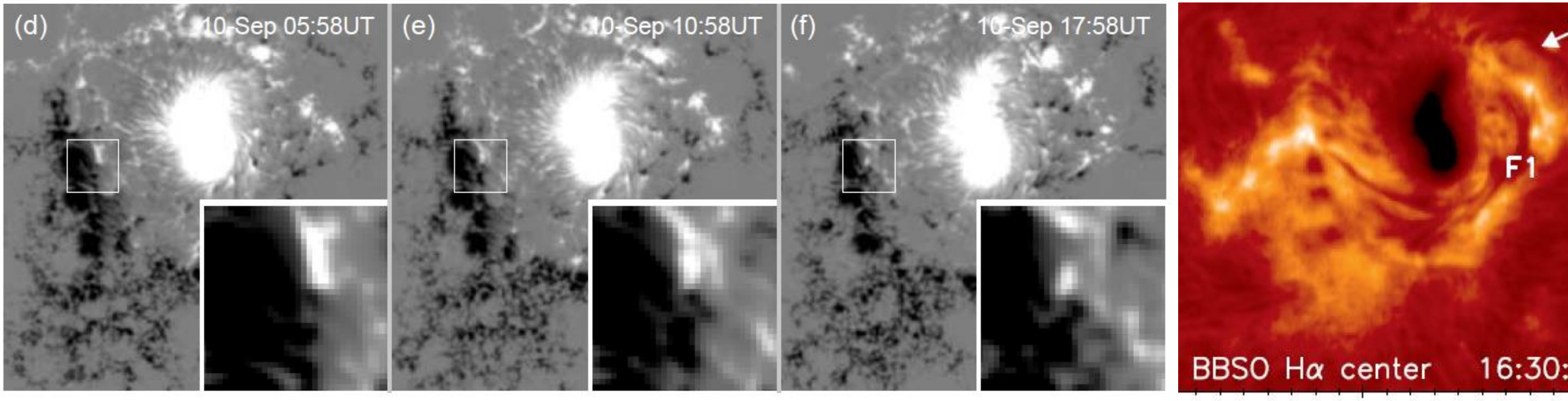

Cheng et al. (2015), ApJ, 804, 82

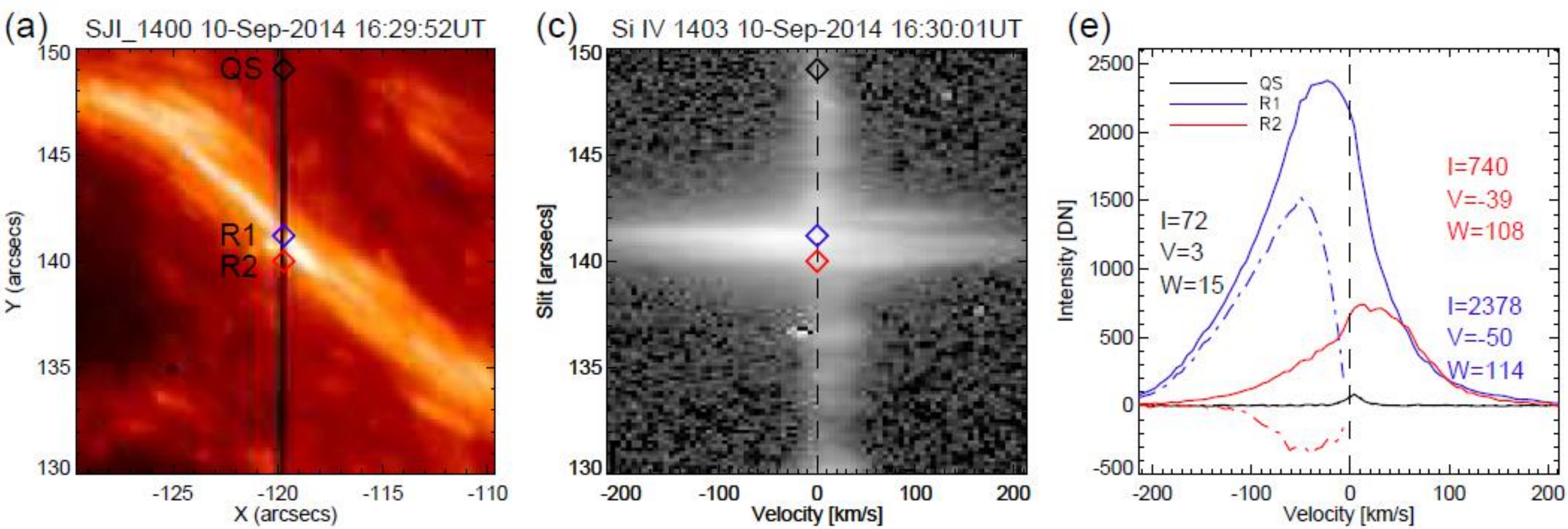

Tether-cutting Reconnection

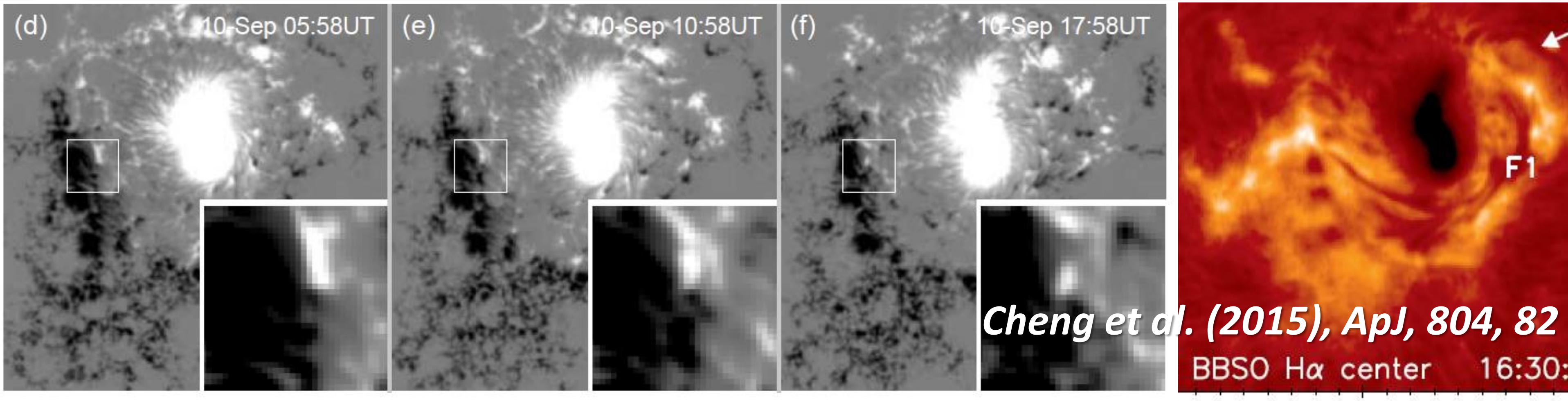

Cheng et al. (2015), ApJ, 804, 82

- 2D: Tether-cutting adds to the filament/flux-rope
- Allows for explanation of the observed Doppler velocities

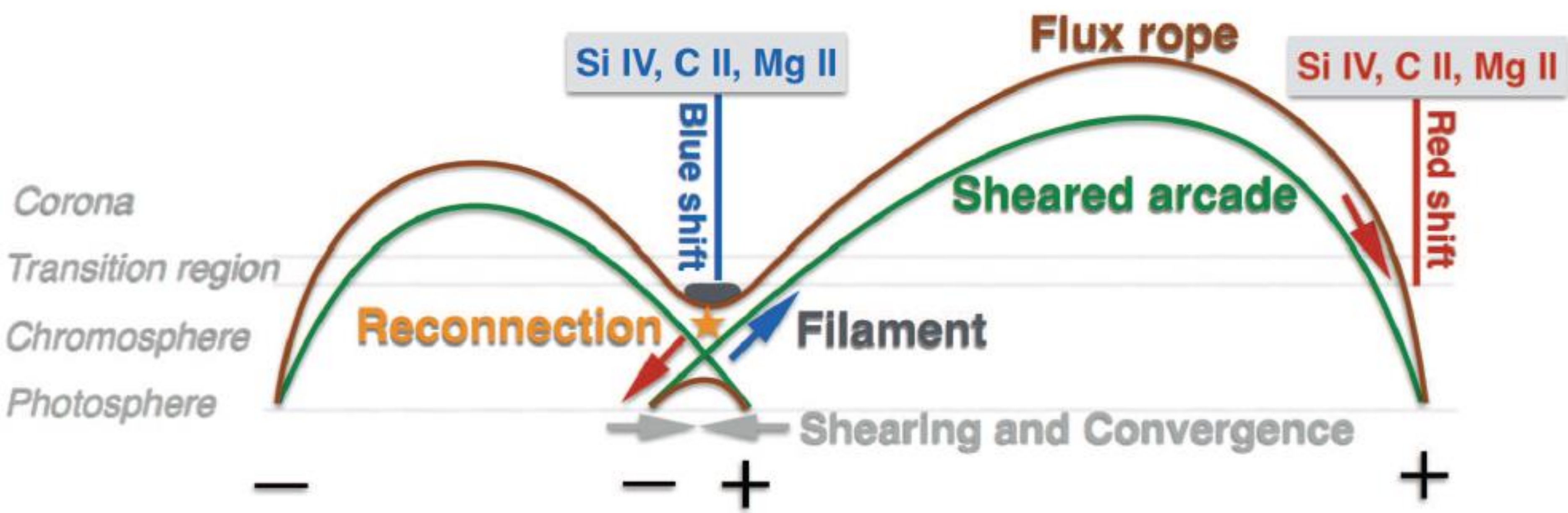

Chromospheric Evaporation

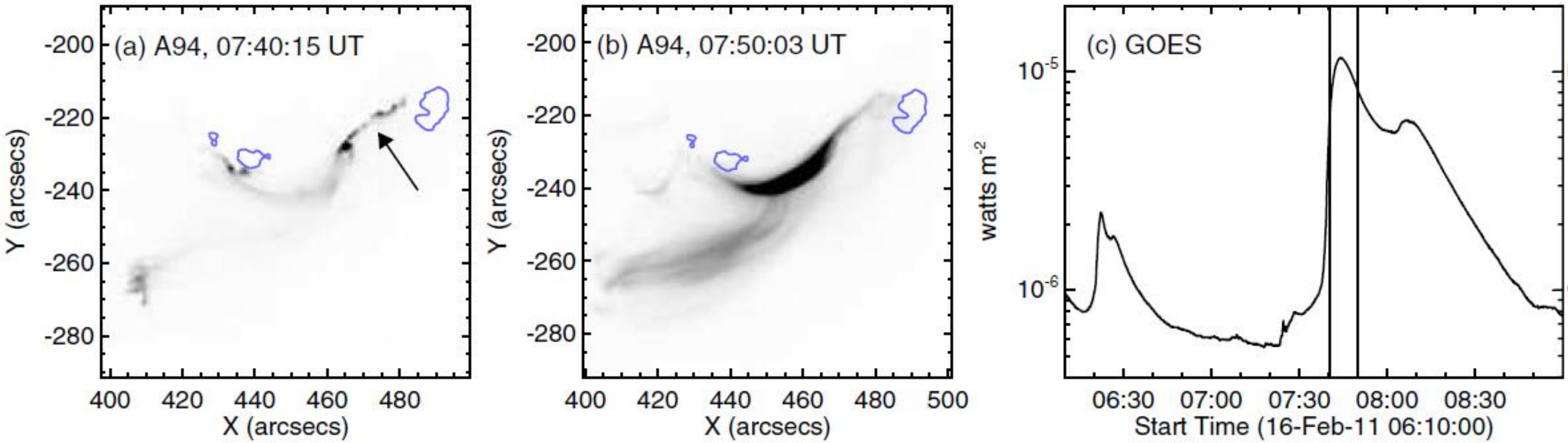

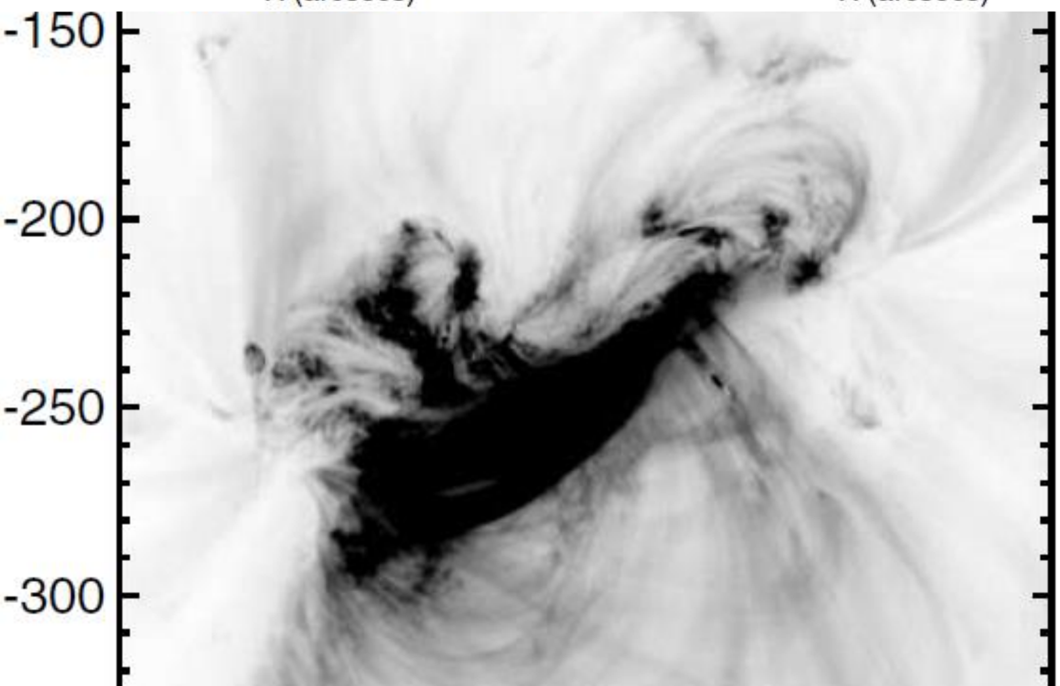

Young et al. (2013), ApJ, 766, 127

- **Observation of an M-class flare with SDO/AIA and Hinode/EIS**
- **Hinode/EIS sparse raster (2'' slit jumps by 5'' in position)**
- **Observed O VI to Fe XXIV**

EIS Sparse Raster “Imaging”

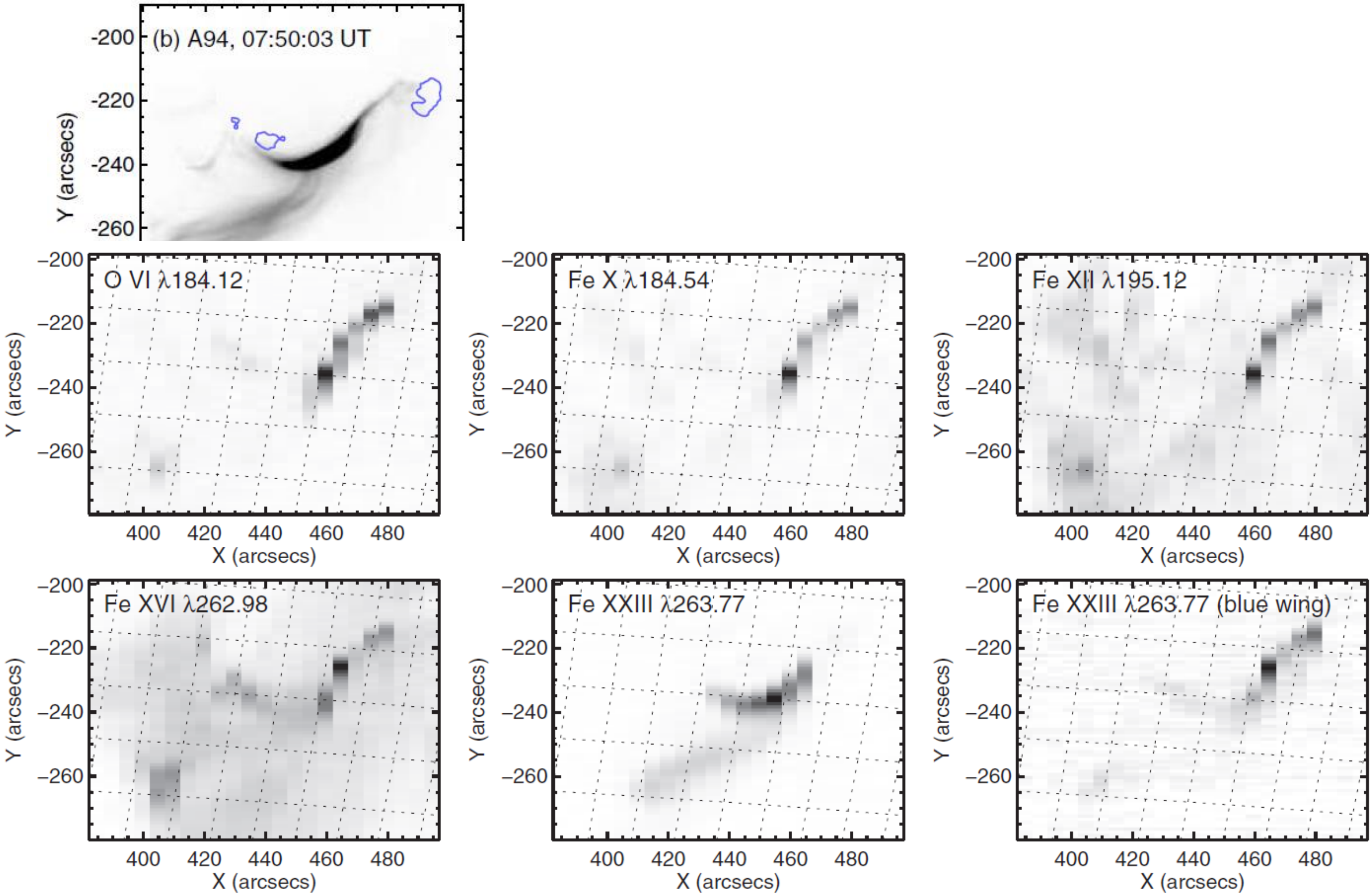

Chromospheric Evaporation

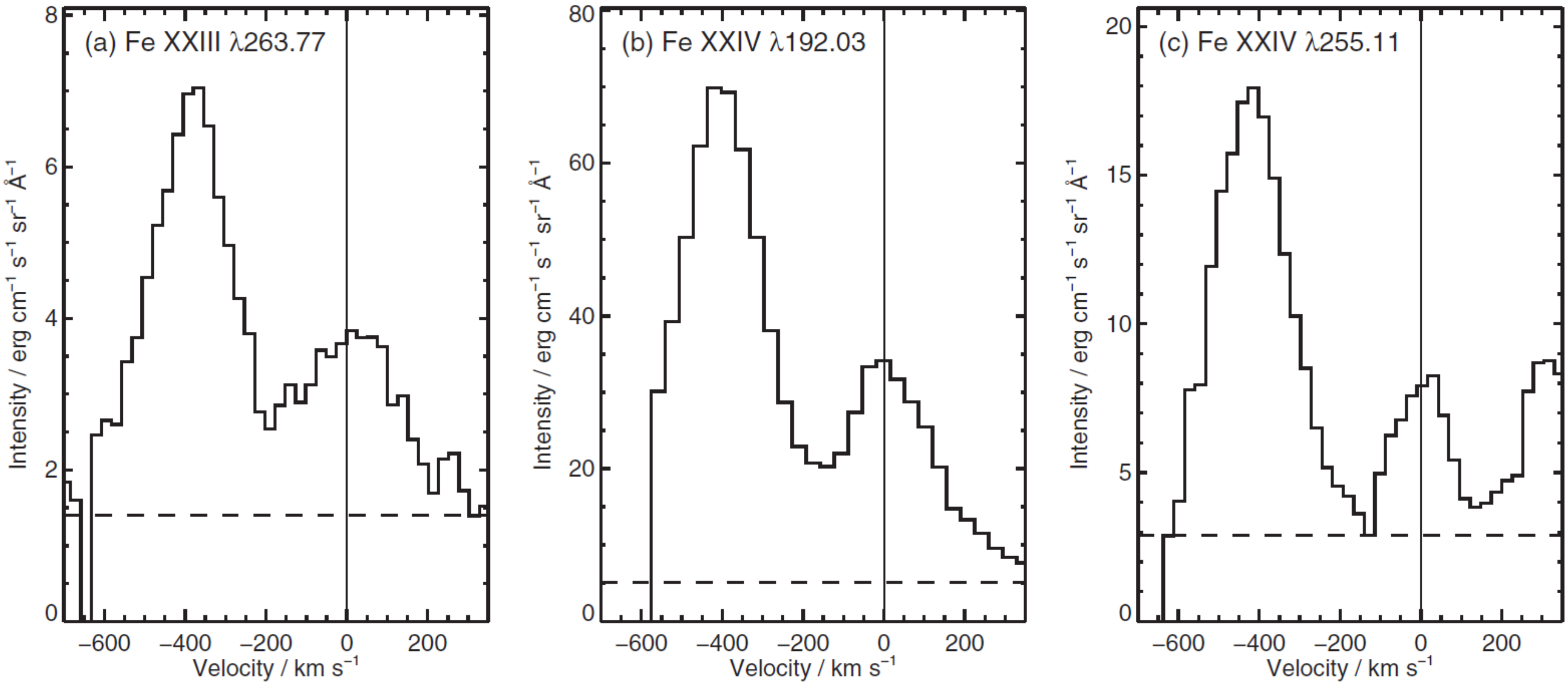

Young et al. (2013), ApJ, 766, 127

- Spectra from a flare kernel
- Very fast (400 km s^{-1}) and very intense upflowing component
- Stationary component slightly red-shifted
- Problems with resolving individual components?

Young et al. (2013), ApJ, 766, 127

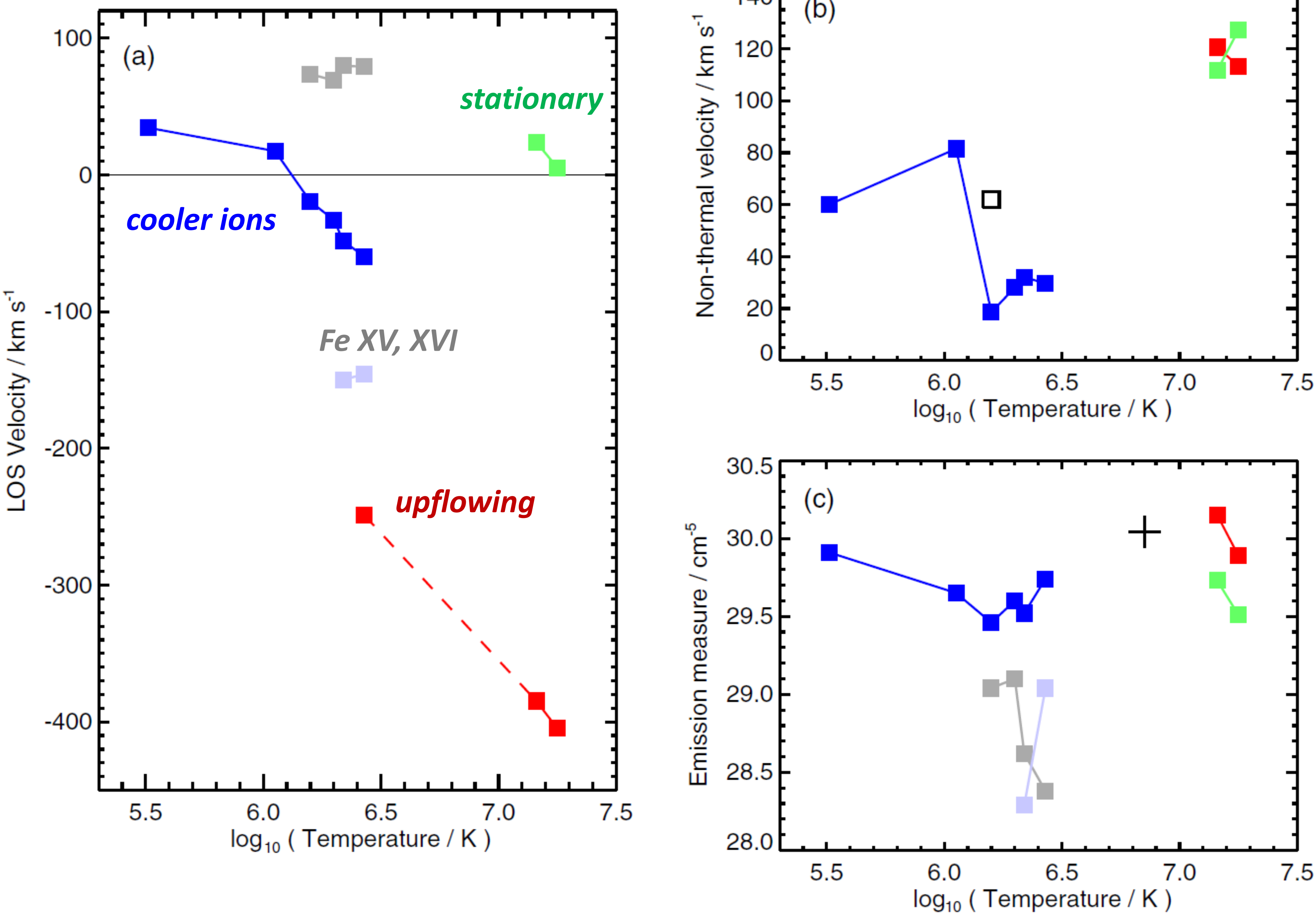

Chromospheric Evaporation

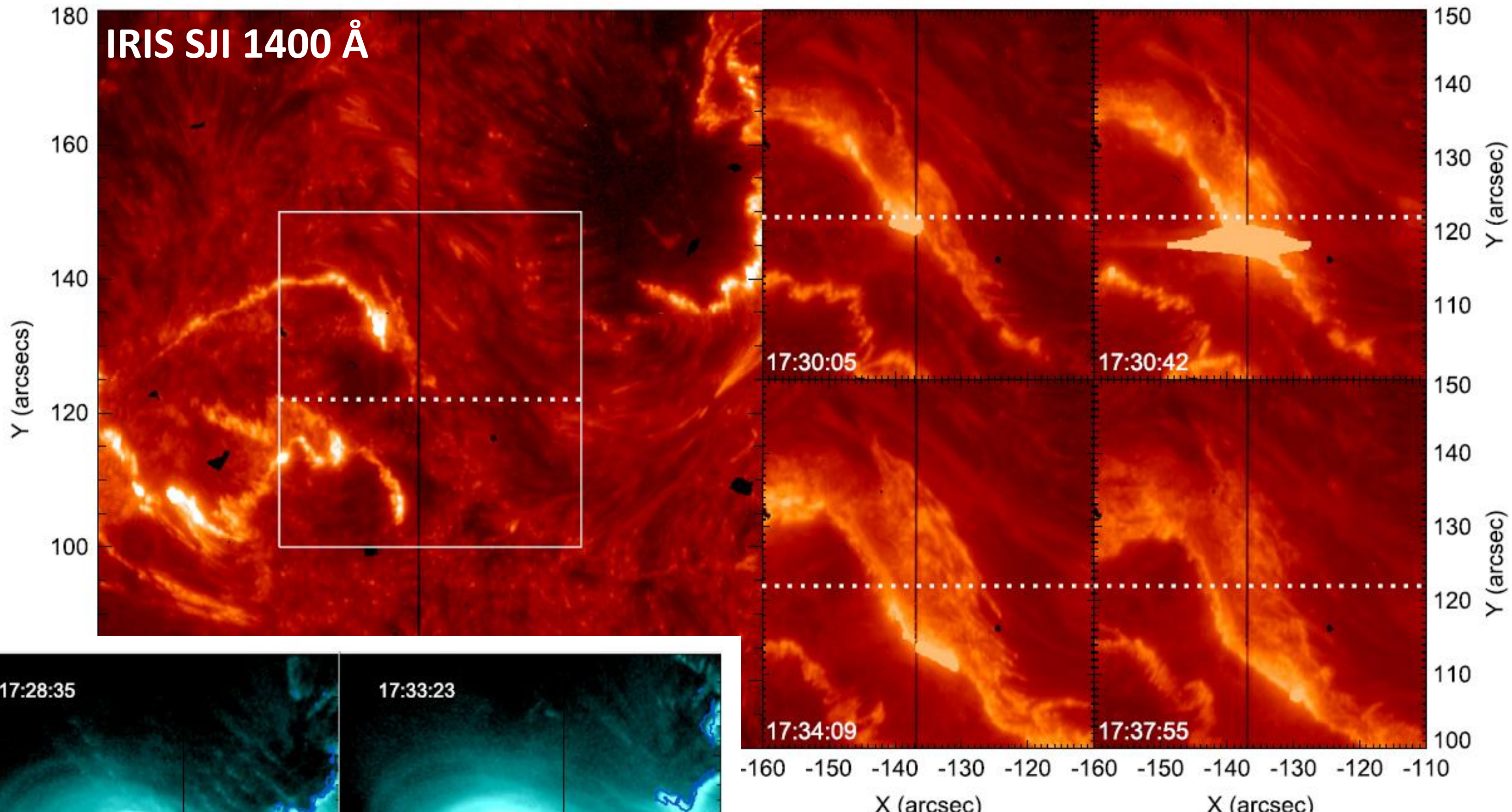

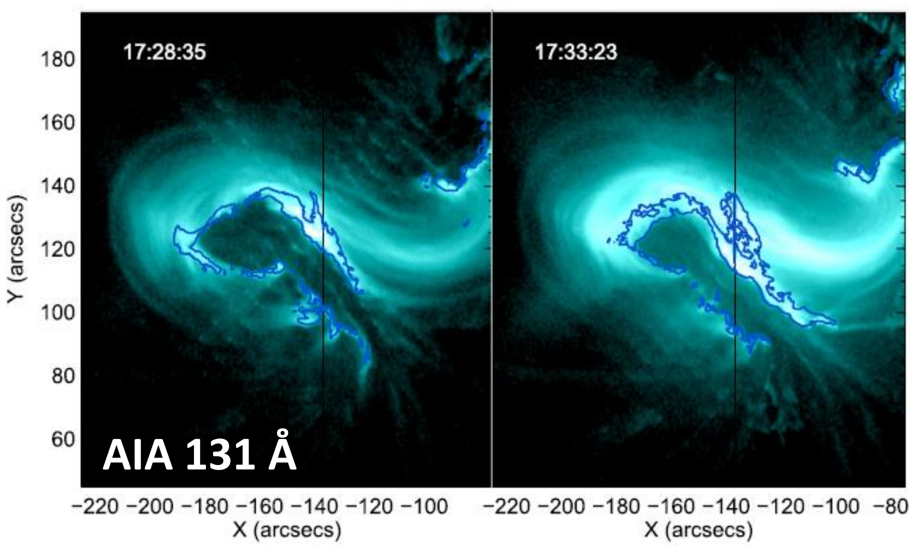

Graham & Cauzzi (2015), ApJ, 807, L22

- 2014 September 10 X1.6-class flare
- IRIS sit-and-stare
  with Mg II and Fe XXI spectra

Evaporation in Individual Kernels

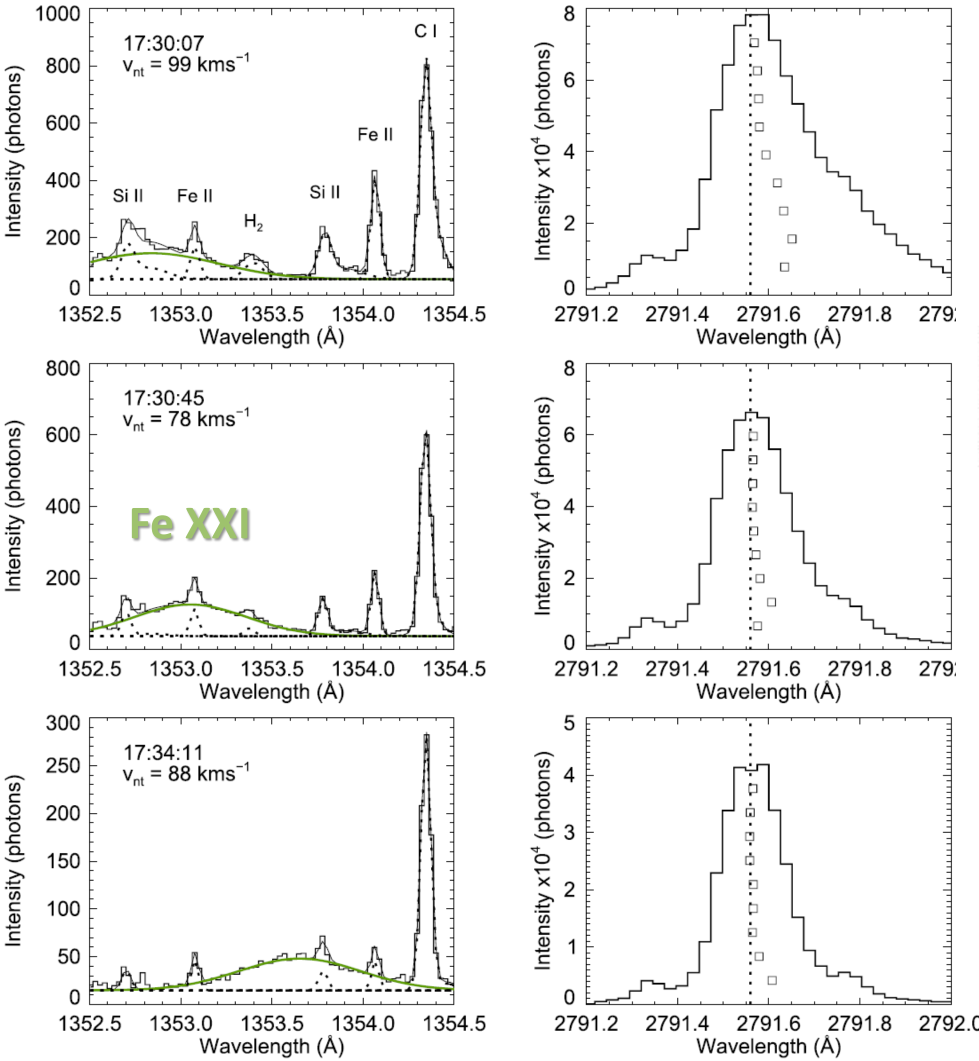

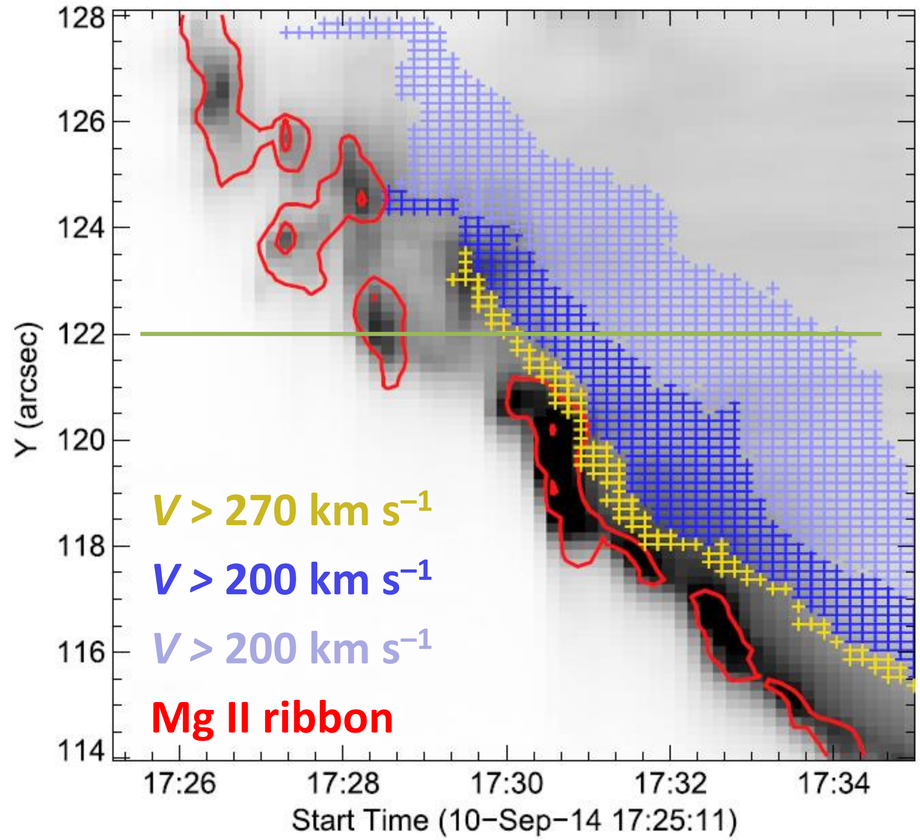

Graham & Cauzzi (2015), ApJ, 807, L22

- Mg II redshifted at ribbon (red)
- Individual kernels have similar behavior: evaporation starts at about 300 km s^{-1} and *lags* behind the ribbon

Evaporation: Evolution

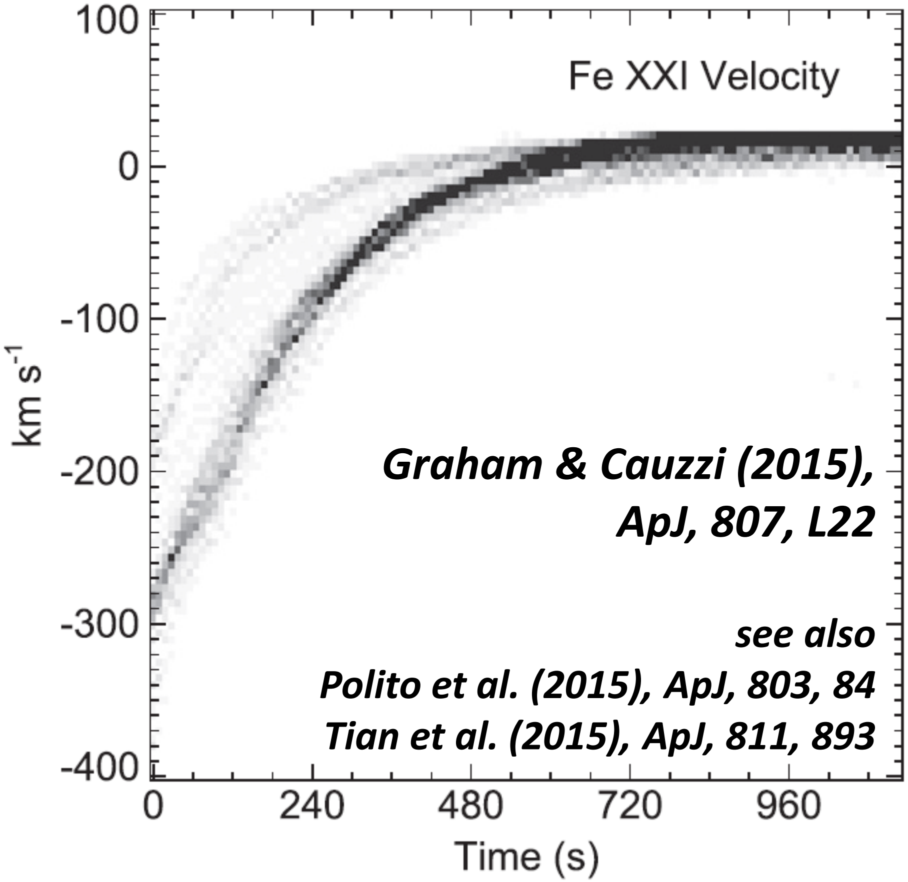

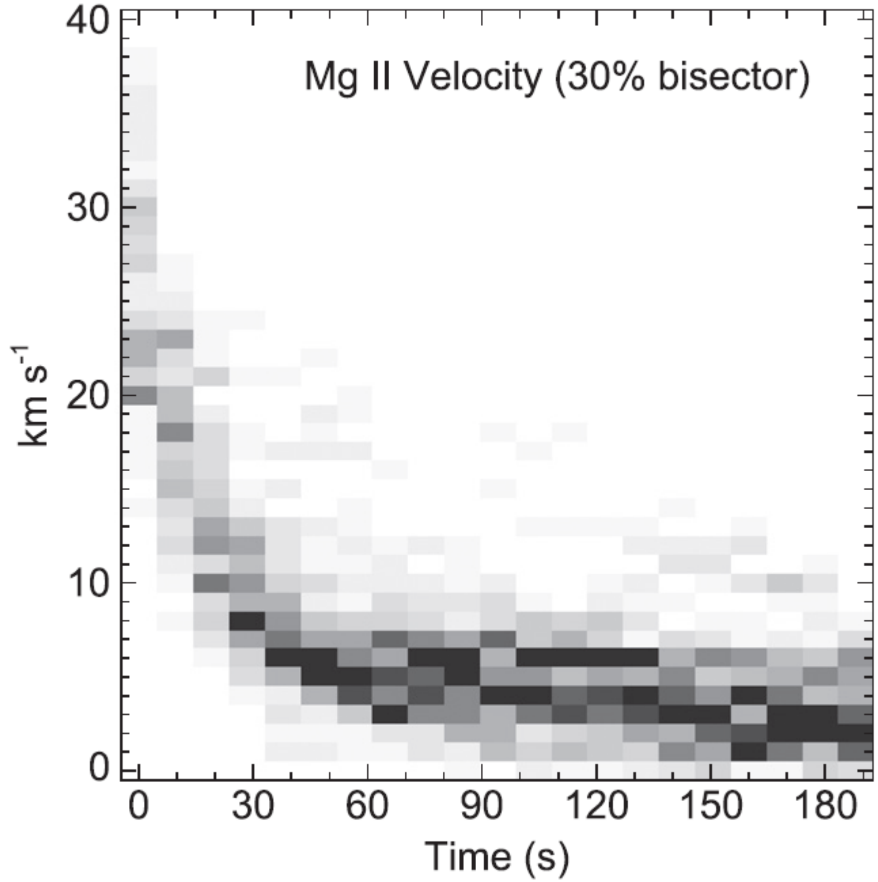

- Superposed analysis: curves for each line and kernel shifted to $t = 0$ s
- Strikingly similar behavior in every kernel in both Fe XXI and Mg II subordinate line
- Fe XXI upflows last about 6 min, strong condensation donwflows in Mg II, 40 km s^{-1}
- In good agreement with predictions of 1D hydro models: *Fisher (1989), ApJ, 317, 502*

Evaporation: Evolution

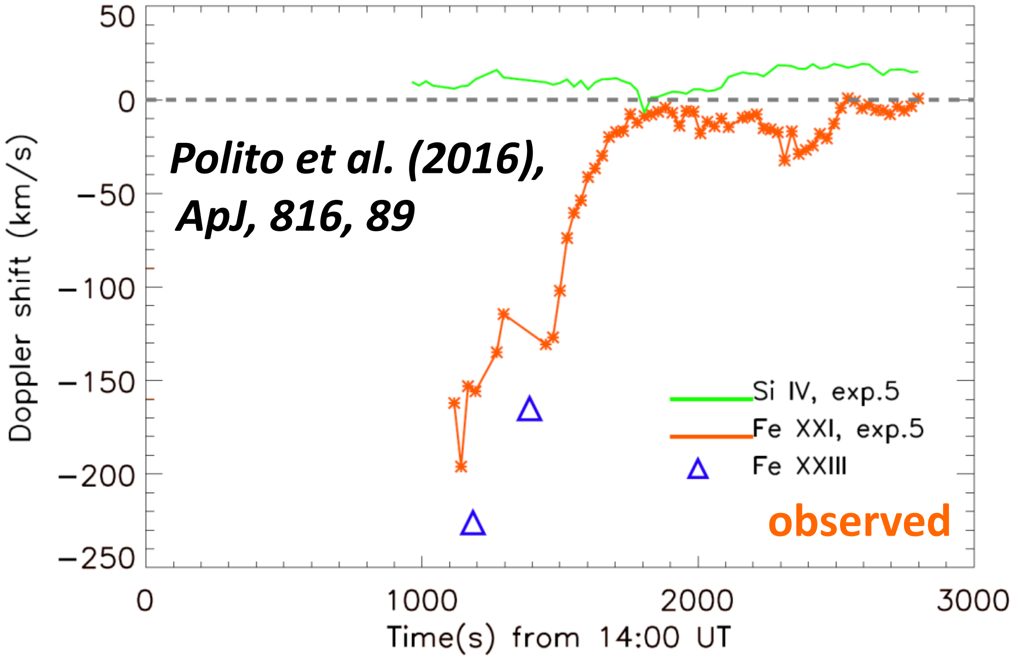

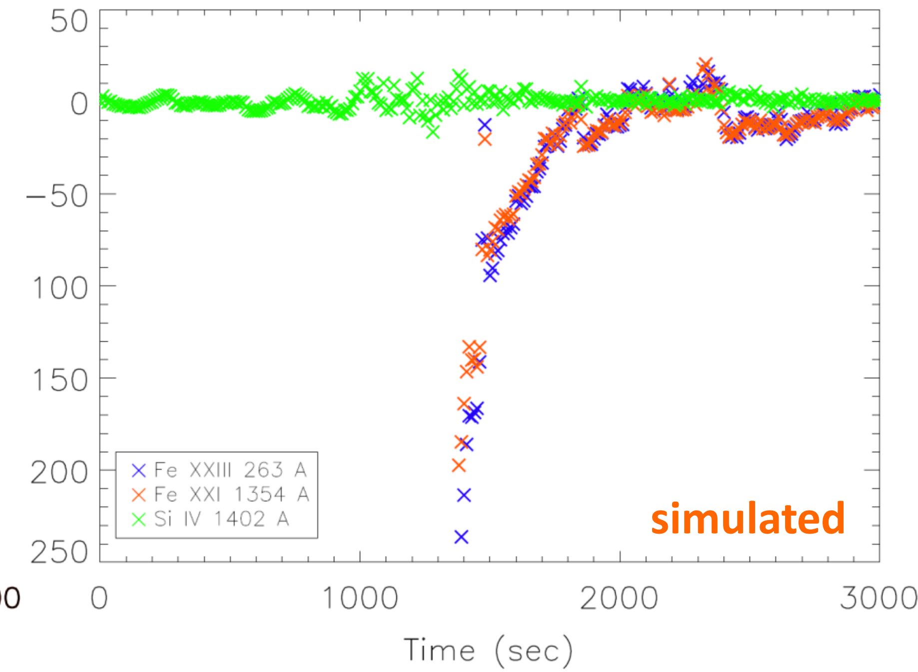

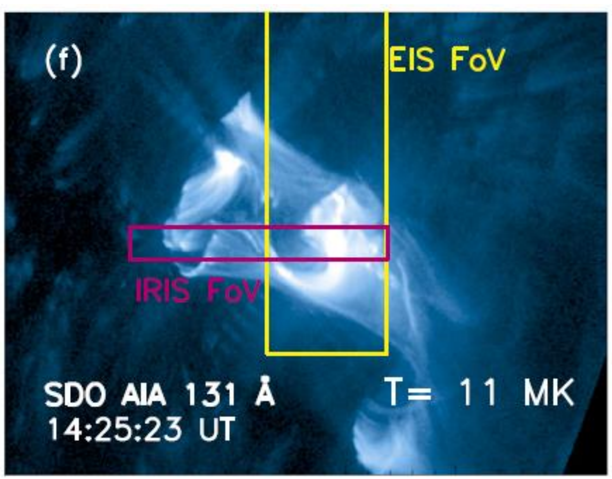

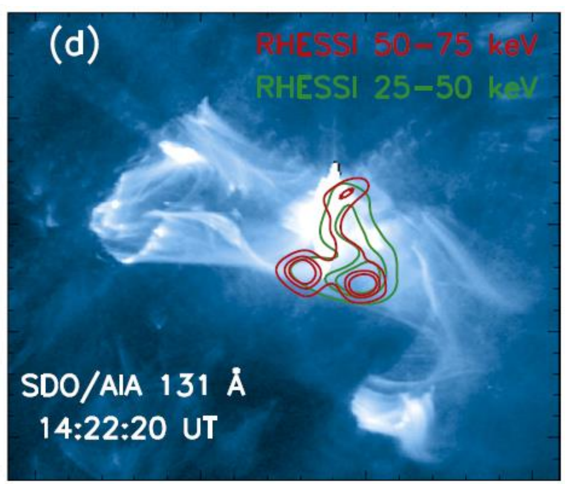

- Fe XXI completely blueshifted
- Fe XXIII asymmetric
- HYDRAD 1D simulations with beam heating
- Cut-off and spectral index given by RHESSI
- *But electron flux 10x lower !*
  (Area? Coronal deposit?)

Evaporation = *f* (Flare Class) ?

Polito et al. (2017), A&A, 601, 39

Doschek et al. (2013), ApJ, 767, 55

- **2012 March 9 recurrent flares confined C to eruptive M in less than 4 hours**
- **Footpoint brightenings K1, K2**

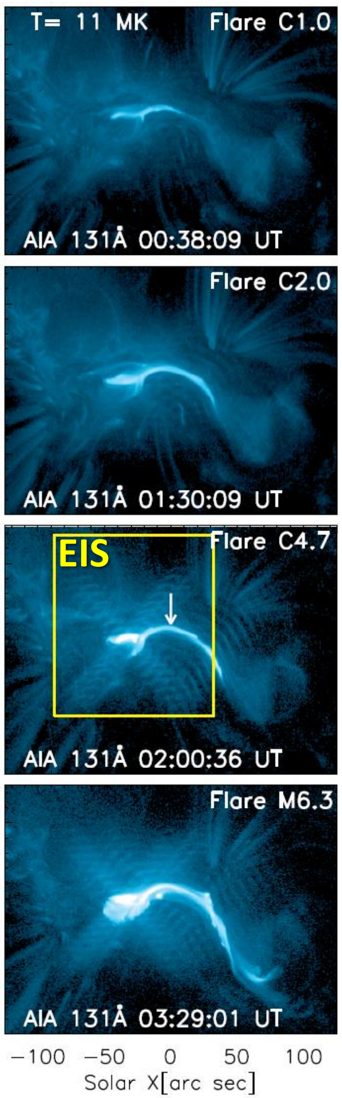

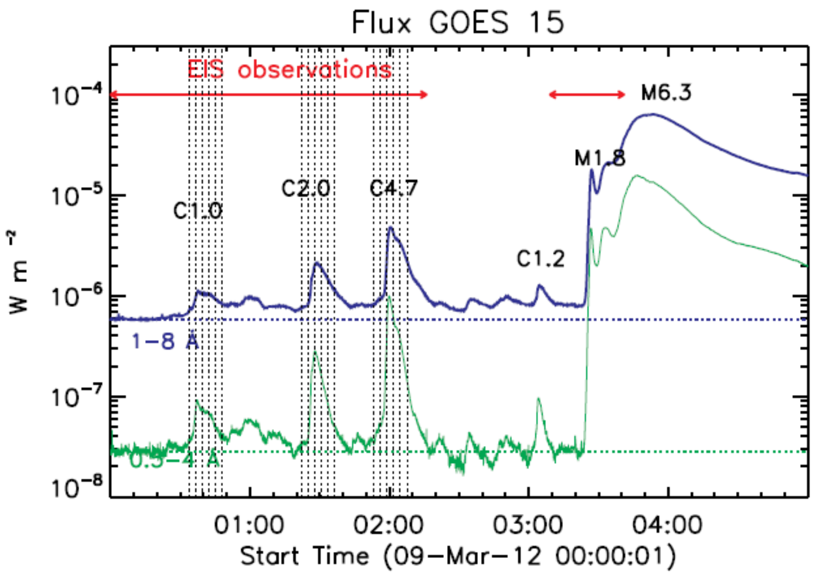

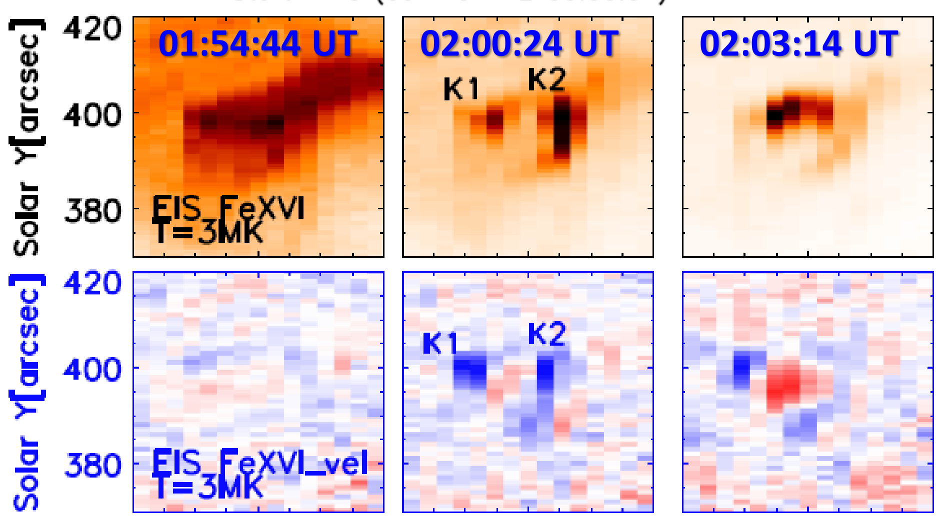

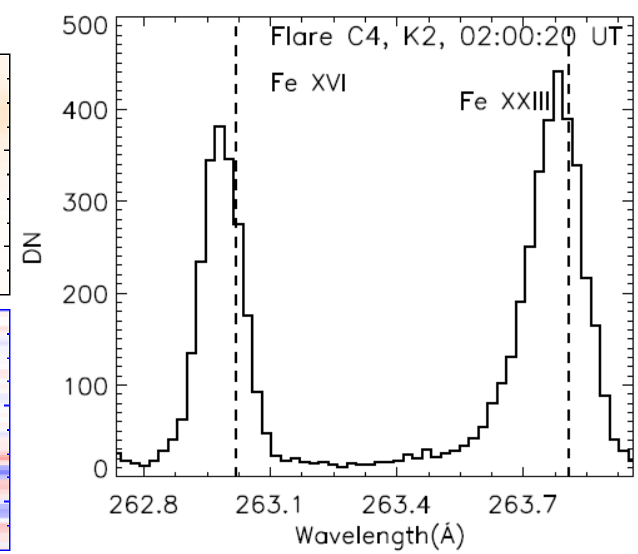

Evaporation = f (Flare Class) ?

Polito et al. (2017), A&A, 601, 39

Doschek et al. (2013), ApJ, 767, 55

Flare	Fe XXIII vel (km s^{-1})		Fe XVI vel (km s^{-1})	
	K1	K2	K1	K2
C2.0	202 ± 14	60 ± 7	76*	12 ± 5
C4.7	146 ± 10	110*	43 ± 5	39 ± 5
M1.8 (Doschek et al. 2013)	150–170		40–60	

- No dependence on flare class
- Not the same kernels

Flare	Log N_e (min, max) cm^{-3}	
	K1	K2
C1.0	10.0 (9.9, 10.2)	10.2 (10.0, 10.4)
C2.0	10.4 (10.2, 10.6)	10.7 (10.4, > 11.0)
C4.7	>11.0 (10.7, >11.0)	11.0 (10.6, >11.0)
M1.0 (Doschek et al. 2013)	>11.0	

- Fe XIV densities
- Dependent on flare class

How *slow* can evaporation be?

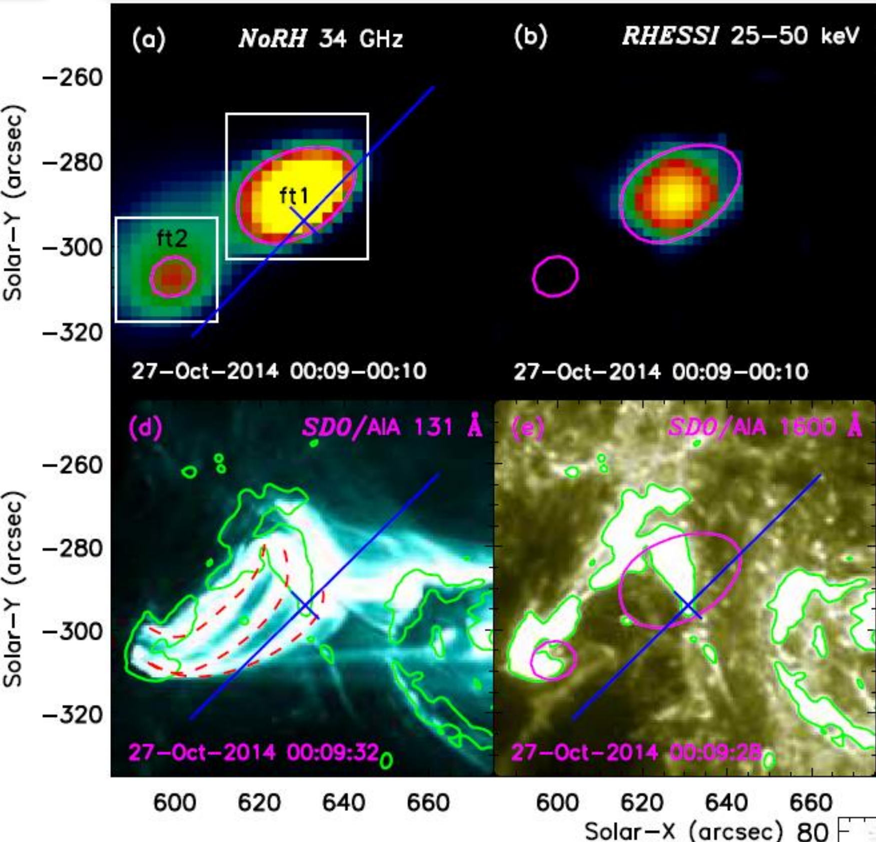

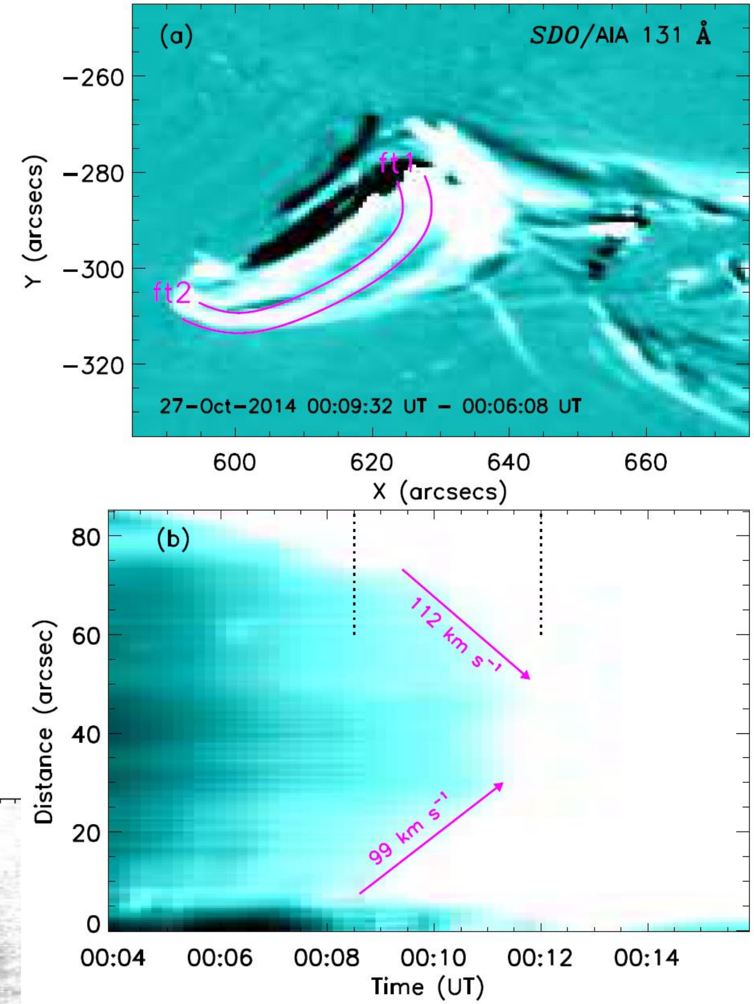

Li et al. (2017), ApJL, 841,

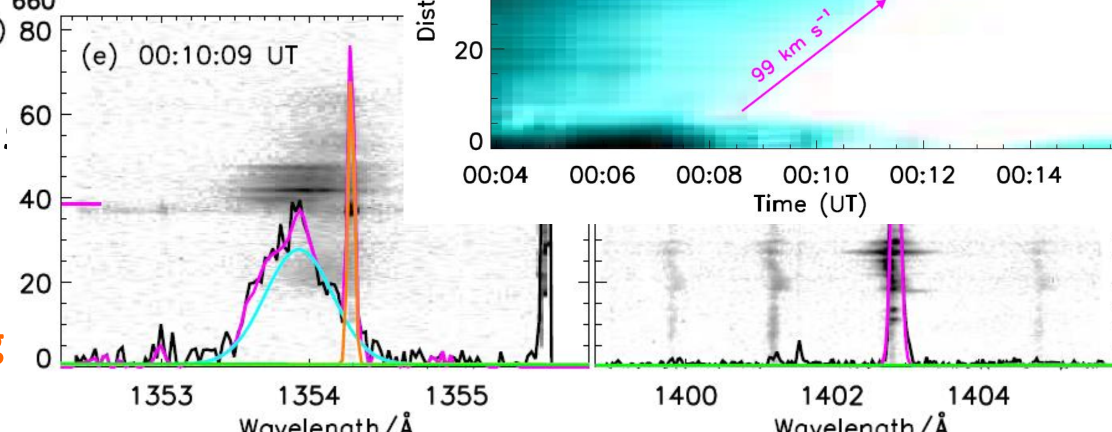

- M7.1 flare of 2014 October 27
- Slow evaporation, 67 km s^{-1} max
- AIA 131 Å loop observed to be filling up with plasma

How *fast* can evaporation be?

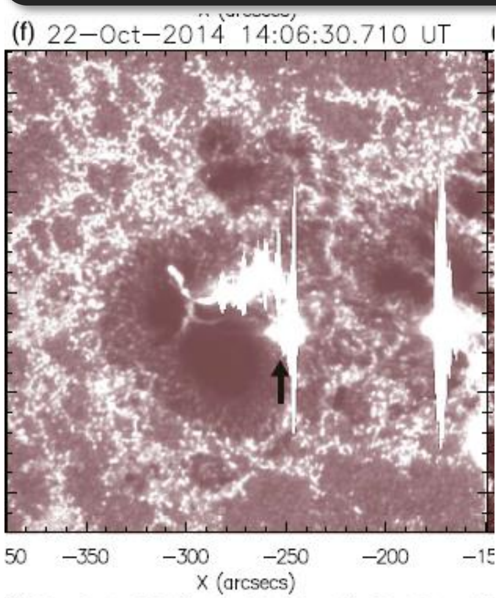

Lee et al. (2017), ApJ, 836, 150

- White-light X1.6 <u>confined</u> flare of *2014 October 22*
- WL kernel (arrow) with HXR peak and HMI continuum enhancement
  (indicative of non-thermal beam heating)
- **Bulk blue-shift of the Fe XXIII and XXIV (rare in EIS)**
- Red-shifts in chromospheric and TR lines observed by IRIS

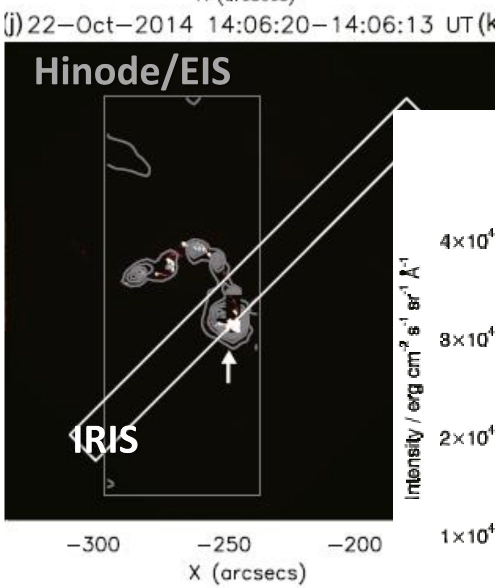

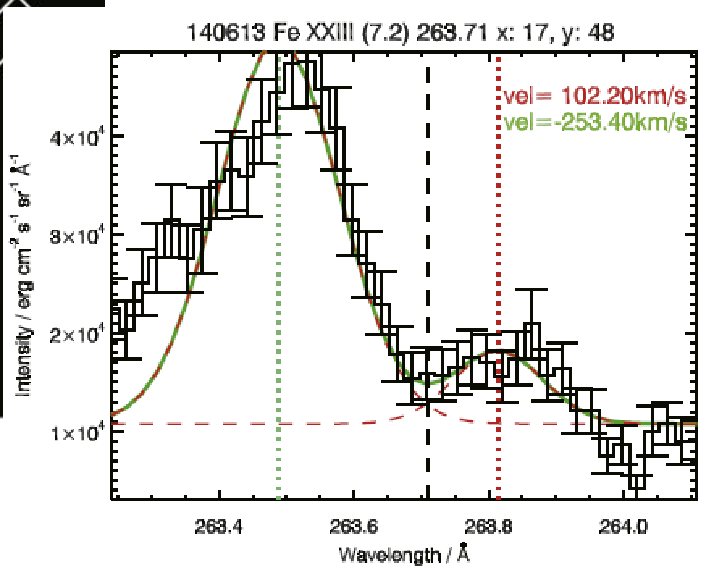

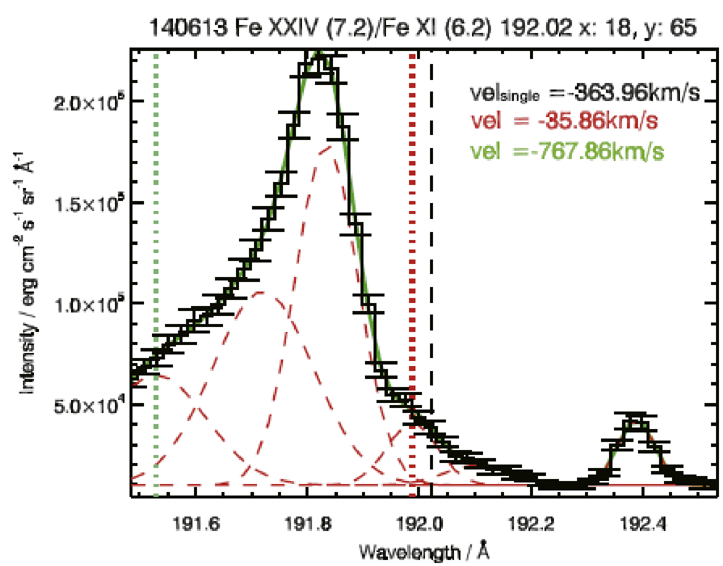

II. Flares and Eruptions are 3D!

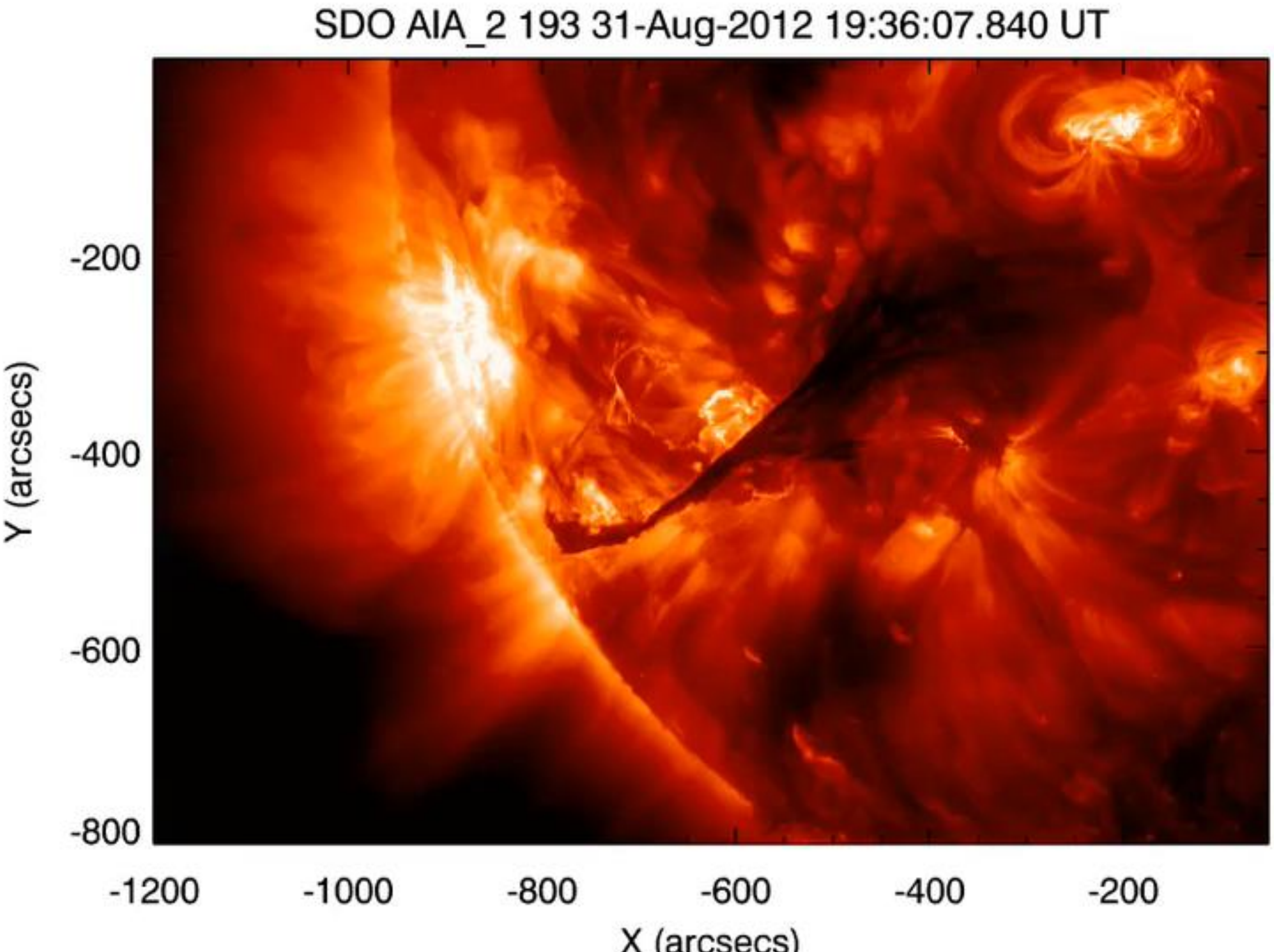

2D → 3D is easy?

- **Asymmetric model of a flare capturing dynamics of:**
- **propagation of brightenings along ribbons**
- **progressive ribbon separation**
- **2.5D**

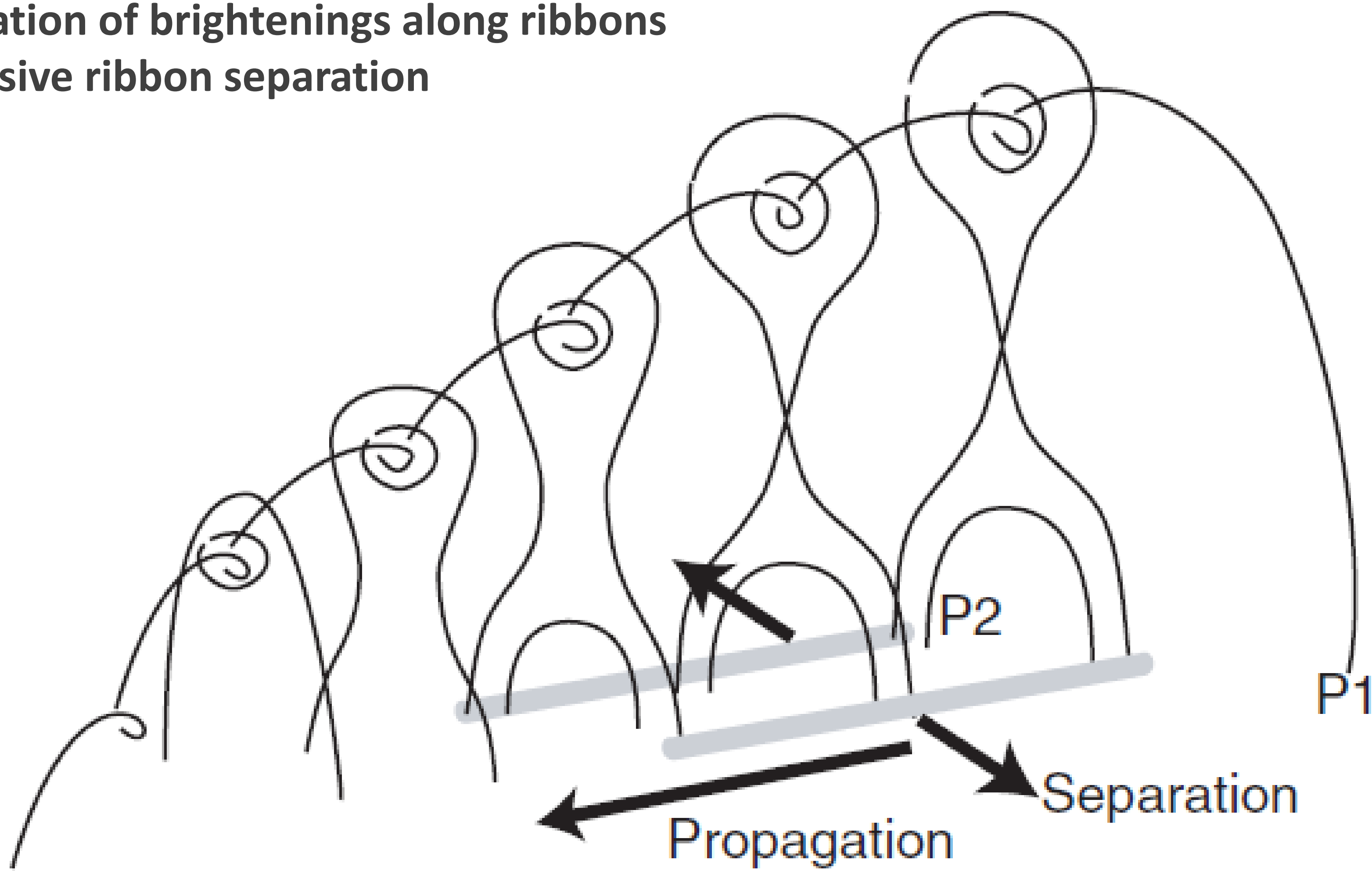

Tripathi, Isobe & Mason (2006), Astron. Astrophys., 453, 1111

III. 2D → 3D Magnetic Null Points

- **Not straightforward to generalize: 2.5D null-points ≠ 3D null-points**

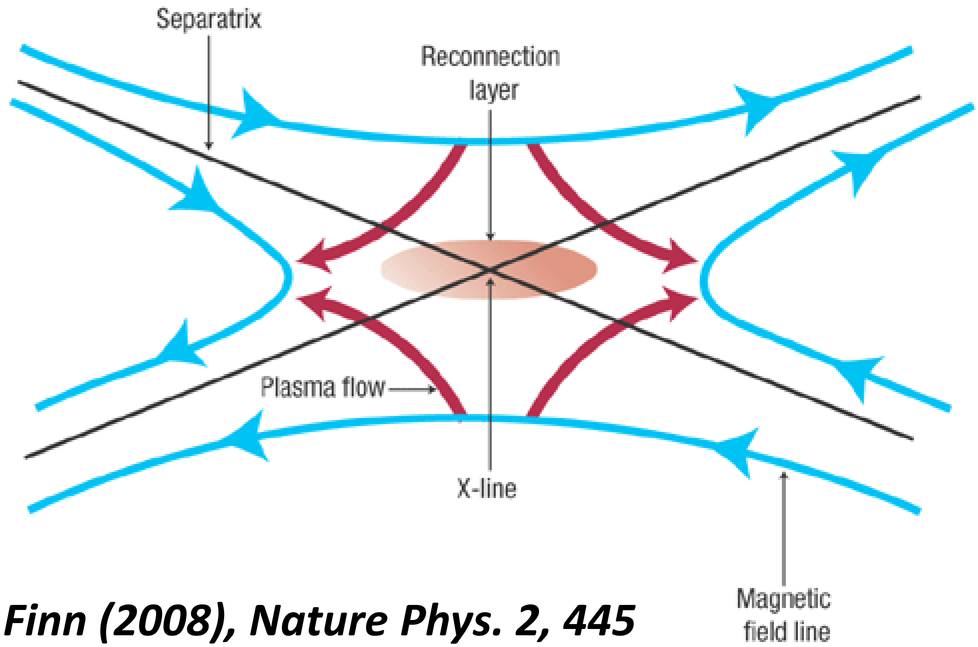

Finn (2008), Nature Phys. 2, 445

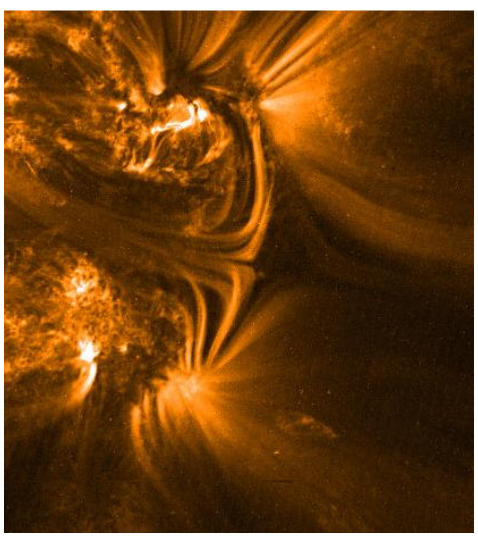

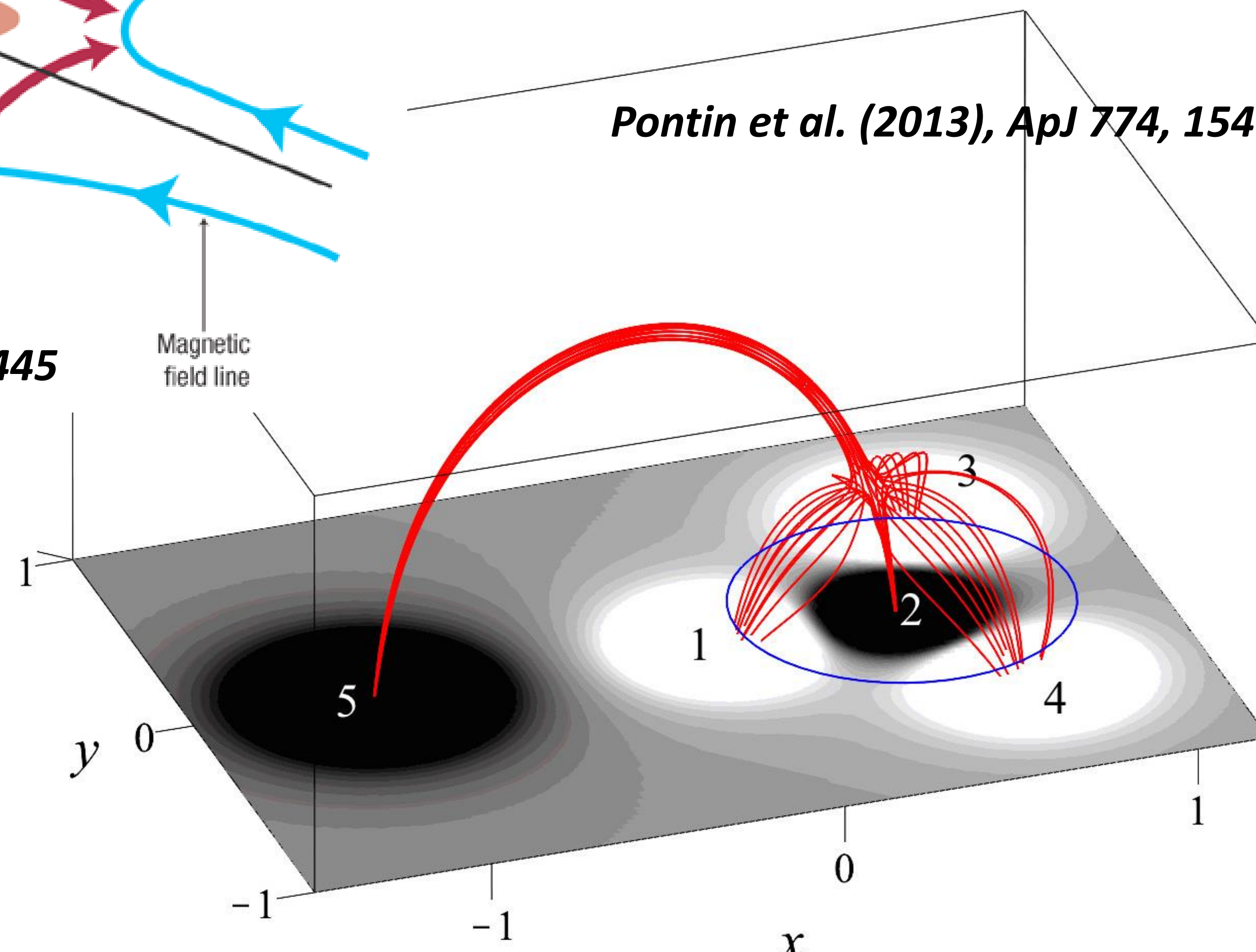

Pontin et al. (2013), ApJ 774, 154

3D Null Point Reconnection

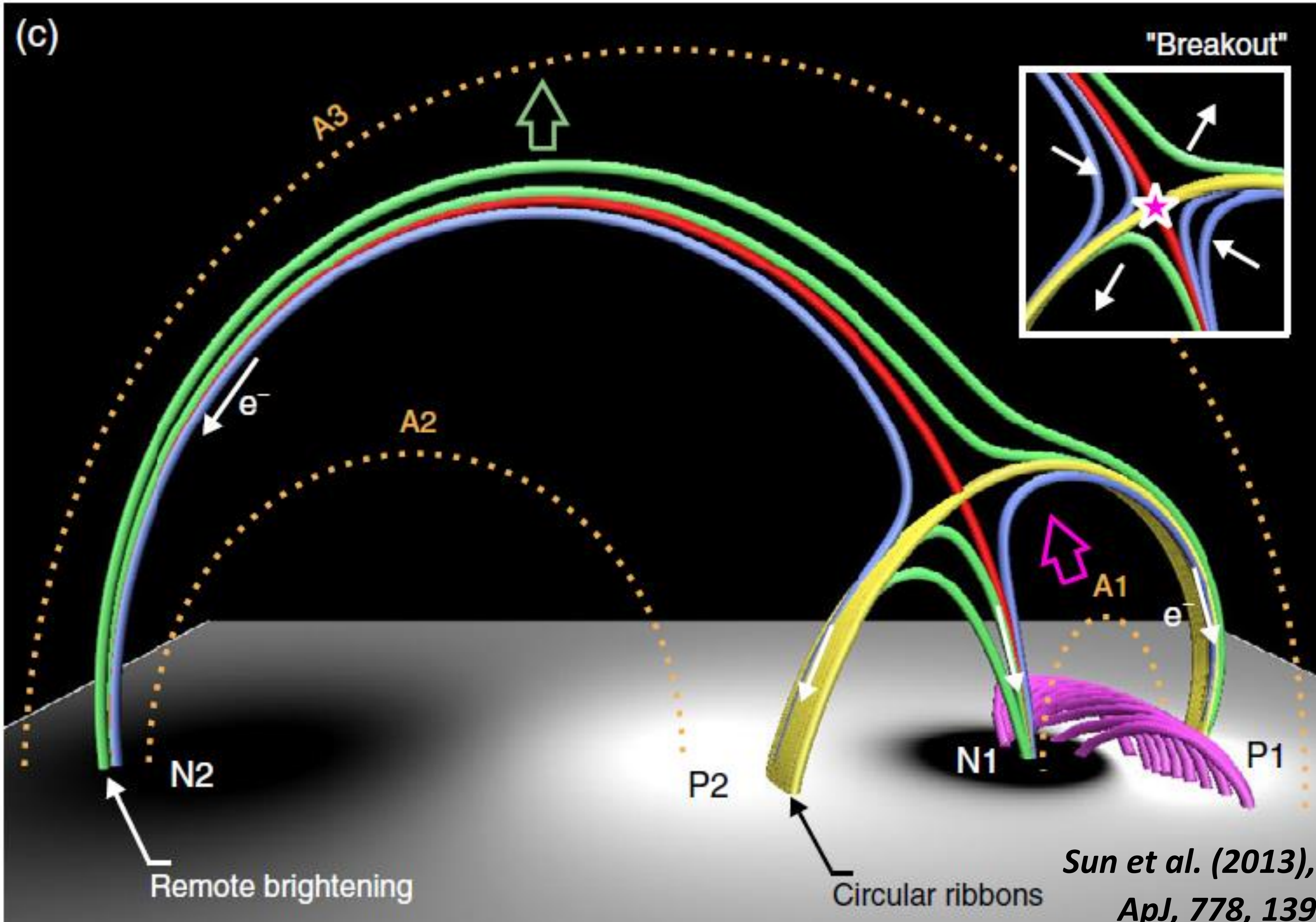

Sun et al. (2013), ApJ, 778, 139

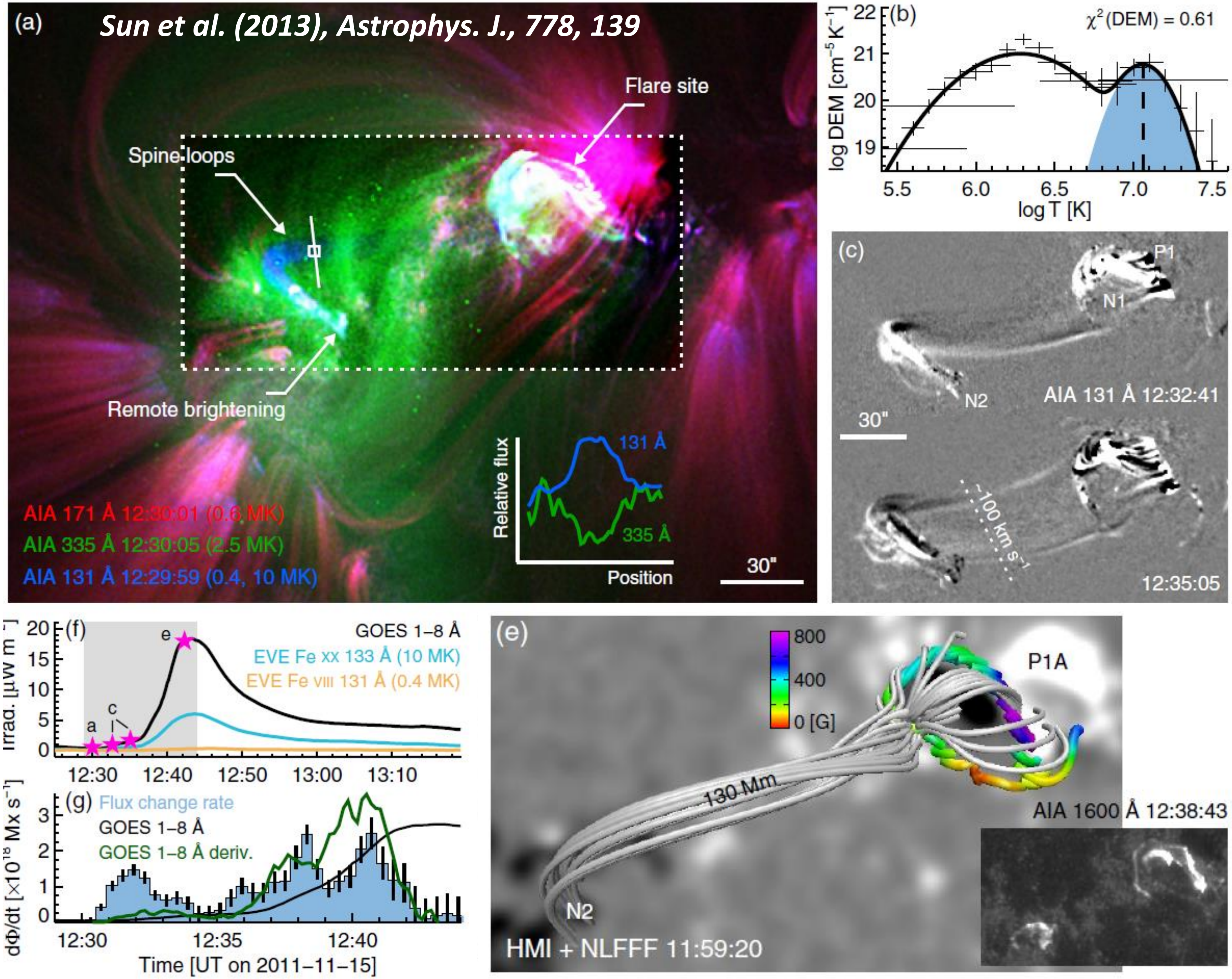

Sun et al. (2013), Astrophys. J., 778, 139
(a)
Flare site
Spine loops
Remote brightening
Relative flux
131 Å
335 Å
Position
30"
AIA 171 Å 12:30:01 (0.6 MK)
AIA 335 Å 12:30:05 (2.5 MK)
AIA 131 Å 12:29:59 (0.4, 10 MK)
(b)
χ^2(DEM) = 0.61
log DEM [cm^{-5} K^{-1}]
log T [K]
(c)
P1
N1
N2
AIA 131 Å 12:32:41
30"
~100 km s^{-1}
12:35:05
(f)
GOES 1–8 Å
EVE Fe XX 133 Å (10 MK)
EVE Fe VIII 131 Å (0.4 MK)
Irrad. [μW m^{-2}]
(g)
Flux change rate
GOES 1–8 Å
GOES 1–8 Å deriv.
dΦ/dt [$\times 10^{18}$ Mx s^{-1}]
Time [UT on 2011–11–15]
(e)
P1A
800
400
0 [G]
130 Mm
N2
AIA 1600 Å 12:38:43
HMI + NLFFF 11:59:20

Three Loop Systems

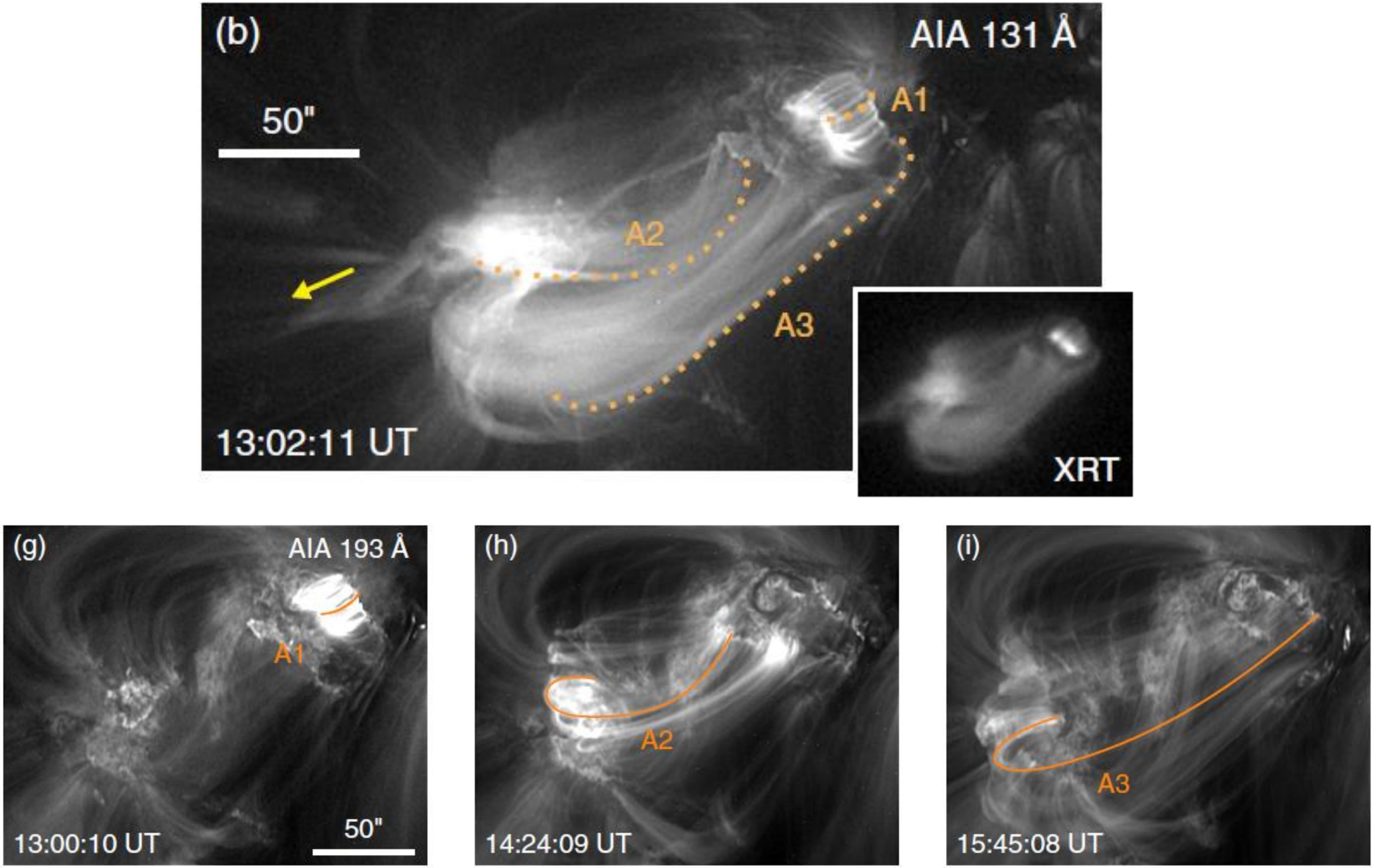

3D Null Point Reconnection

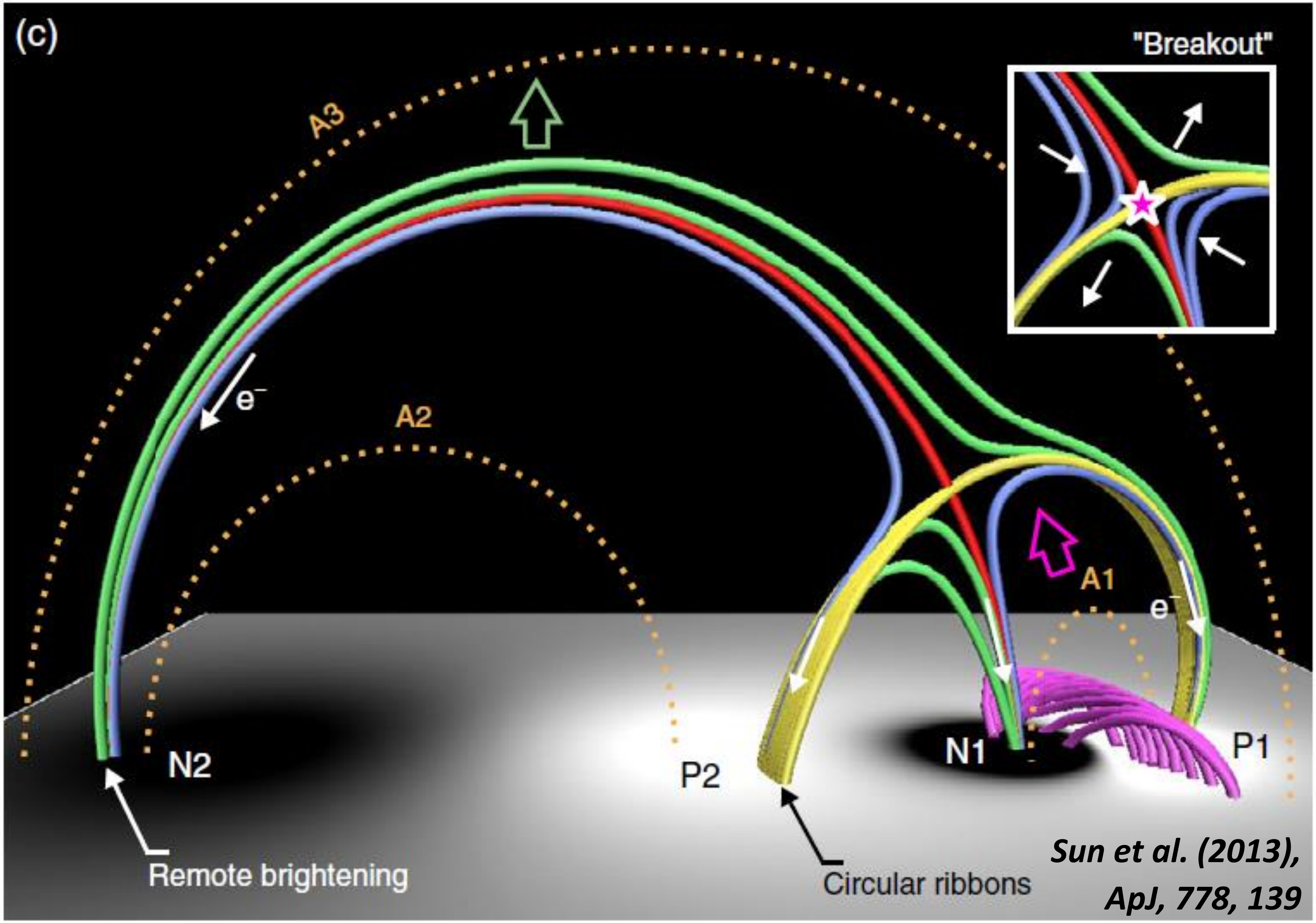

Sun et al. (2013), ApJ, 778, 139

EUV Late Phase of Solar Flares

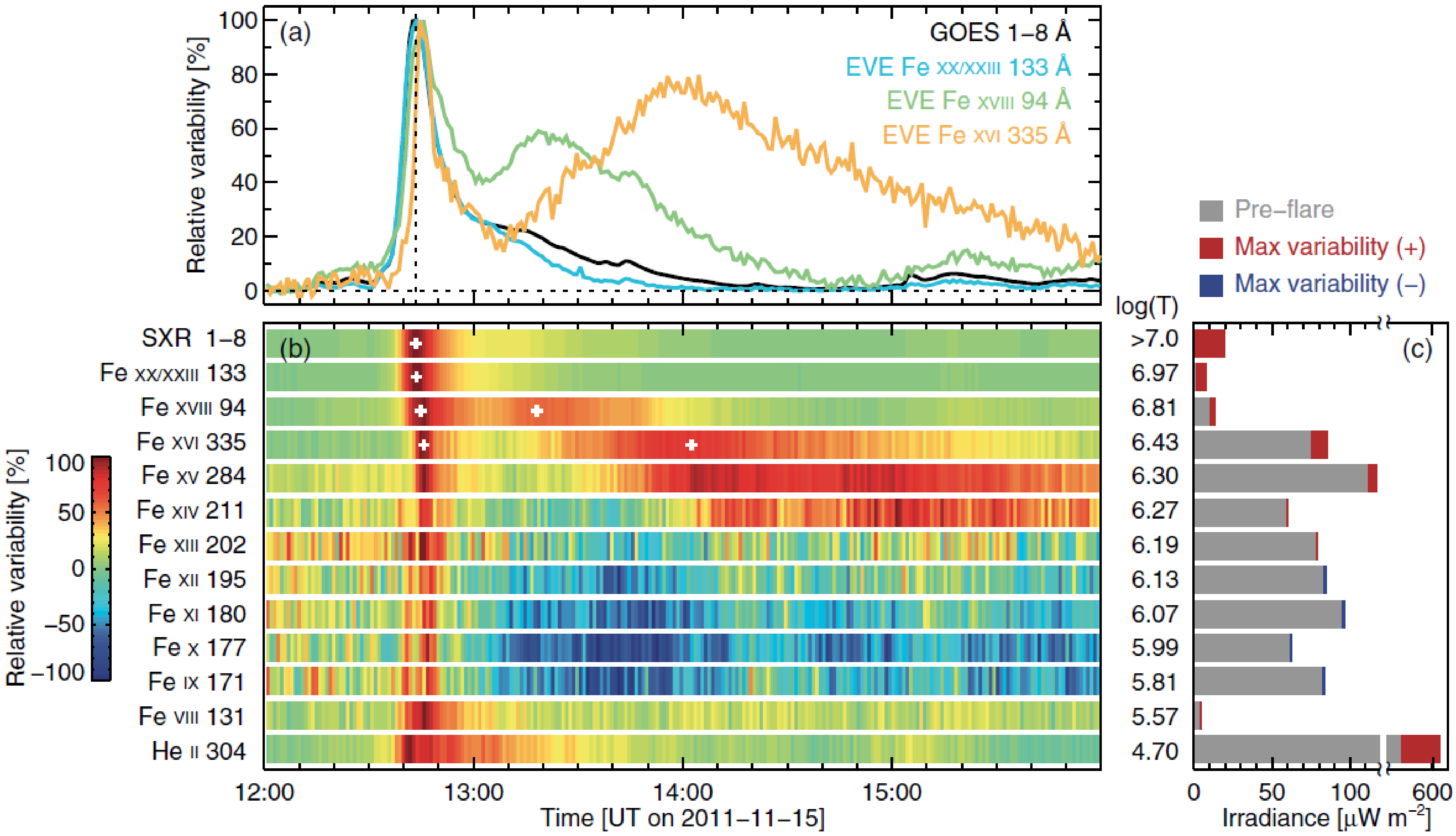

EUV Late Phase of Solar Flares

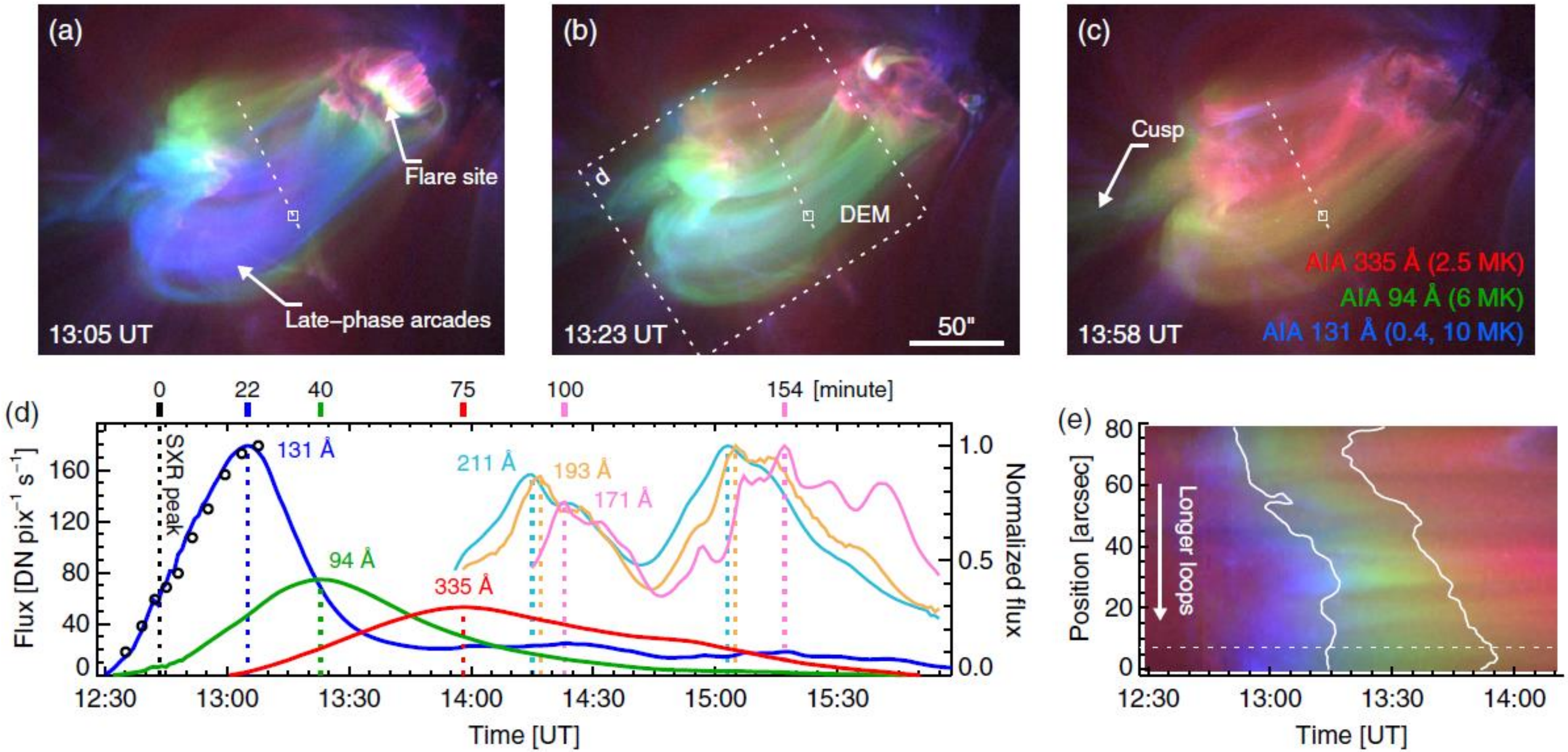

- Three different loop systems evolve on different timescales
- For A3, cooling is the longest

Cargill (2014), ApJ, 784, 49: $\tau_{\rm cool} = \left(\frac{2-\alpha}{1-\alpha}\right) 3k \left(\frac{1}{\kappa_0^{4-2\alpha}\chi^7}\frac{L^{8-4\alpha}}{(n_0 T_0)^{3+2\alpha}}\right)^{1/(11-2\alpha)}$

Cooling of Flare Loops

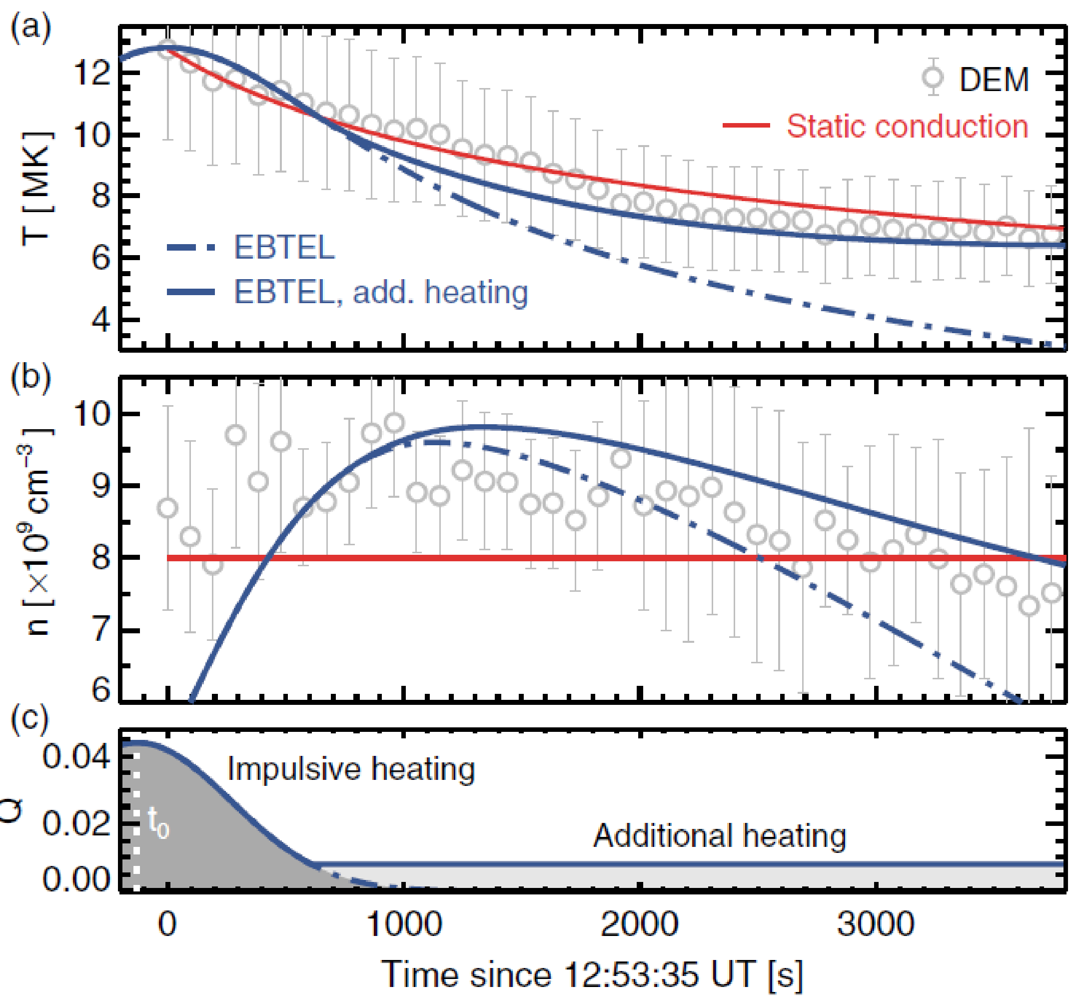

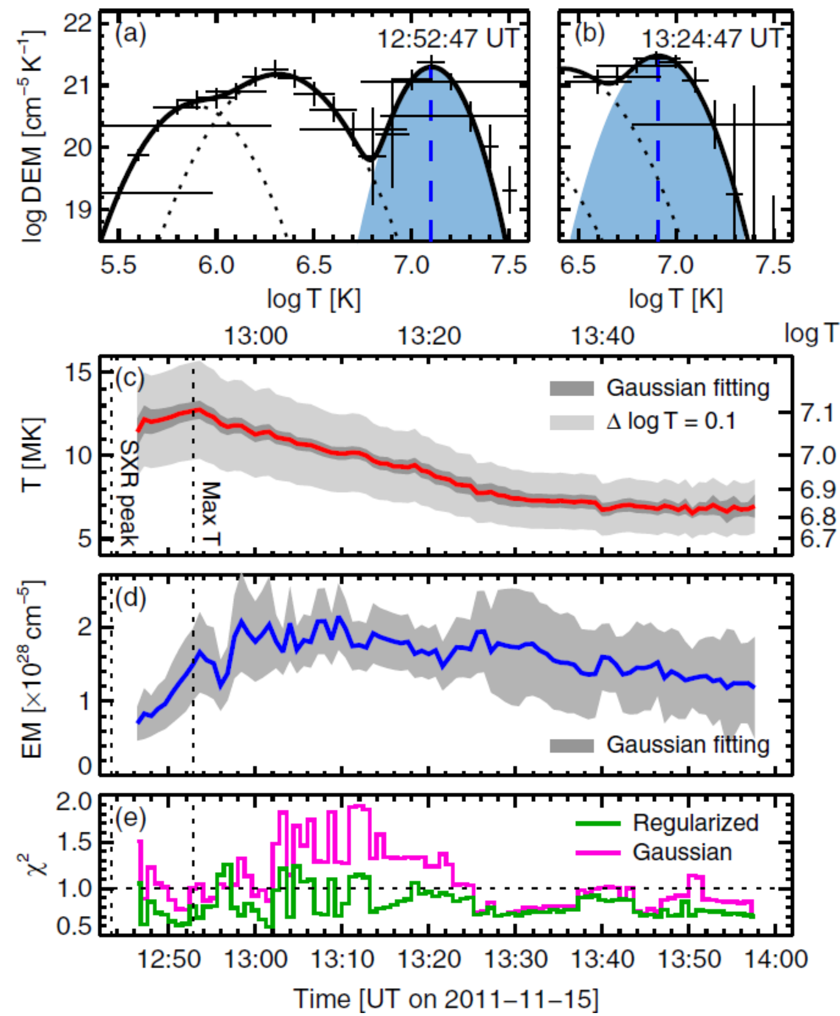

- **Conductive cooling times dependent on loop length *L***
- **Additional heating during gradual phase required to explain the observed lightcurves: Ongoing reconnection**

IV. 3D Magnetic Topology

QSLs: Geometrical structures with high gradients of connectivity

1. **Suppose we project one magnetic polarity to the other:** $\underset{+-}{\Pi} : \vec{r}_+ \rightarrow \vec{r}_-,$ $\underset{-+}{\Pi} : \vec{r}_- \rightarrow \vec{r}_+,$

2. **Jacobi matrices:**

$$\underset{+-}{\mathcal{D}} = \begin{pmatrix} \dfrac{\partial X_-}{\partial x_+} & \dfrac{\partial X_-}{\partial y_+} \\ \dfrac{\partial Y_-}{\partial x_+} & \dfrac{\partial Y_-}{\partial y_+} \end{pmatrix}, \qquad \underset{-+}{\mathcal{D}} = \begin{pmatrix} \dfrac{\partial X_+}{\partial x_-} & \dfrac{\partial X_+}{\partial y_-} \\ \dfrac{\partial Y_+}{\partial x_-} & \dfrac{\partial Y_+}{\partial y_-} \end{pmatrix}.$$

3. **We can then define following quantities:**

$$N_\pm = \sqrt{\left(\frac{\partial X_\pm}{\partial x_\mp}\right)^2 + \left(\frac{\partial X_\pm}{\partial y_\mp}\right)^2 + \left(\frac{\partial Y_\pm}{\partial x_\mp}\right)^2 + \left(\frac{\partial Y_\pm}{\partial y_\mp}\right)^2},$$

$$Q = \frac{N_+^2}{|\det(D_+)|} = \frac{N_-^2}{|\det(D_-)|},$$

$$K = \ln|\det(D_+)| = -\ln|\det(D_-)|.$$

Q and the Quasi-Separatrix Layers

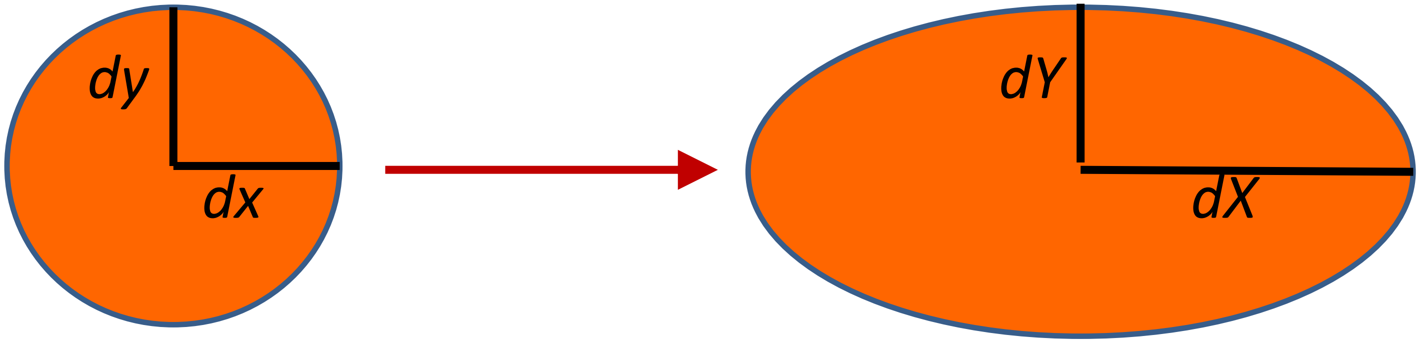

- **By definition:** $$Q = \frac{\sqrt{\left(\frac{dX}{dx}\right)^2 + \left(\frac{dY}{dy}\right)^2}}{\left(\frac{dX}{dx}\right)\left(\frac{dY}{dy}\right)} = \frac{dX^2+dY^2}{dXdY},$$

$$K = \ln \left\| \frac{dXdY}{dxdy} \right\| = \ln \left\| \frac{\pi dXdY}{\pi dx^2} \right\|$$

- **Quasi-separatrix layers are places constituted by magnetic field-lines having very high *Q >> 2.***

Démoulin et al. (1997), Astron. Astrophys, 325, 305

Titov, Hornig & Démoulin (2002), J. Geophys. Res. 107, 1164

QSLs and Flare Ribbons

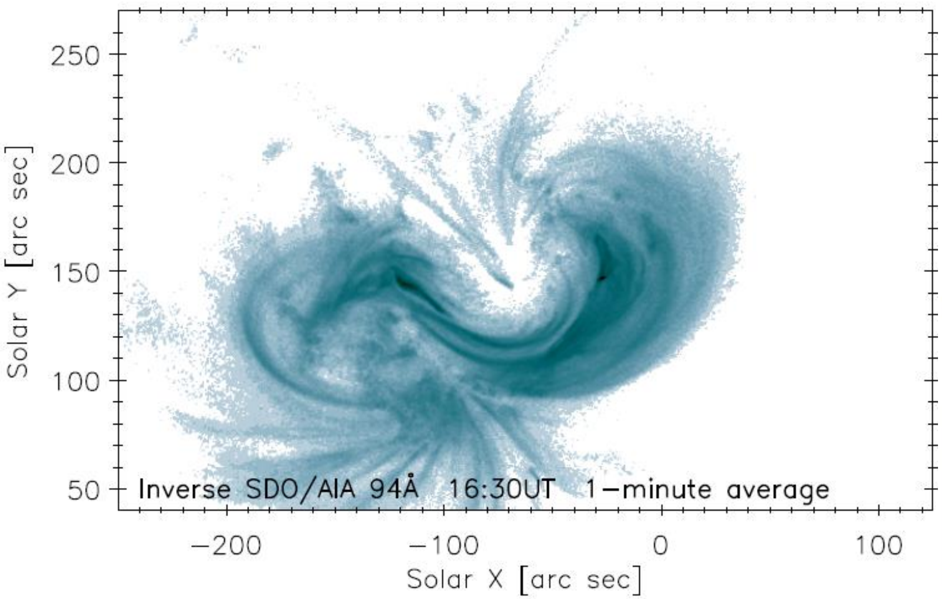

Zhao et al. (2016), ApJ, 823, 62

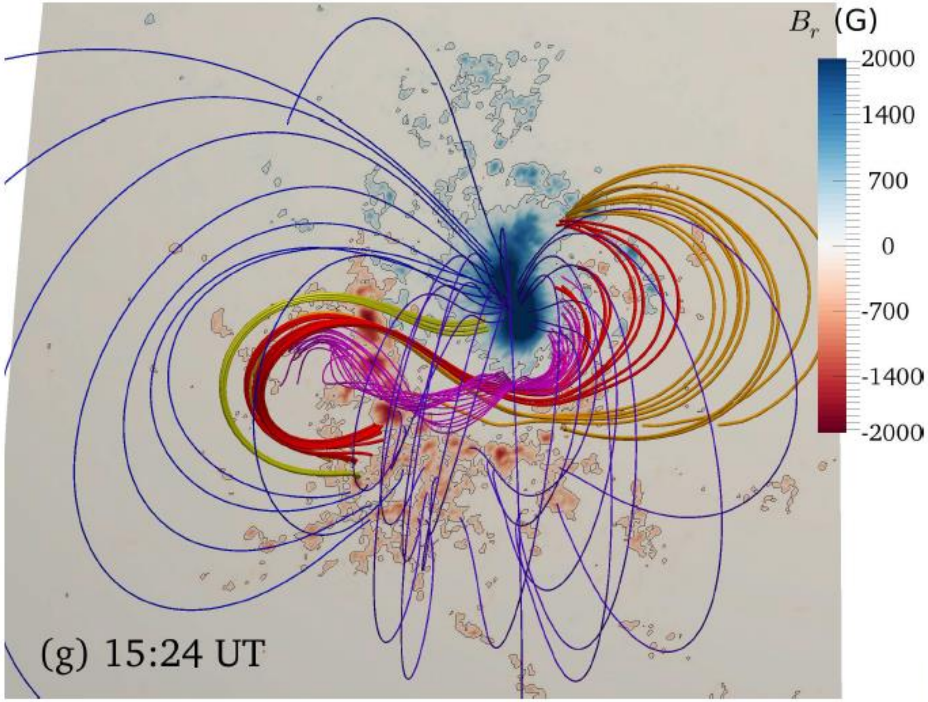

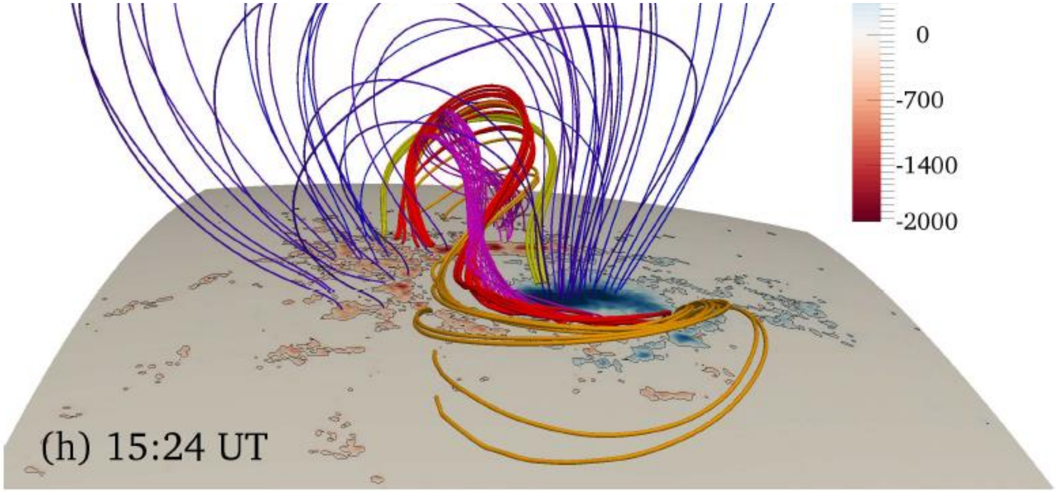

- NLFFF extrapolation of the pre-flare state at 2014 September 10
- Flux rope and sigmoid
- Overlying field
- Complex topological structure

QSLs and Flare Ribbons

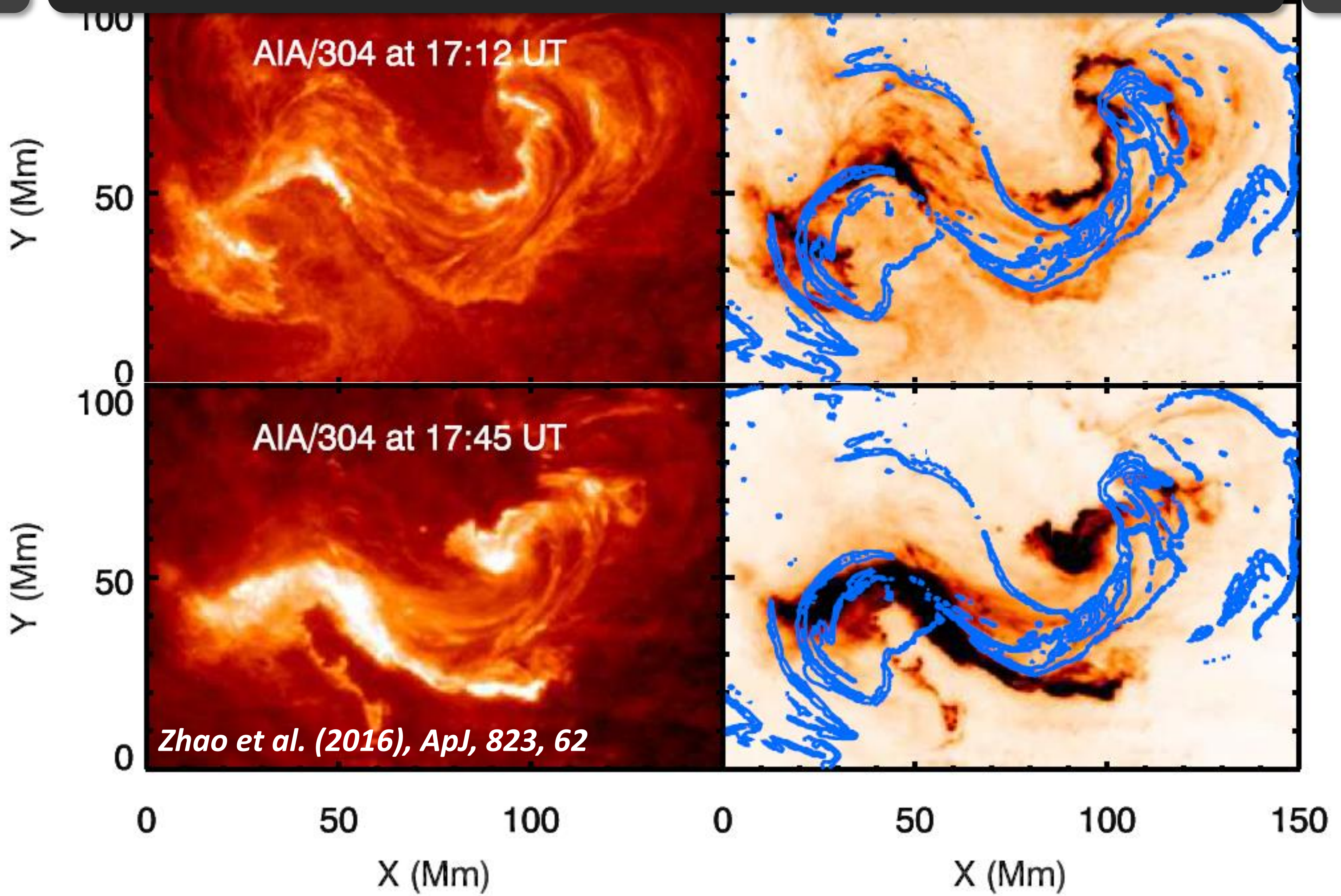

QSLs: Flux Rope and Sigmoid

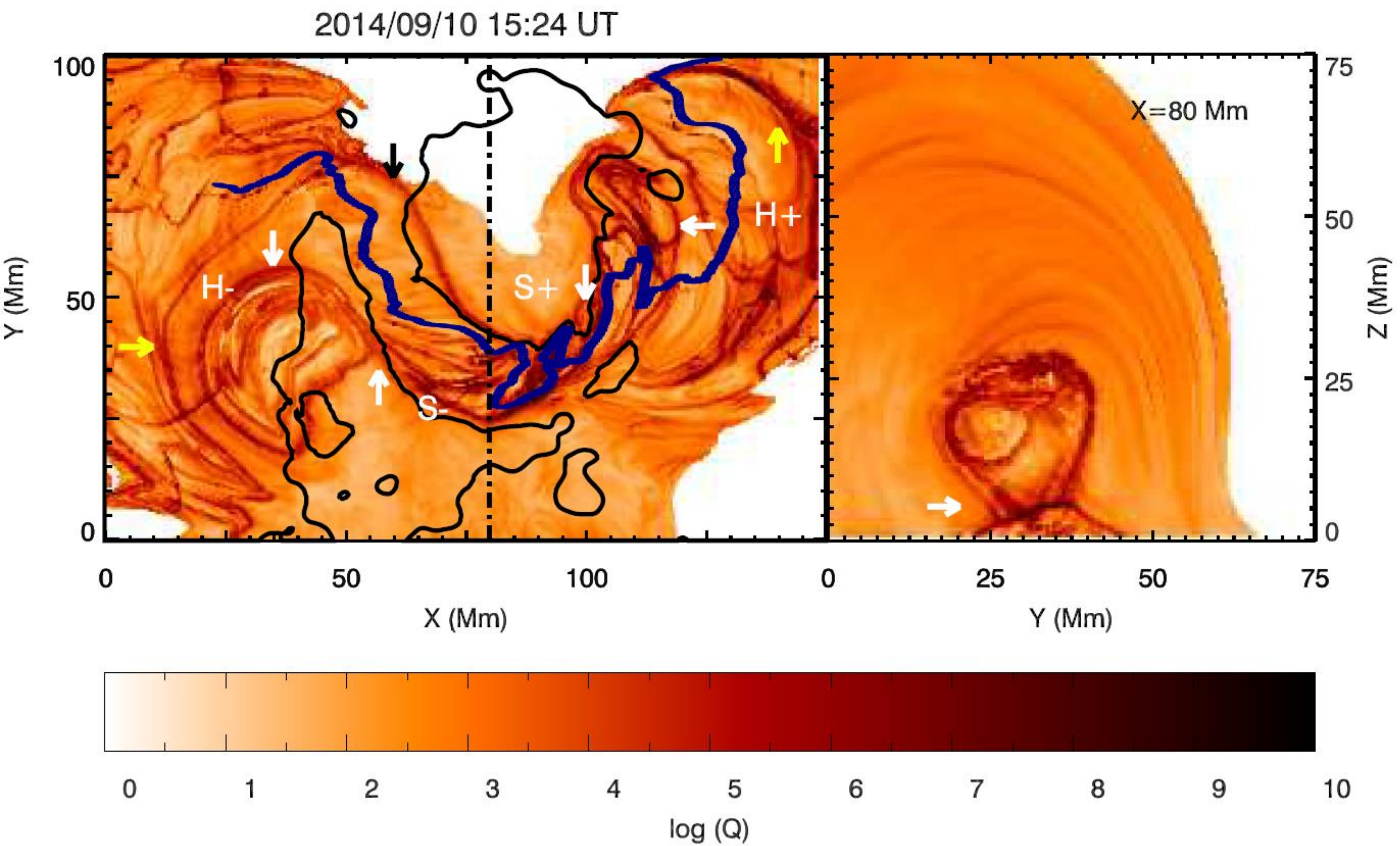

Standard Solar Flare Model in 3D

- MHD model with zero-temperature
- **Flux imbalance and hooked QSLs**

Aulanier et al. (2012), A&A, 534, A110; Janvier et al. (2013), A&A, 555, A77

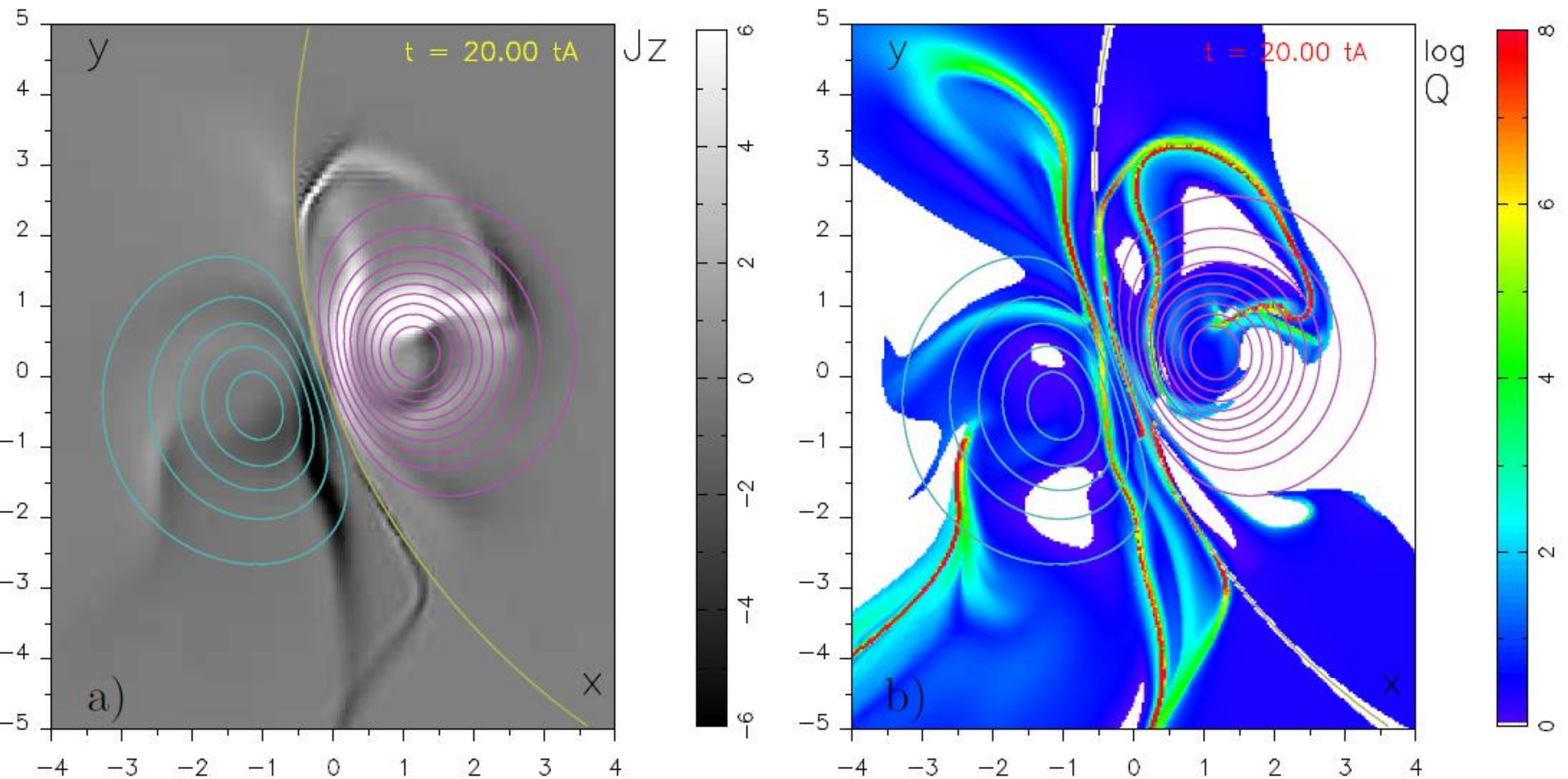

Standard Solar Flare Model in 3D

Aulanier et al. (2012), A&A 534, A110

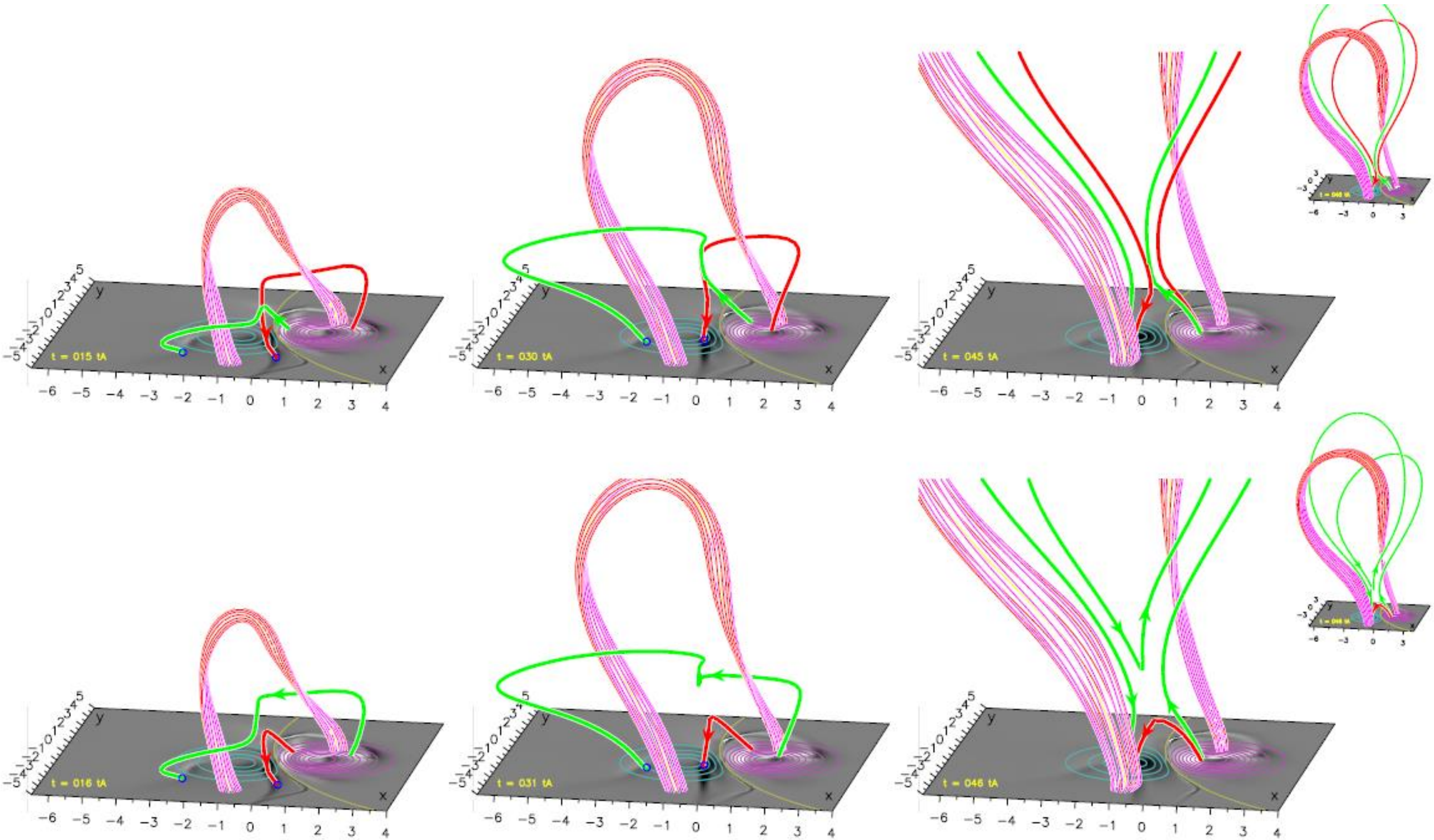

How to Get a Flux Rope

van Ballegooijen & Martens (1989), ApJ, 343, 971

- **Shearing motions:** (a) –> (b)
- **Flux cancellation at the polarity inversion line (PIL)** (c) –> (d)
- **Reconnection at PIL producing a long field line**

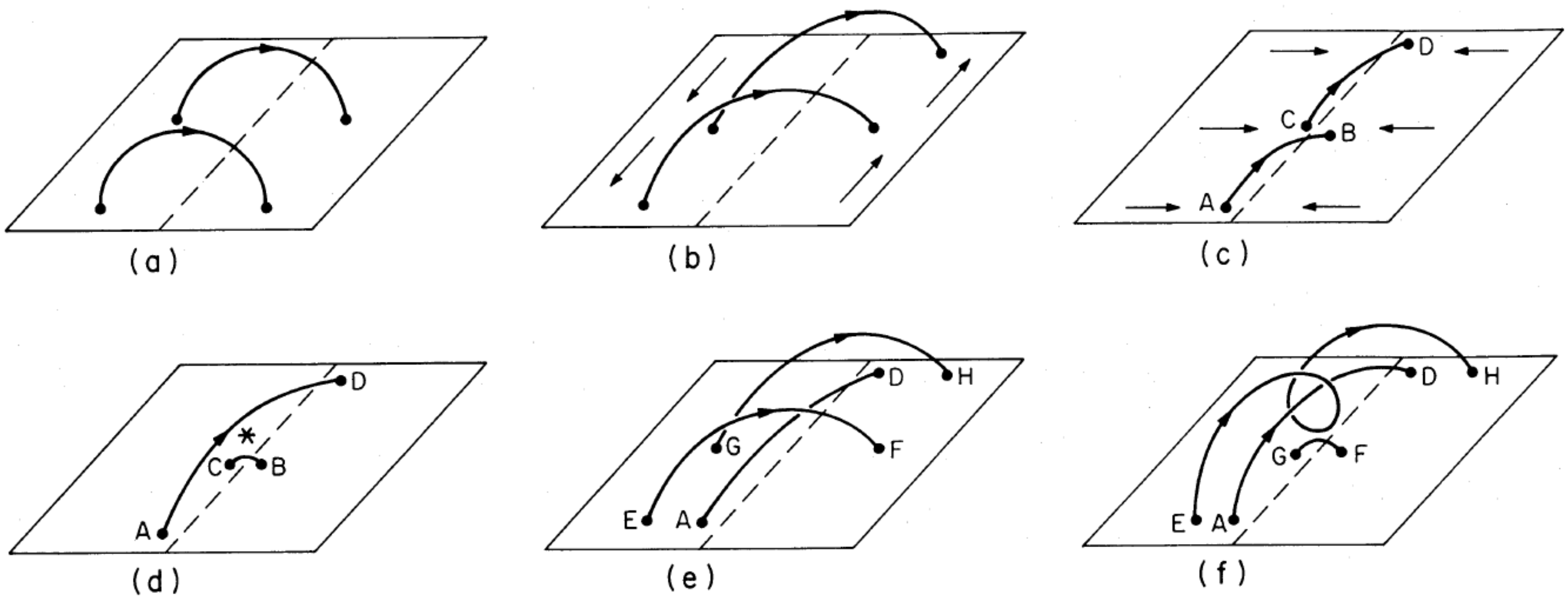

FIG. 1.—Flux cancellation in a sheared magnetic field. The rectangle represents the solar photosphere, and the dashed line is the neutral line separating two regions of opposite magnetic polarity. (*a*) Initial potential field; (*b*) sheared magnetic field produced by flows along the neutral line; (*c*) magnetic shear is increased further due to flows toward the neutral line; (*d*) reconnection produces long loop AD and a shorter loop CB which subsequently submerges; (*e*) overlying loops EF and GH are pushed to the neutral line; (*f*) reconnection produces the helical loop EH and a shorter loop GF which again submerges.

Movie courtesy of Francesco P. Zuccarello

Zuccarello et al. (2016), 821, 23

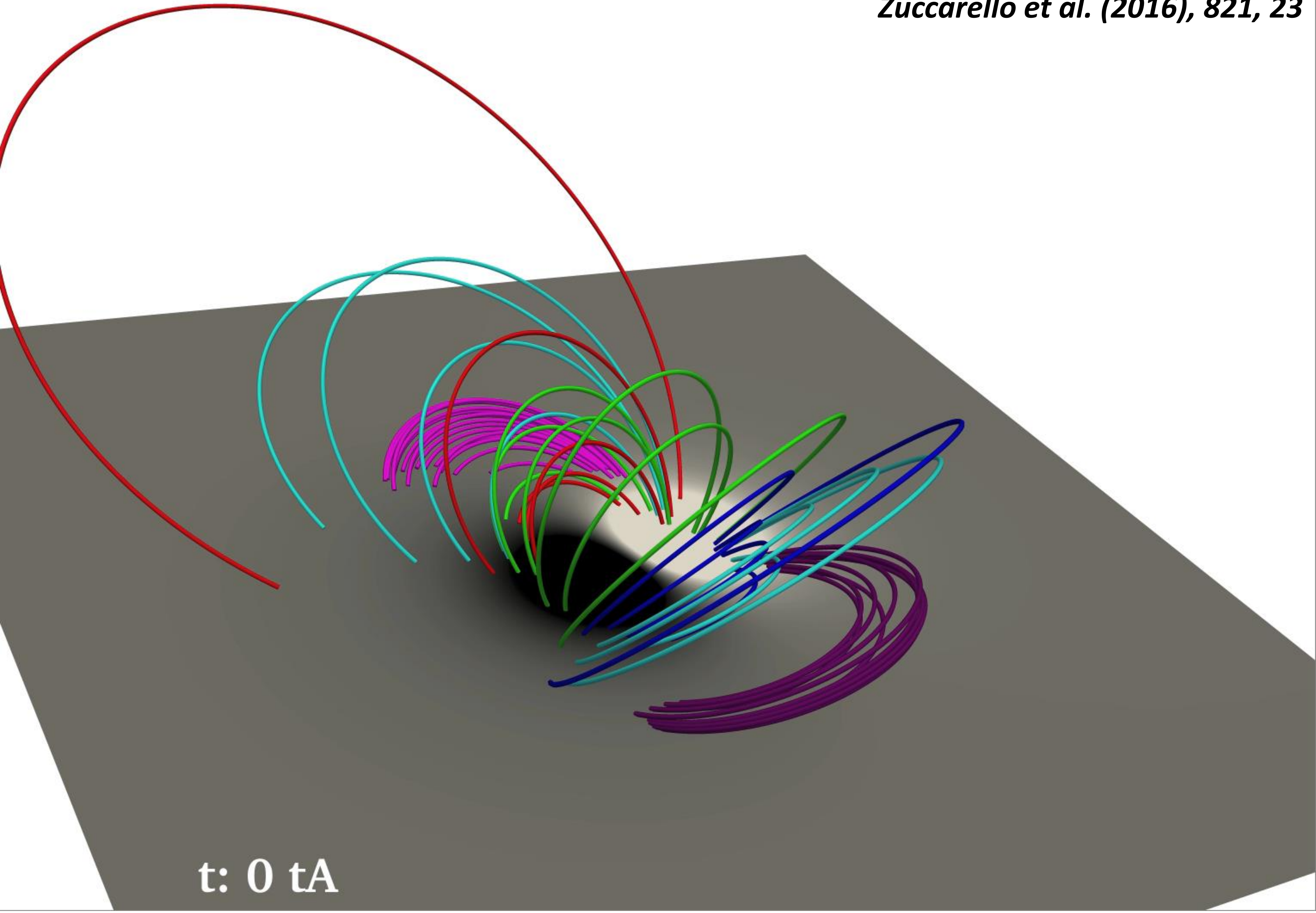

Q and Electric Current Density

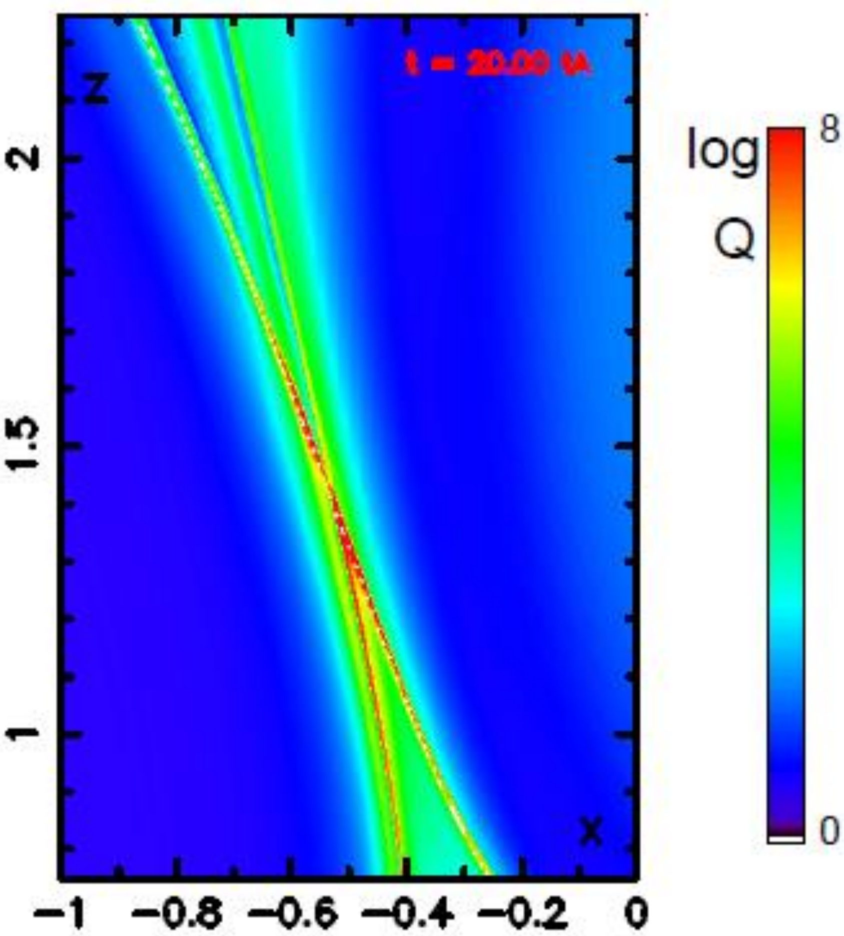

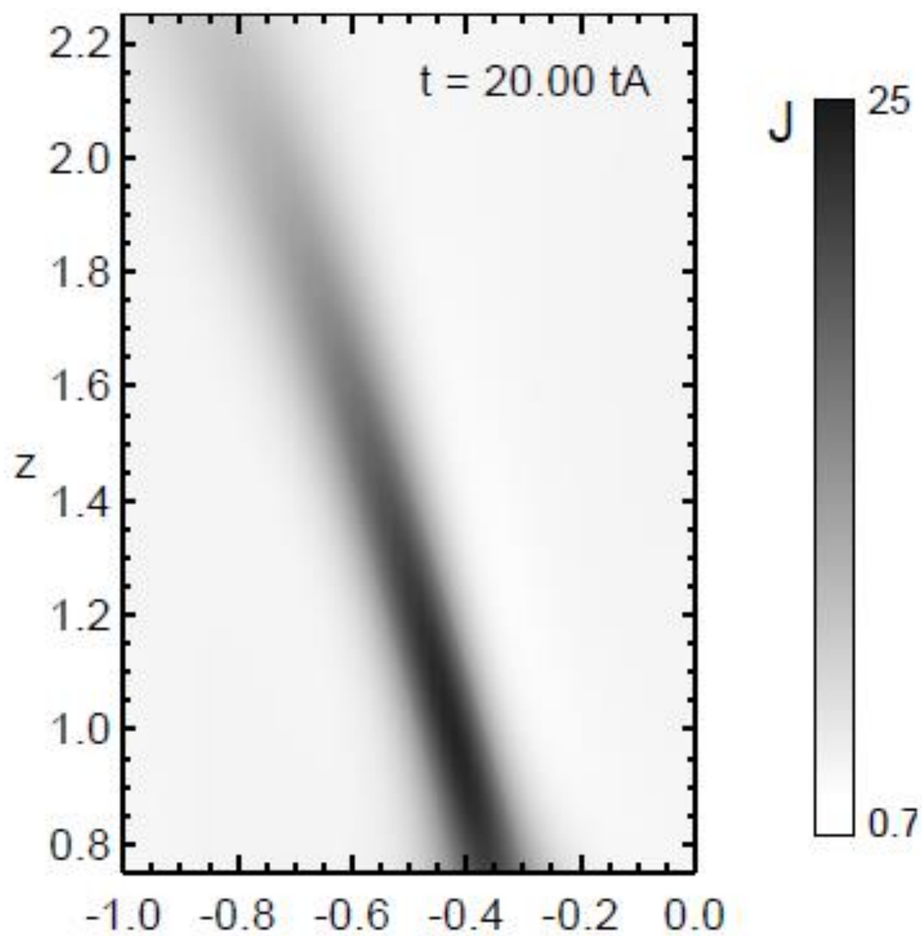

Slipping Reco. in the 3D Model

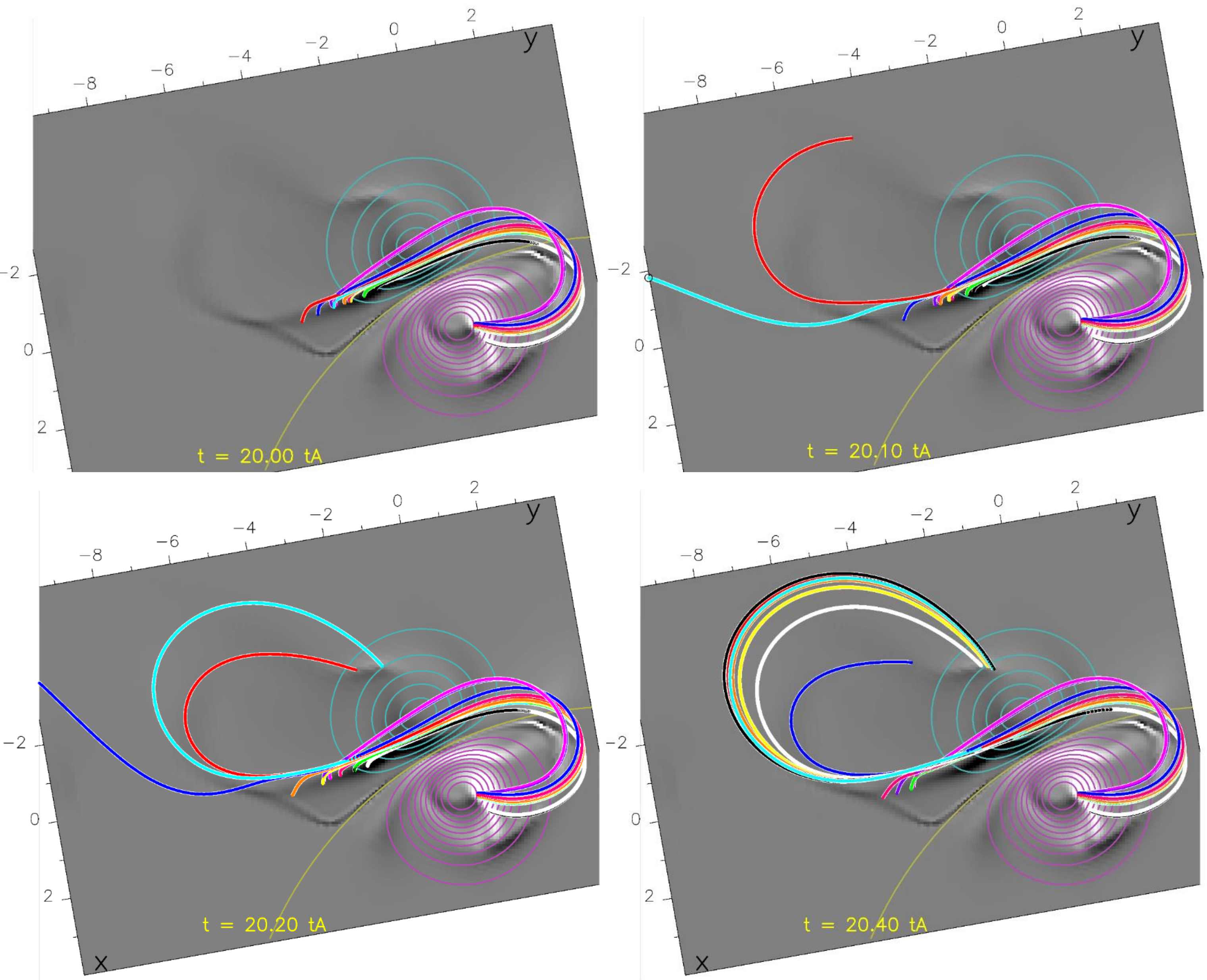

- Hooked QSL traces in the photosphere
- Grayscale: *el. current density j*
- Slipping reconnection in QSLs
- fixed footpoints
- Only one set of field lines is shown
- Images after ***Janvier et al. (2013), A&A, 555, A77***

Slipping Magnetic Reconnection

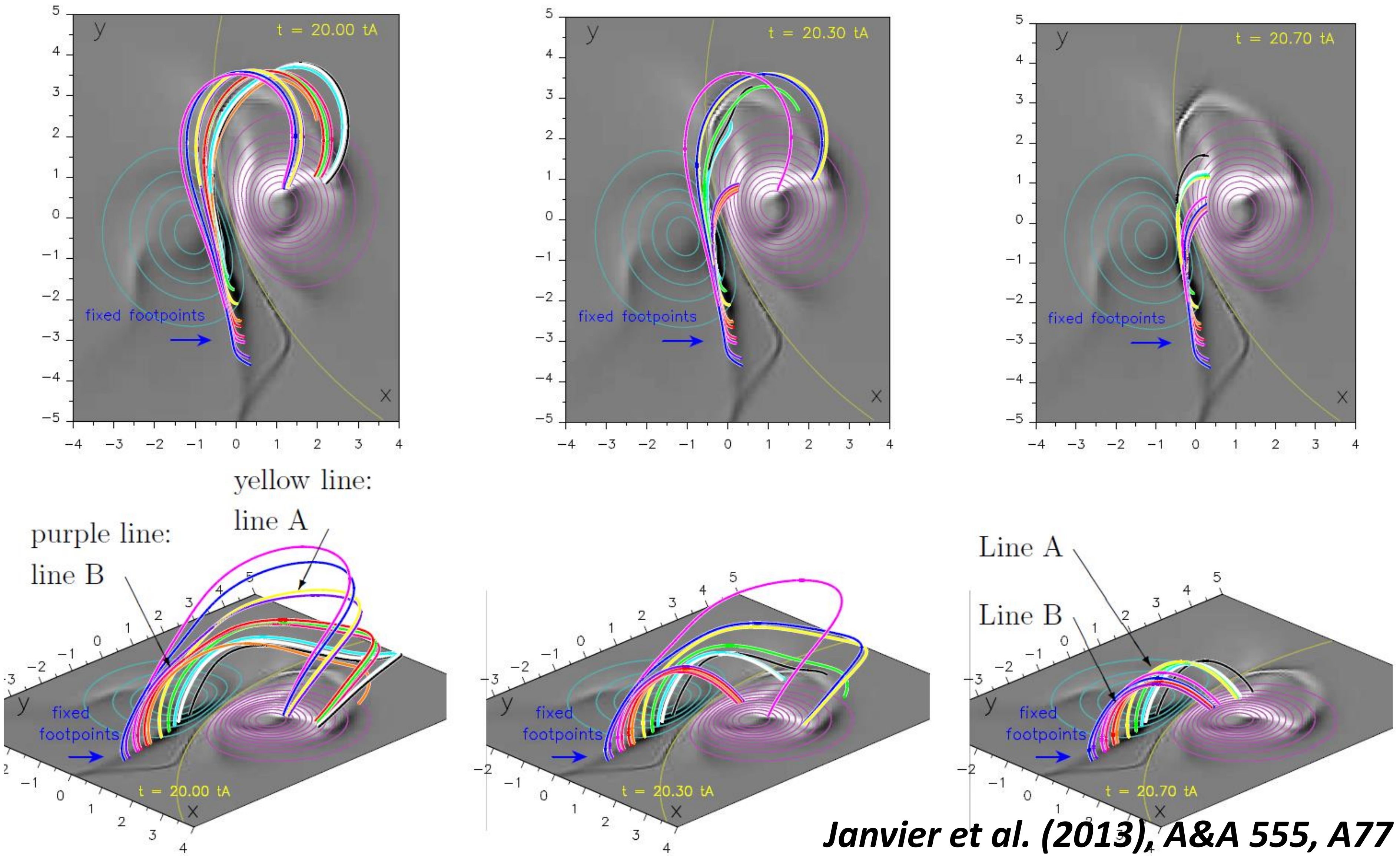

Janvier et al. (2013), A&A 555, A77

Slipping Magnetic Reconnection

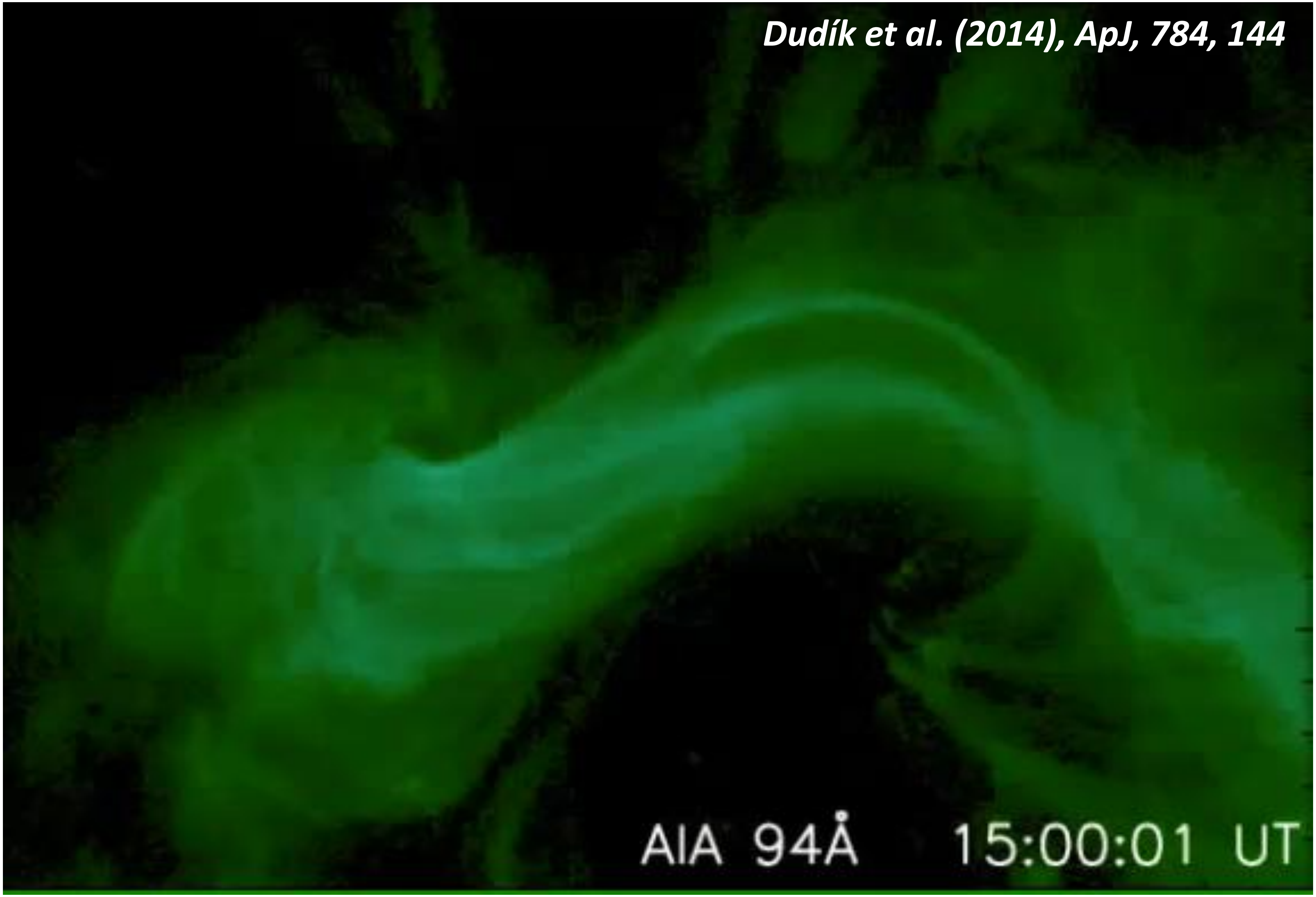

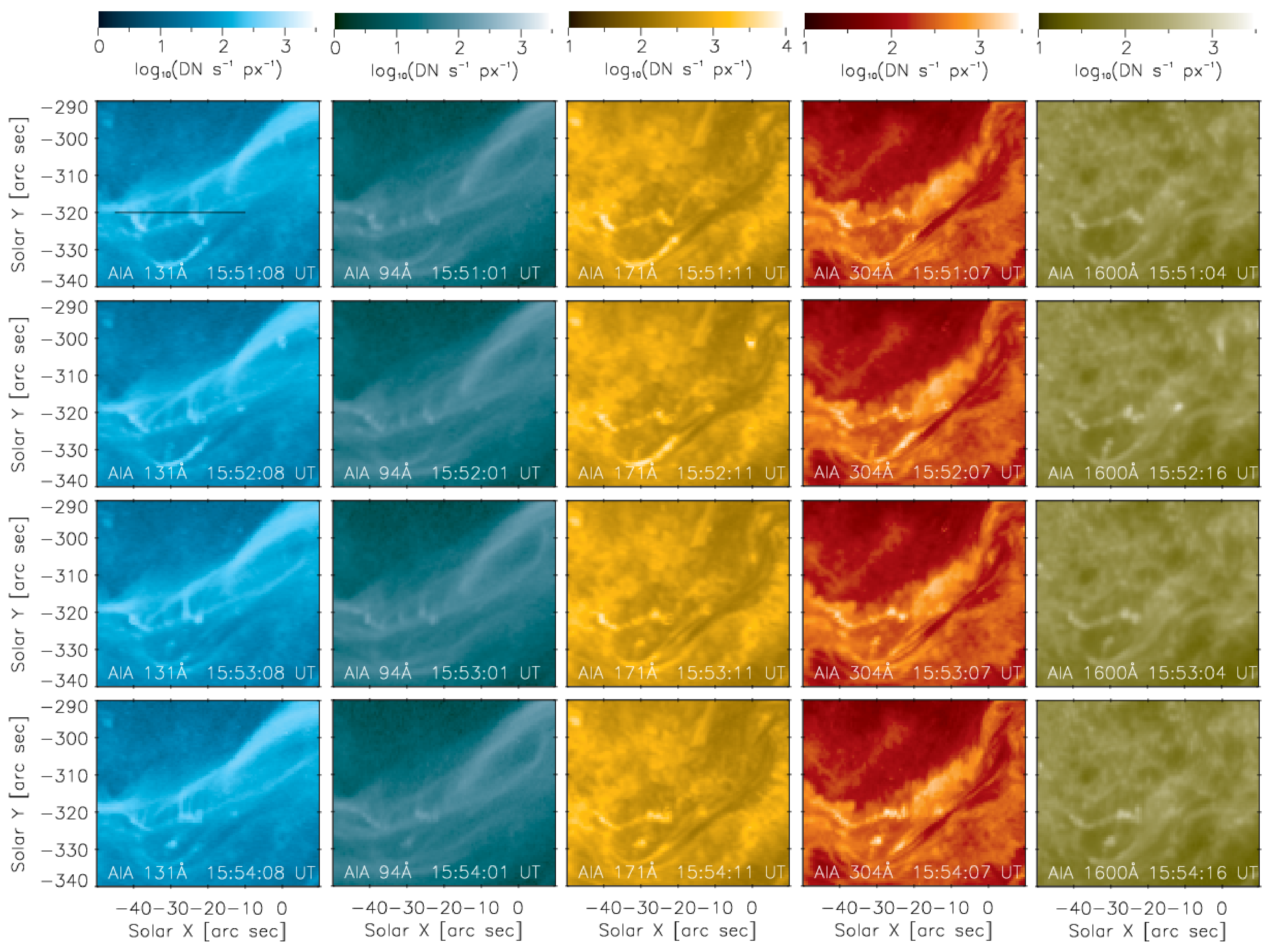

log₁₀(DN s⁻¹ px⁻¹)
Solar Y [arc sec]
Solar X [arc sec]
AIA 131Å 15:51:08 UT
AIA 94Å 15:51:01 UT
AIA 171Å 15:51:11 UT
AIA 304Å 15:51:07 UT
AIA 1600Å 15:51:04 UT
AIA 131Å 15:52:08 UT
AIA 94Å 15:52:01 UT
AIA 171Å 15:52:11 UT
AIA 304Å 15:52:07 UT
AIA 1600Å 15:52:16 UT
AIA 131Å 15:53:08 UT
AIA 94Å 15:53:01 UT
AIA 171Å 15:53:11 UT
AIA 304Å 15:53:07 UT
AIA 1600Å 15:53:04 UT
AIA 131Å 15:54:08 UT
AIA 94Å 15:54:01 UT
AIA 171Å 15:54:11 UT
AIA 304Å 15:54:07 UT
AIA 1600Å 15:54:16 UT

Slipping Loops

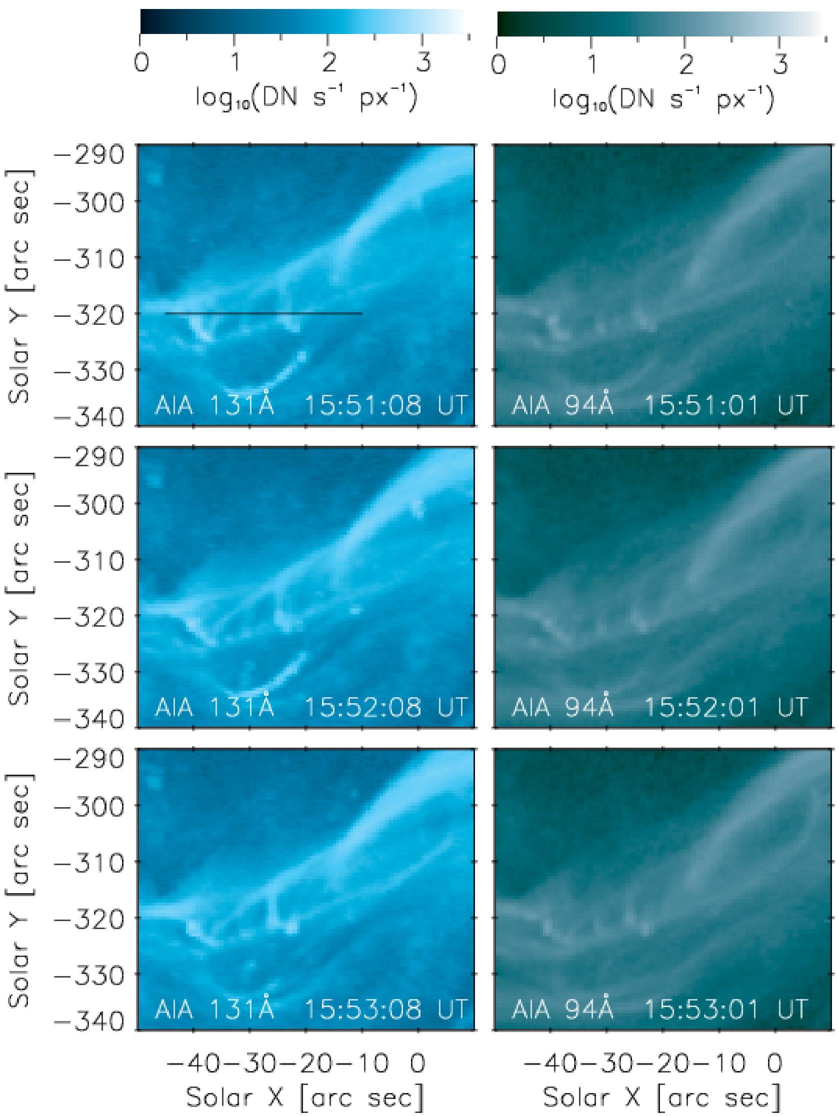

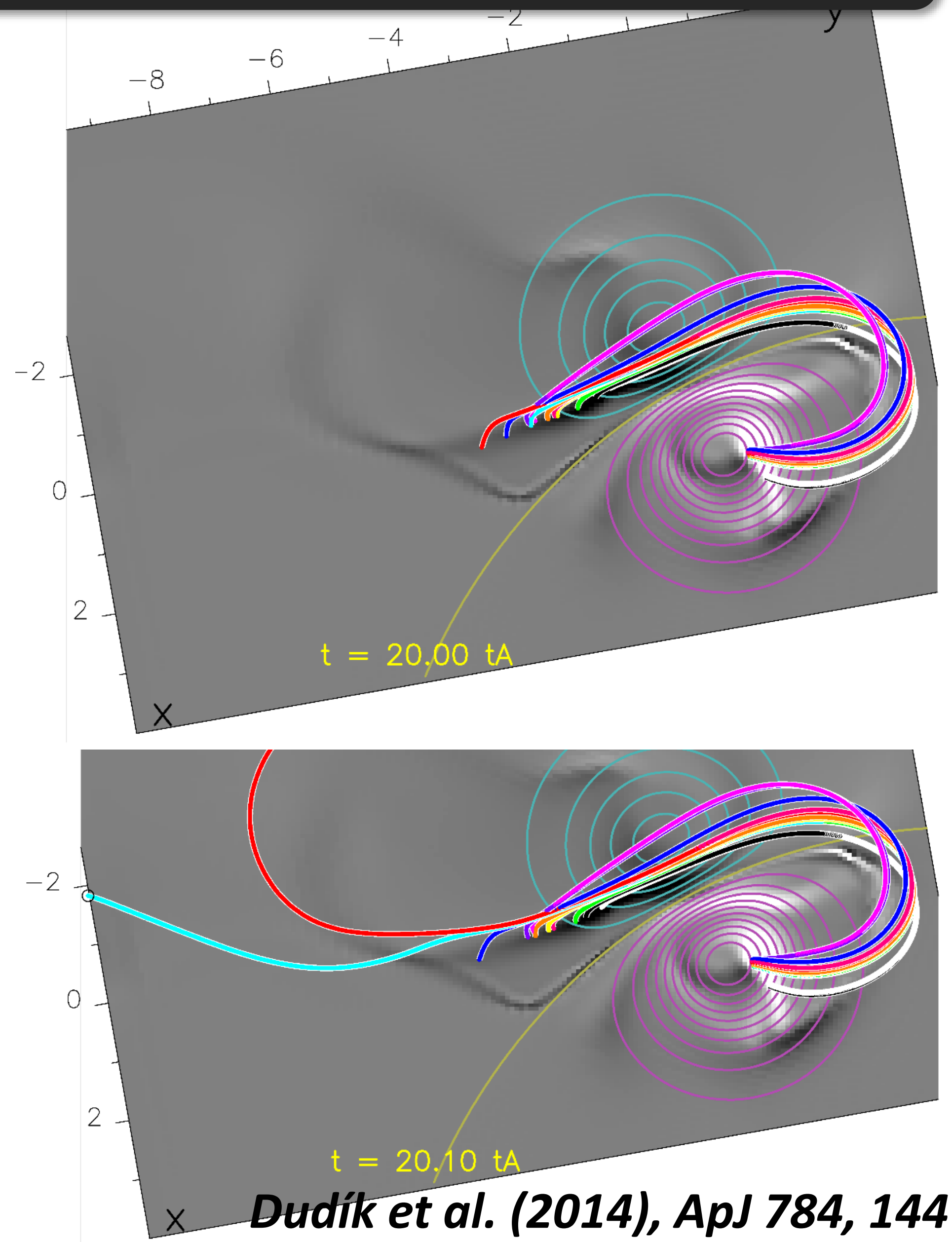

Dudík et al. (2014), ApJ 784, 144

Kinematics of Slipping Loops

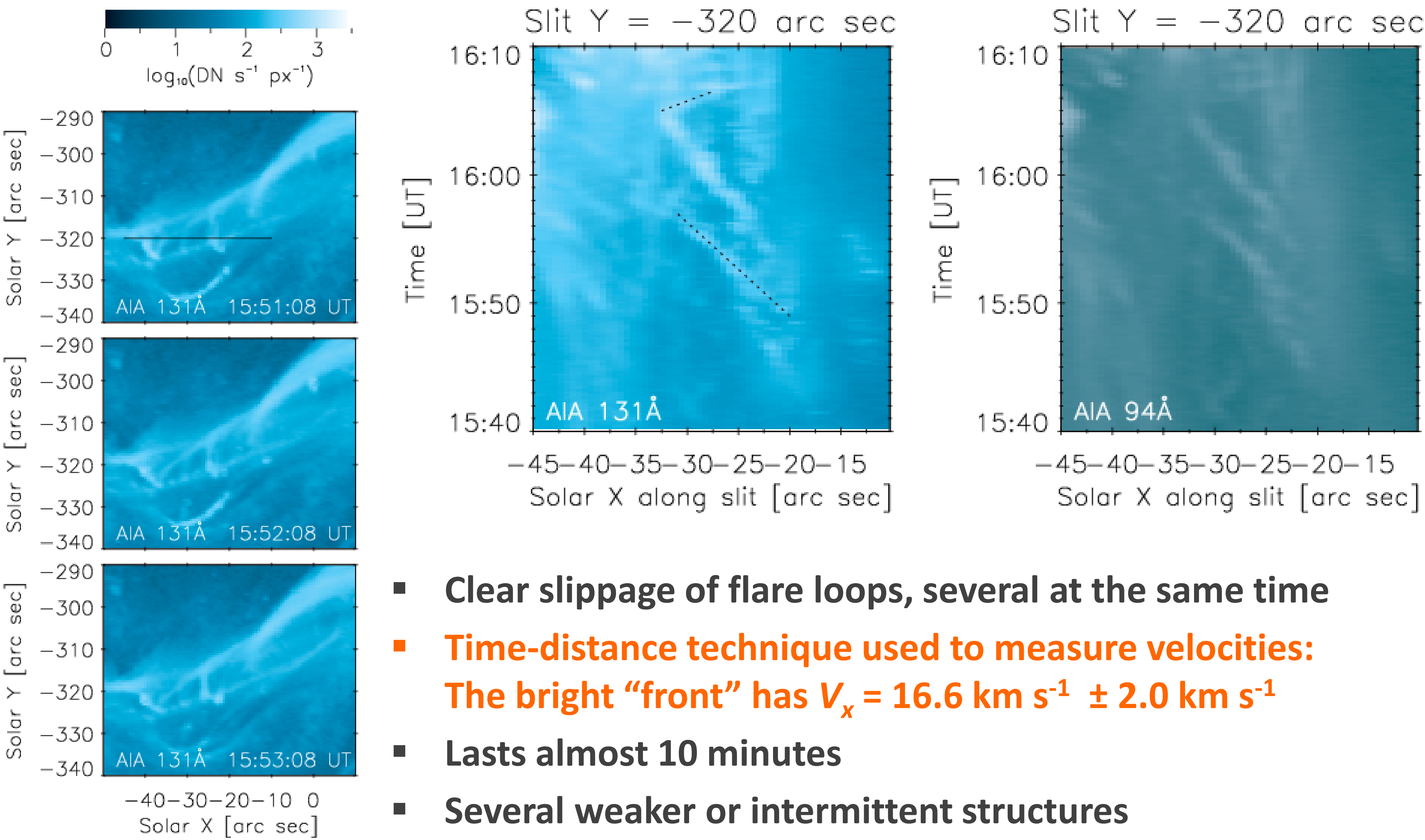

- **Clear slippage of flare loops, several at the same time**
- **Time-distance technique used to measure velocities: The bright "front" has V_x = 16.6 km s^{-1} ± 2.0 km s^{-1}**
- **Lasts almost 10 minutes**
- **Several weaker or intermittent structures slipping in the opposite direction**

Radio Signatures of Slipping?

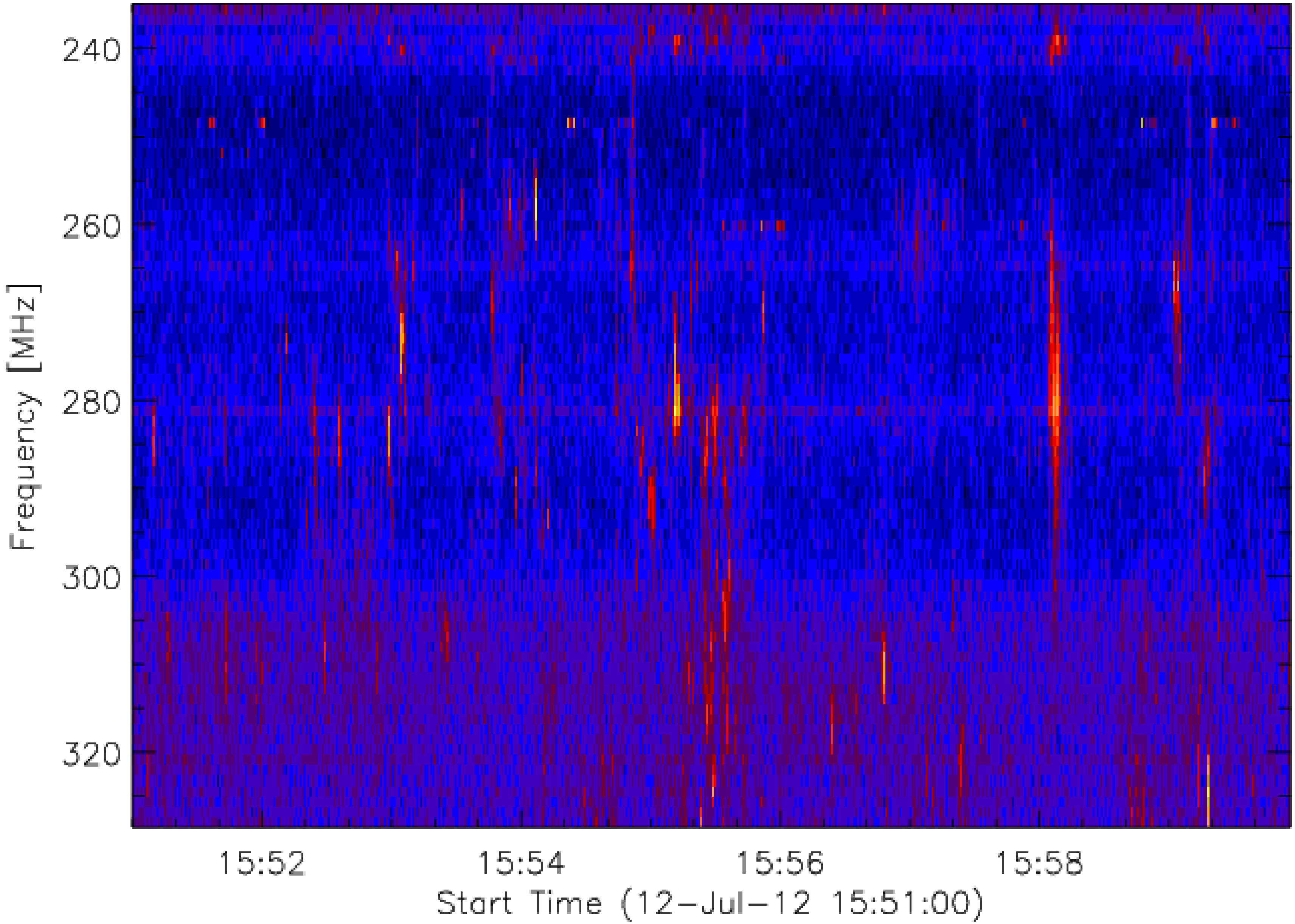

Eruption of the Flux Rope

- Flux rope core
- Slipping loops (set 1)
- Slipping loops (set 2)

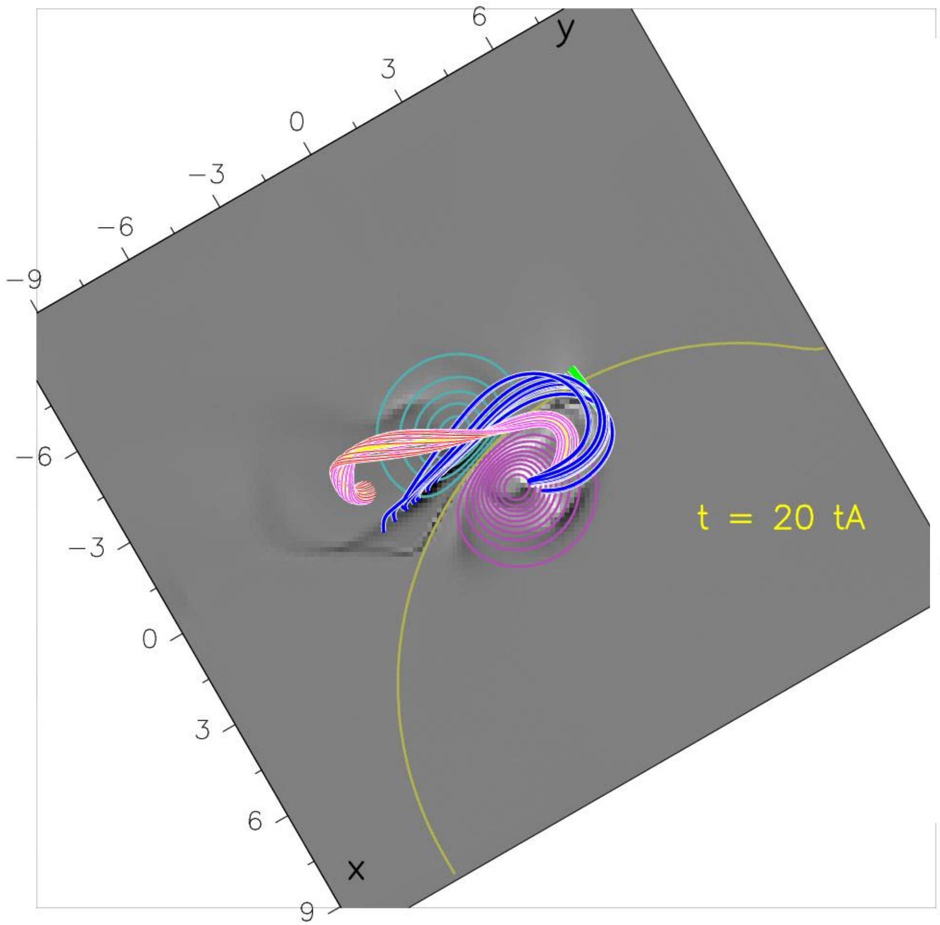

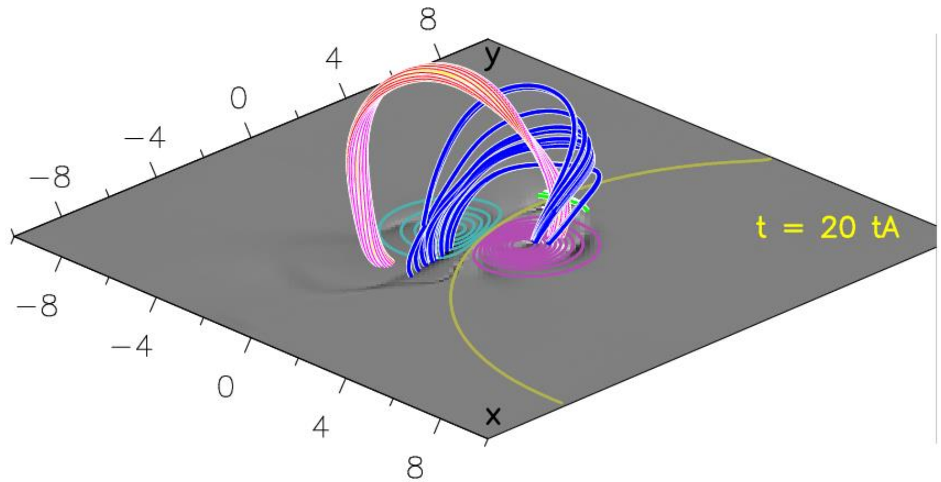

Eruption of the Flux Rope

- Flux rope core - unstable, rising
- Slipping loops (set 1) - @ end of the hook, part of the FR
- Slipping loops (set 2) - moving along QSL

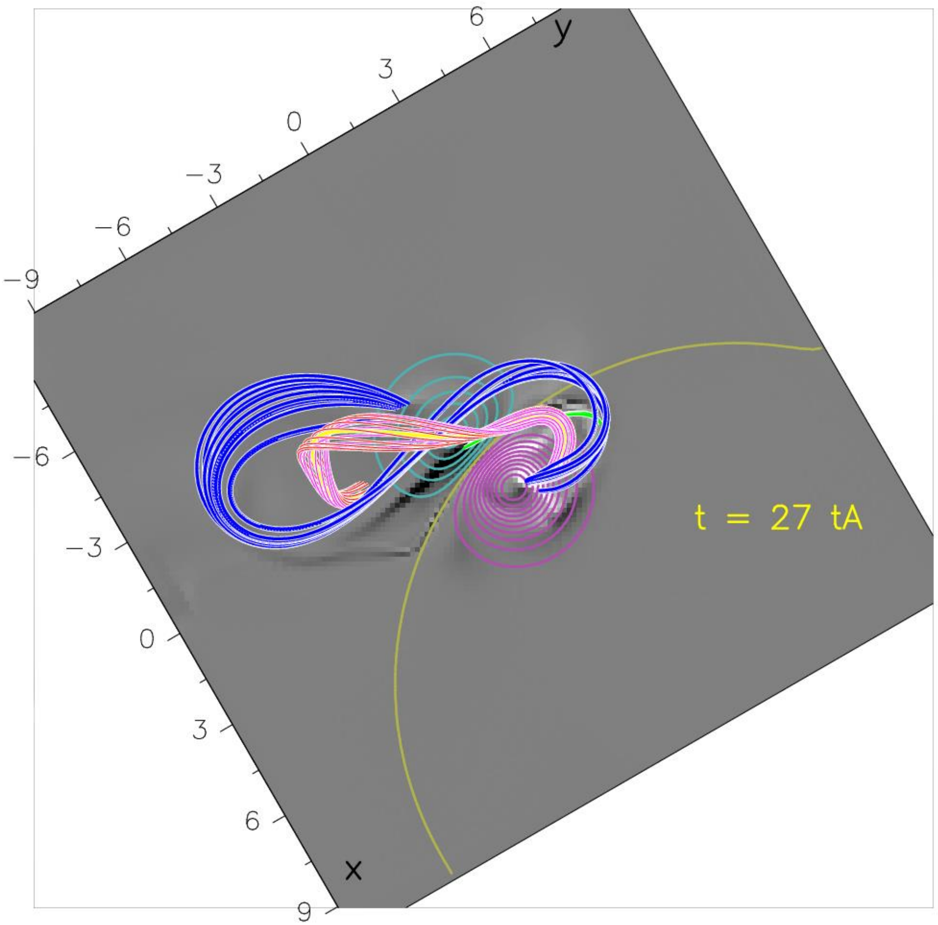

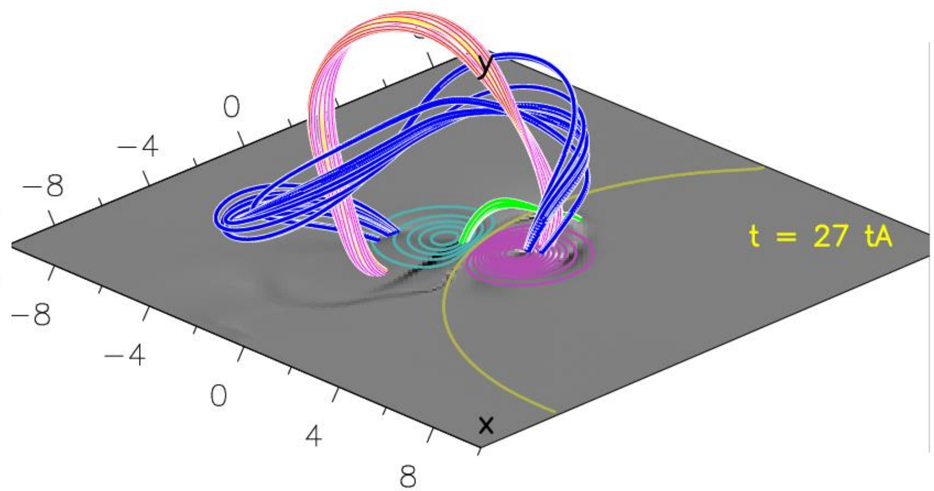

Eruption of the Flux Rope

- Flux rope core - unstable, rising, expanding
- Slipping loops (set 1) - part of the flux rope (envelope)
- Slipping loops (set 2) - @ end of the hook

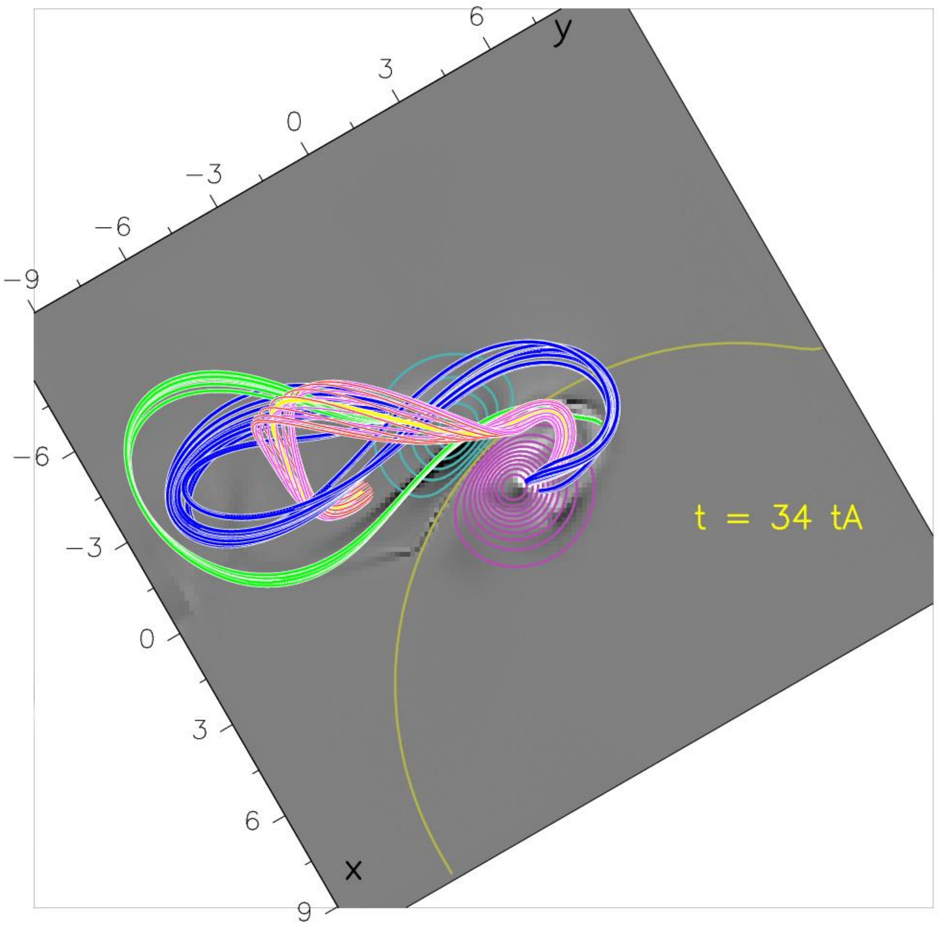

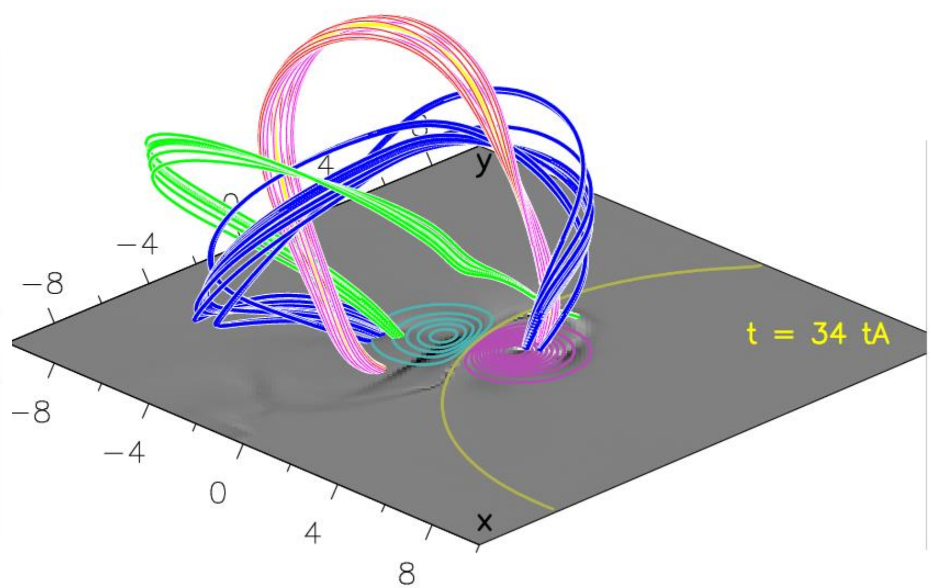

Eruption of the Flux Rope

- Flux rope core - unstable, rising, expanding
- Slipping loops (set 1) - part of the flux rope
- Slipping loops (set 2) - part of the flux rope (envelope)

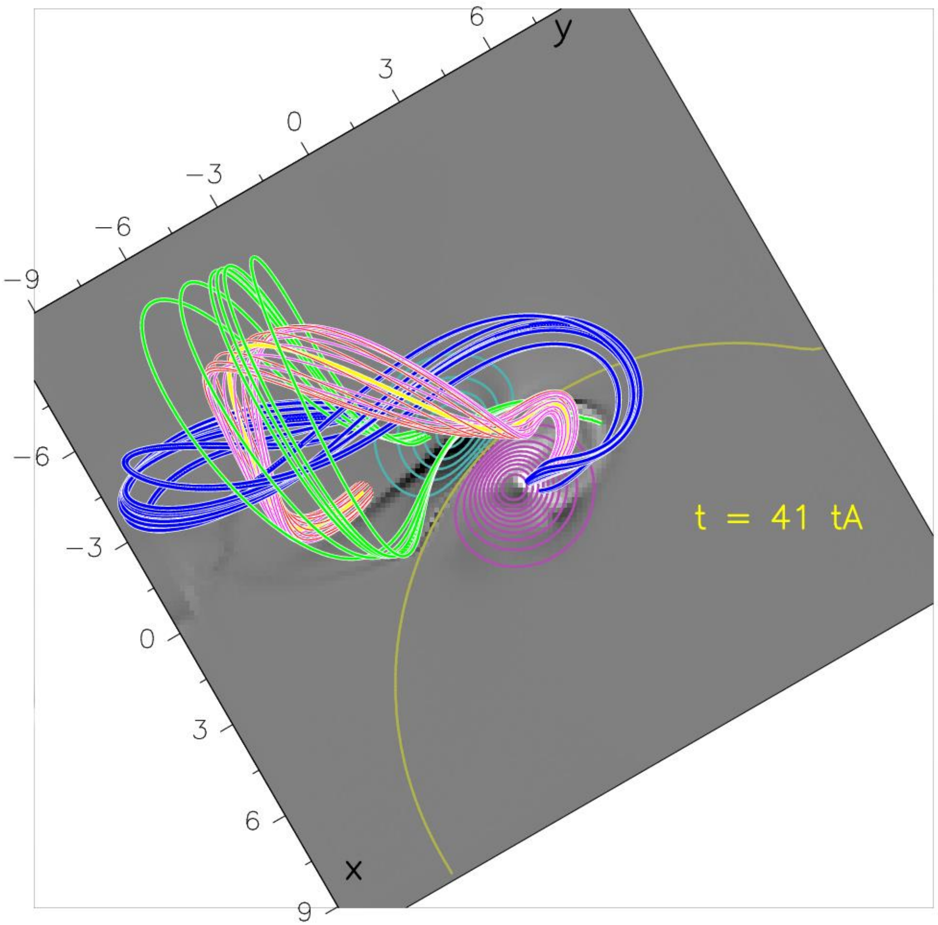

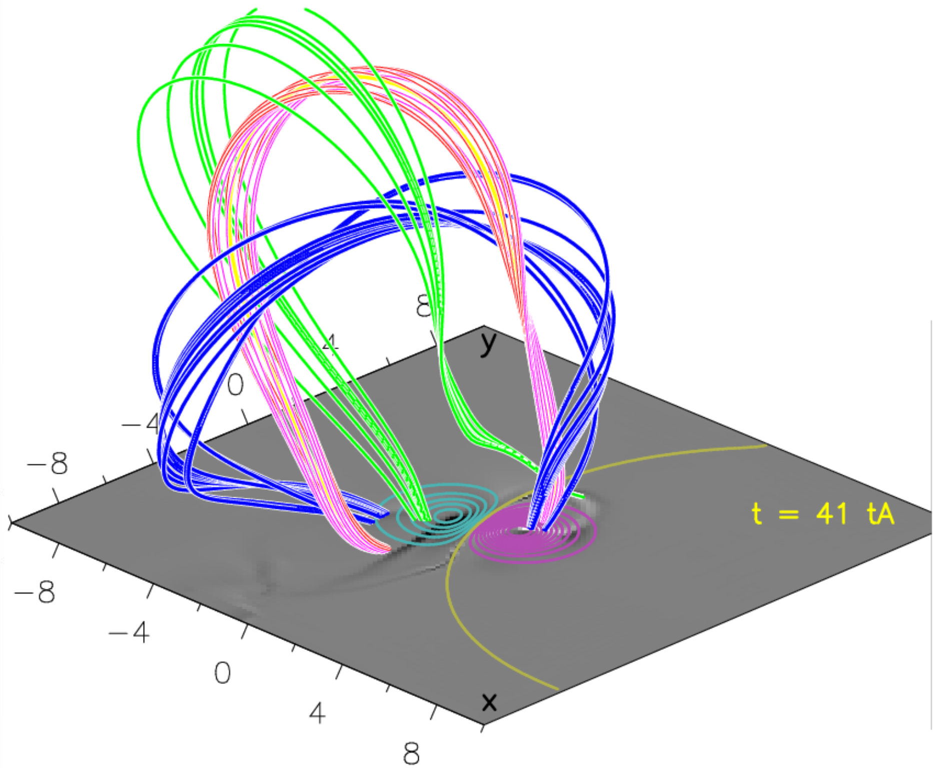

Flux Rope Envelope

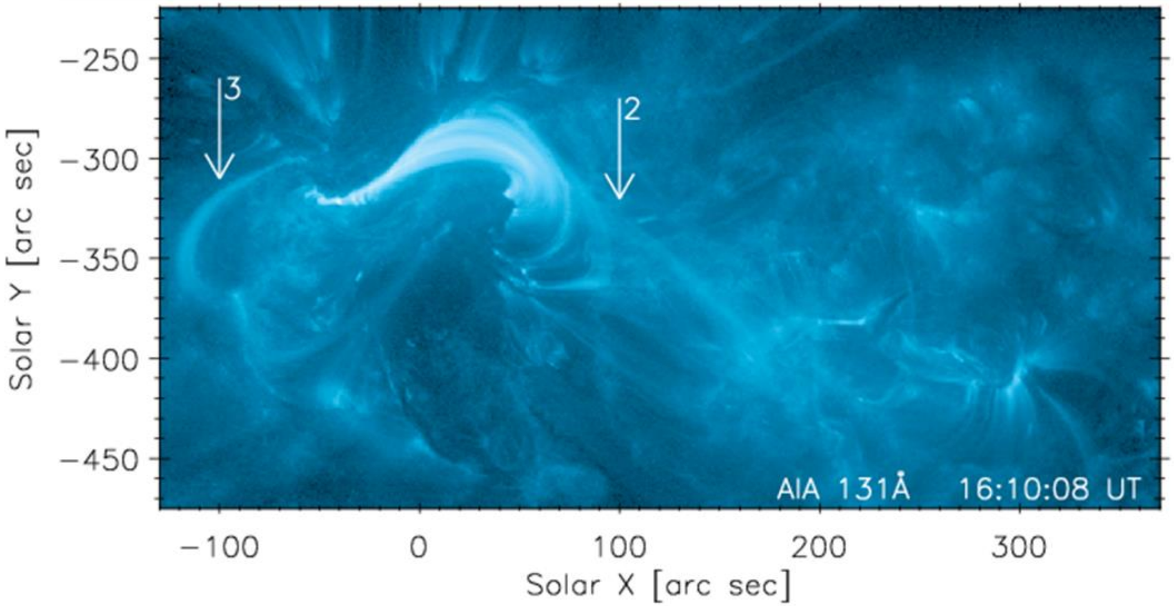

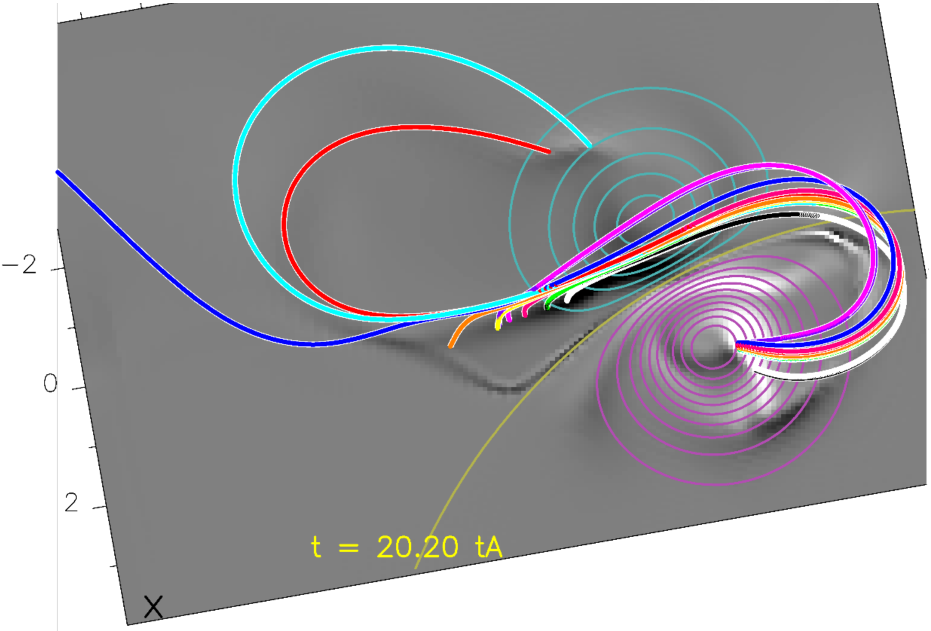

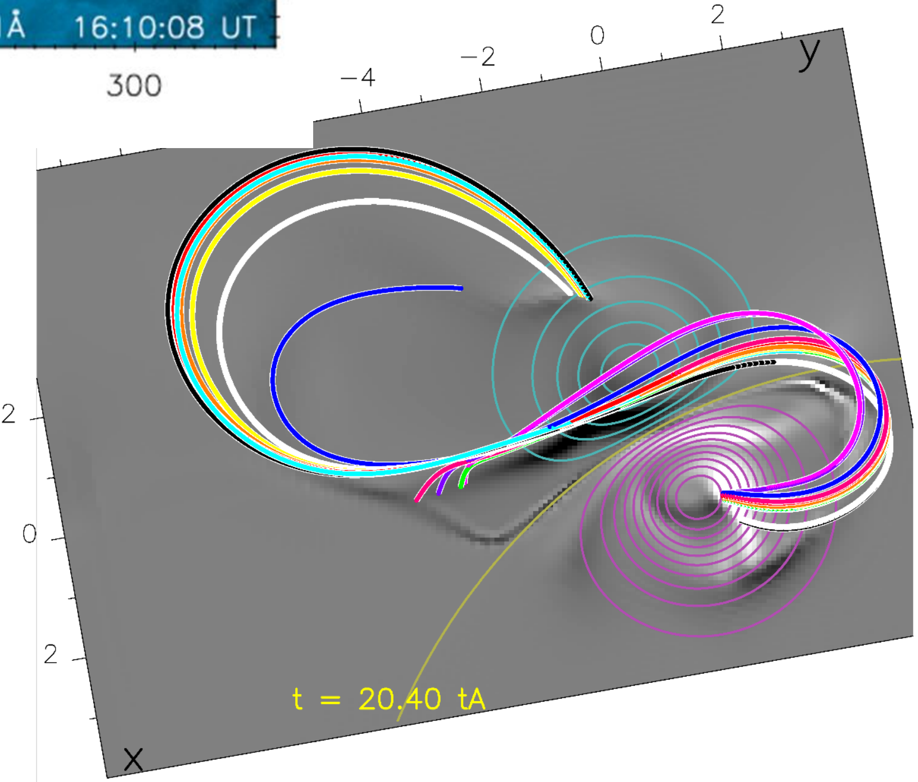

Eruption of Long, Hot, S-Loops

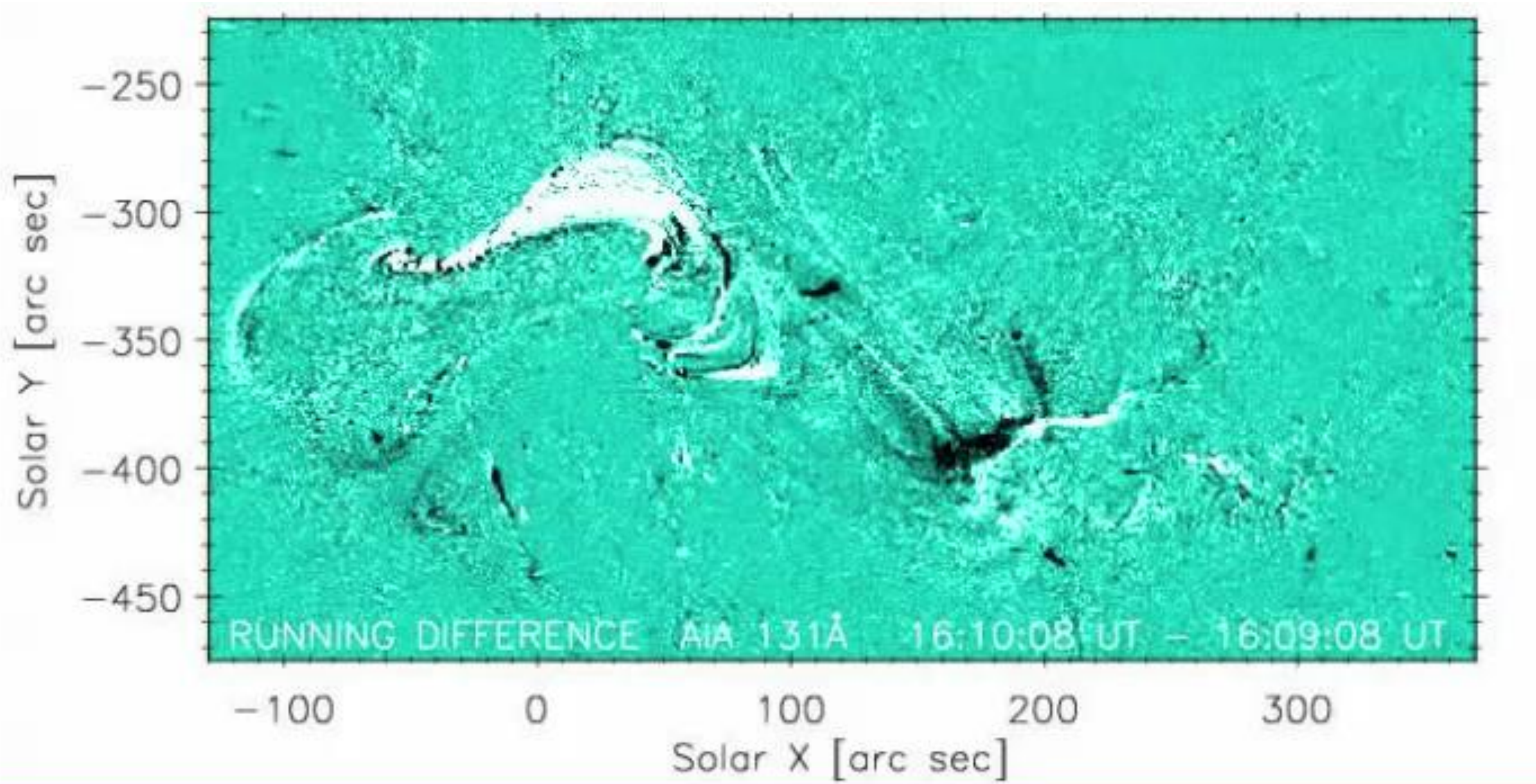

Eruption of Long, Hot, S-Loops

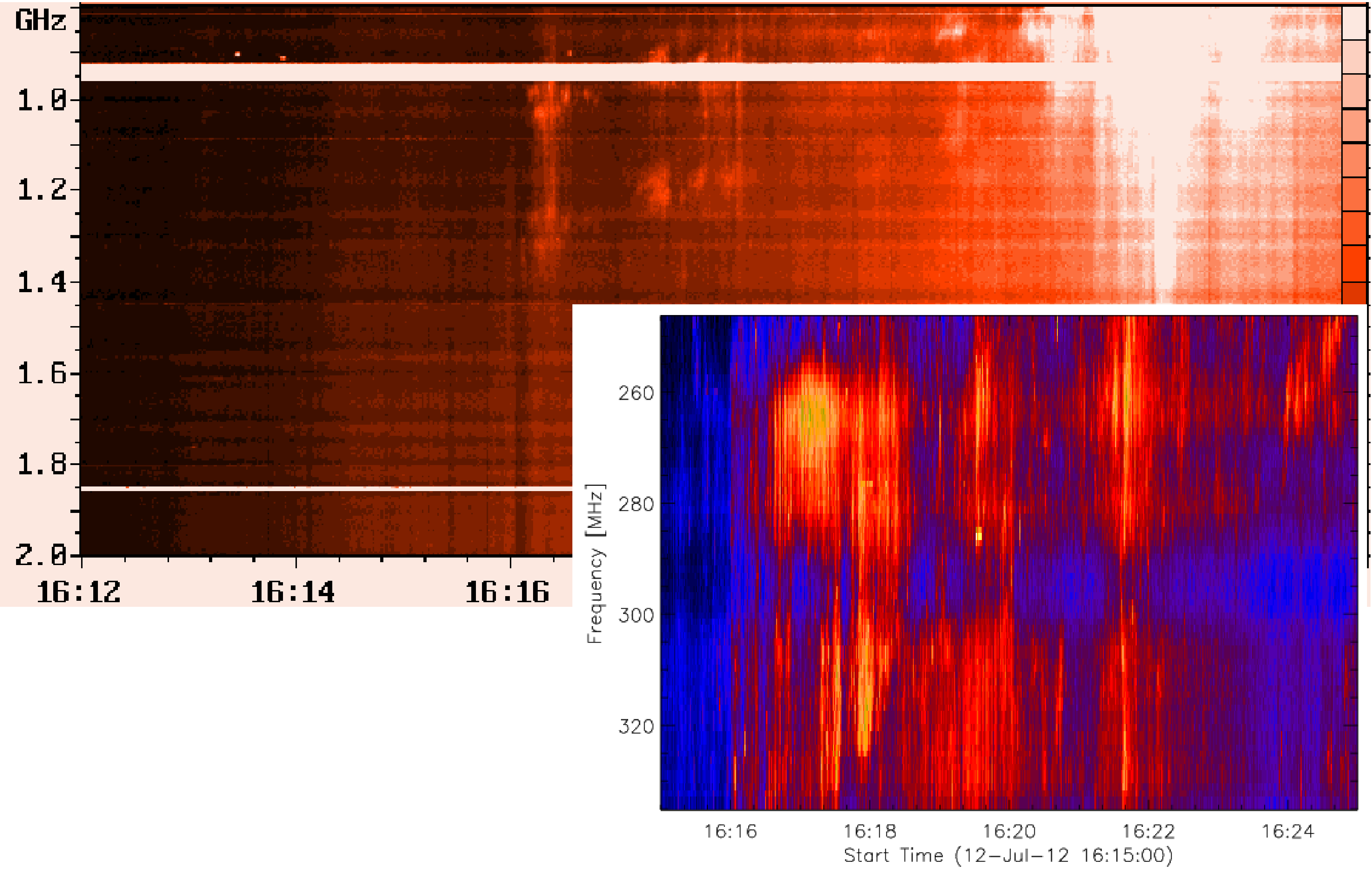

Solar Flare of 2013 Dec 10

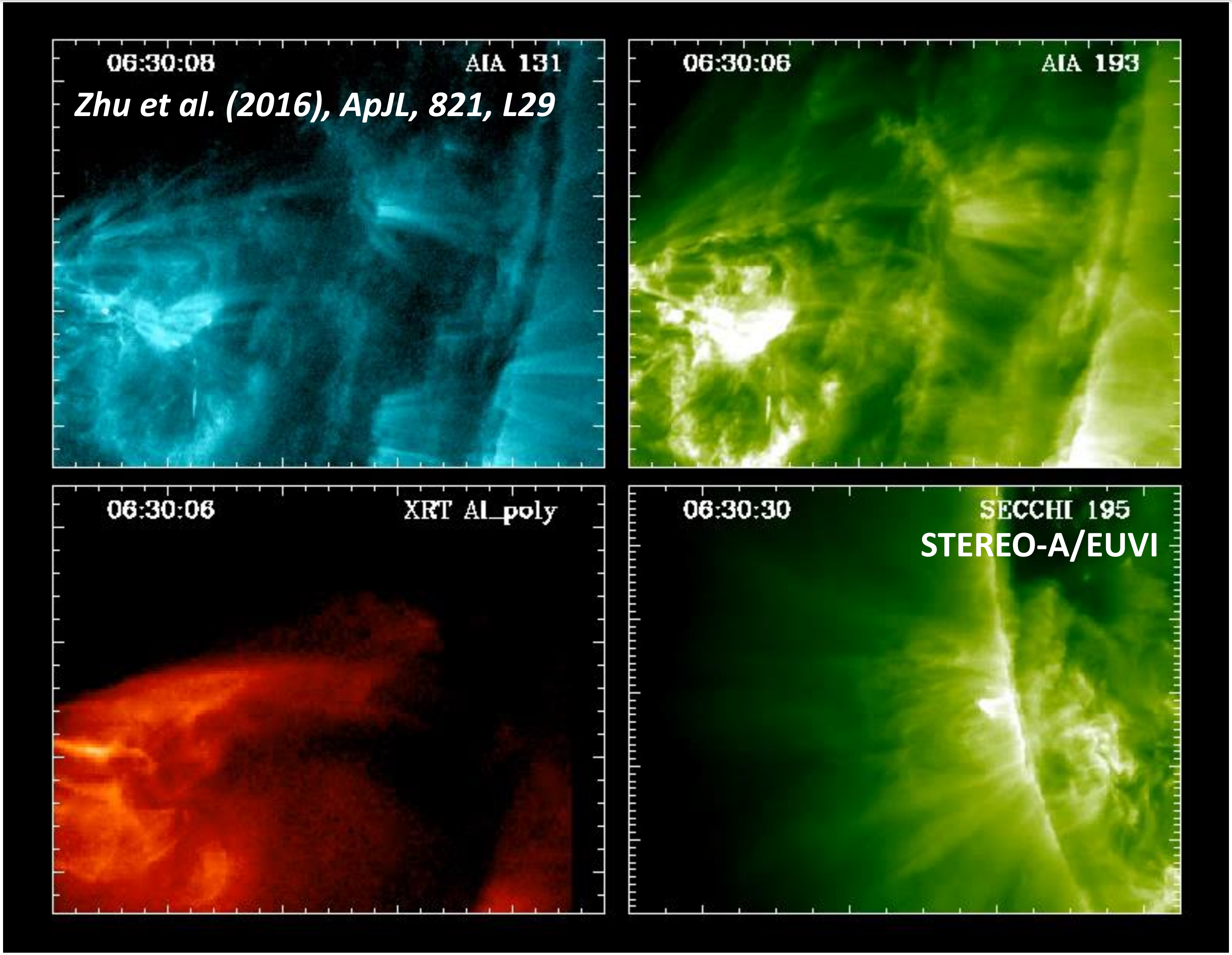

Standard Solar Flare Model in 3D

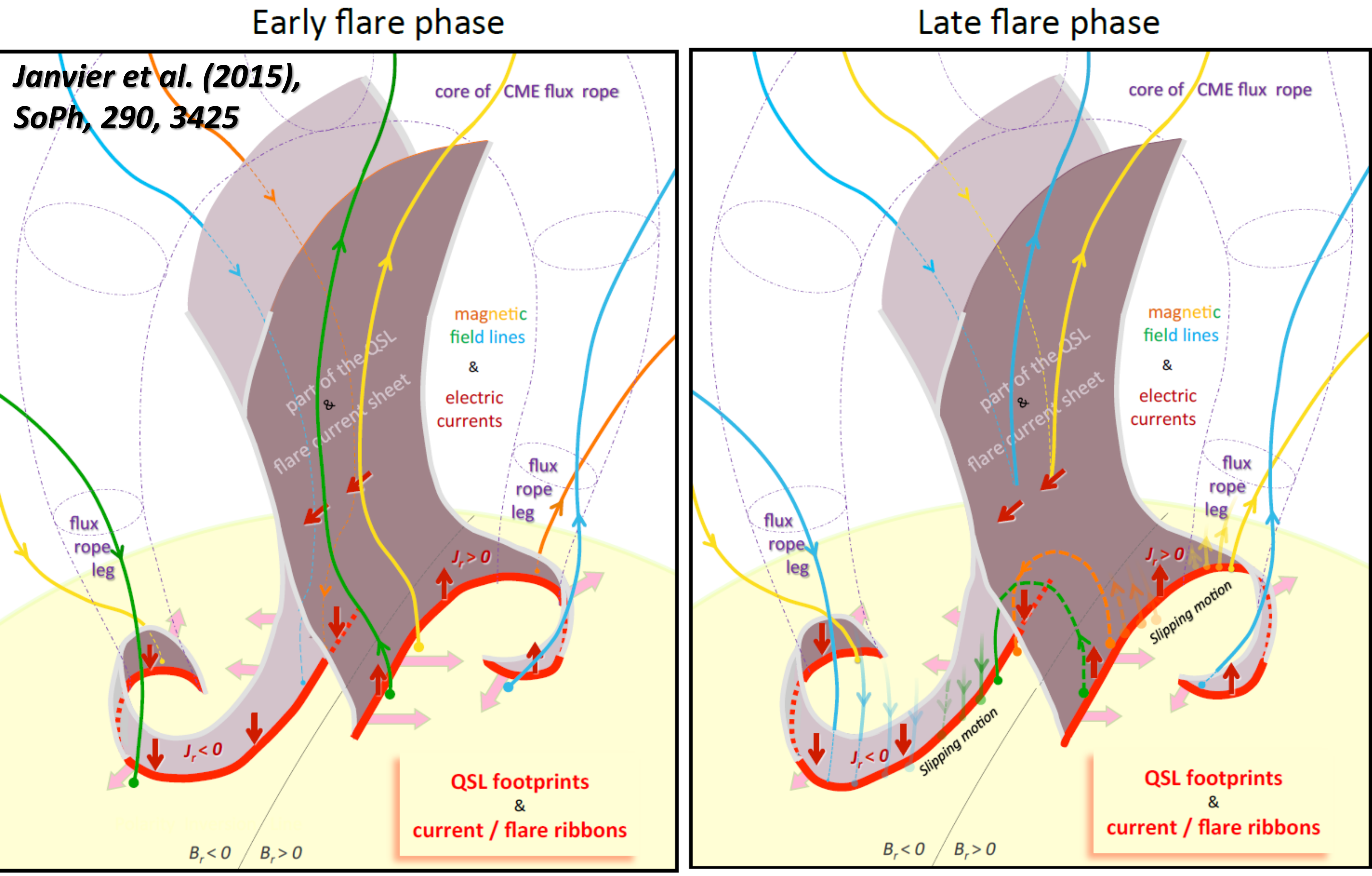

Quasi-periodic Slipping

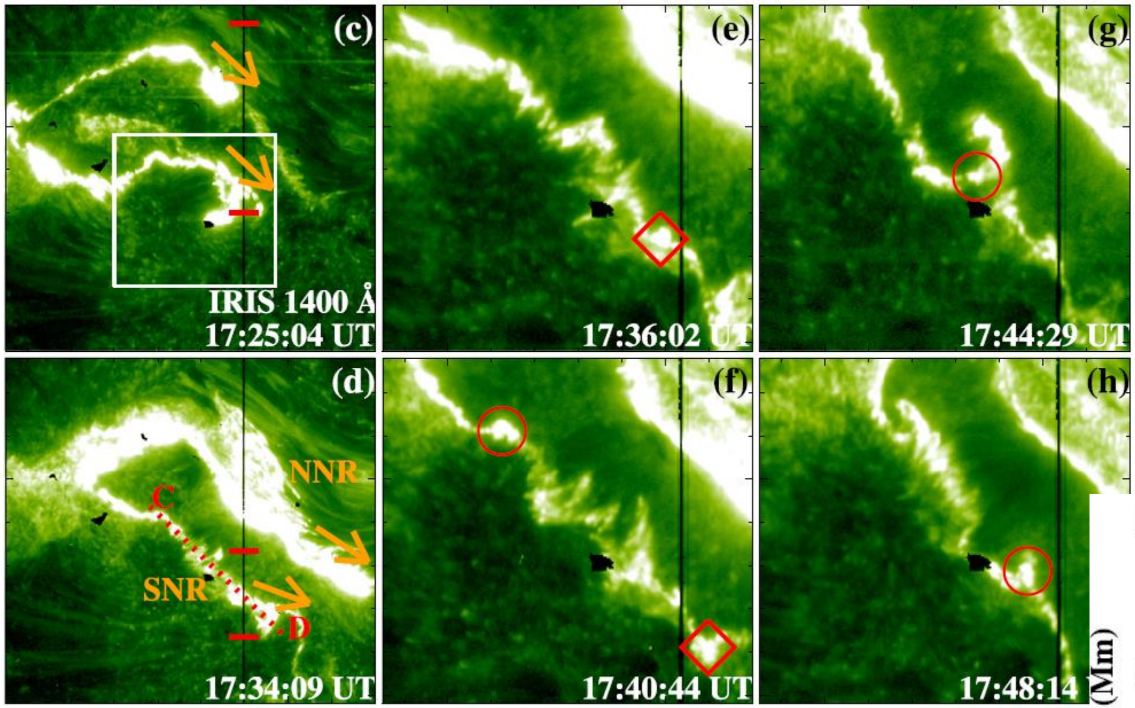

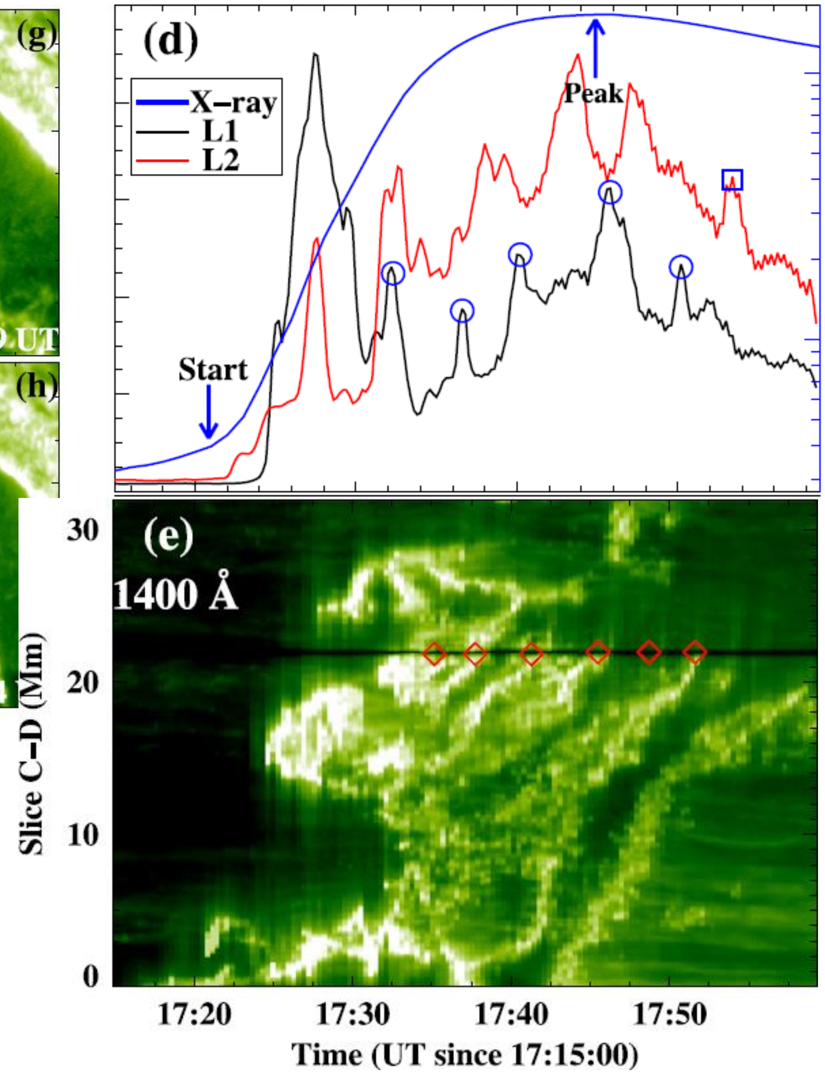

Li & Zhang (2015), ApJL, 804, L8

- Several slipping knots along the ribbon in the 2014 September 10 flare
- Quasi-periodic recurrence of bright knots with periods of 3 – 6 min

Quasi-periodic Slipping

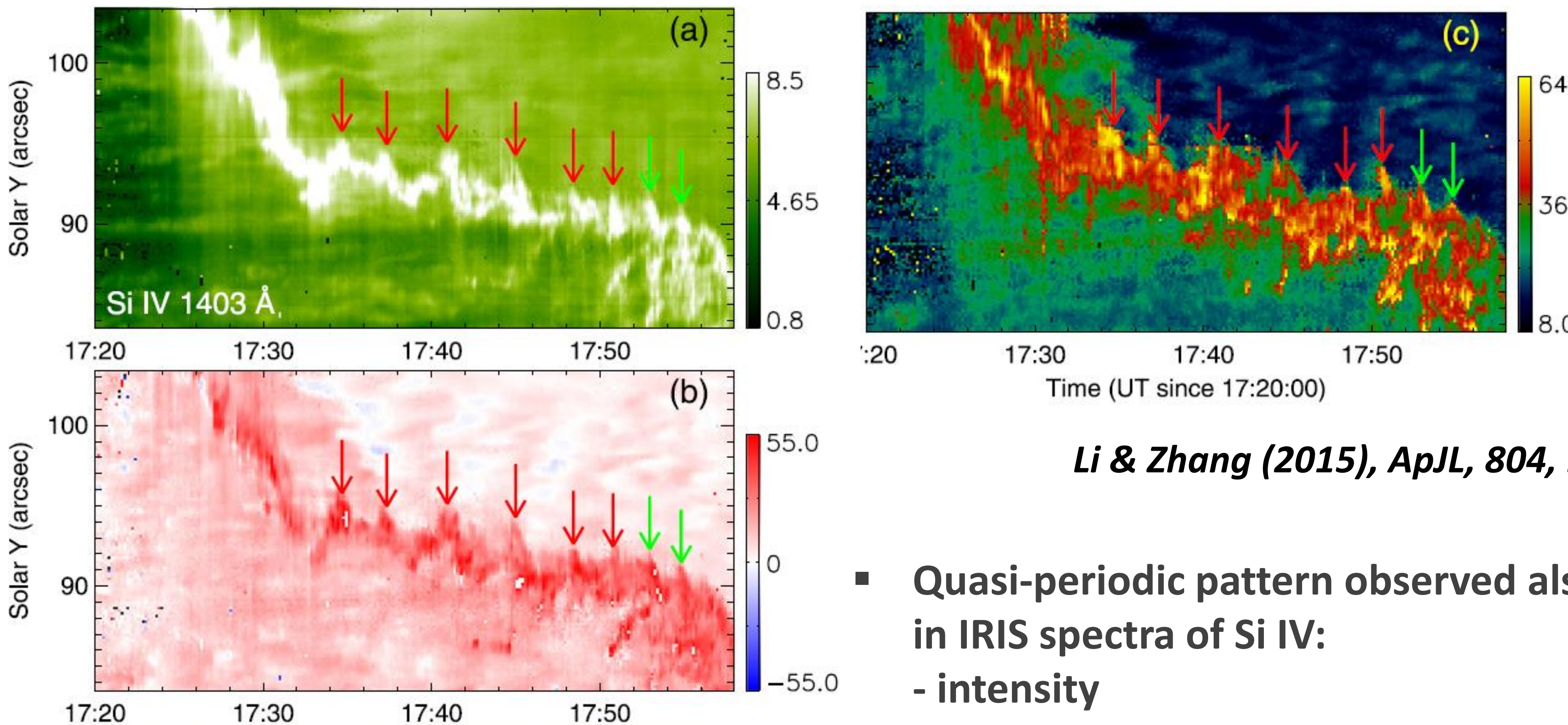

Li & Zhang (2015), ApJL, 804, L8

- **Quasi-periodic pattern observed also in IRIS spectra of Si IV:**
  - intensity
  - Doppler shift
  - non-thermal widths
- **All quantities are higher in the bright slipping knots**

Chromospheric Evaporation

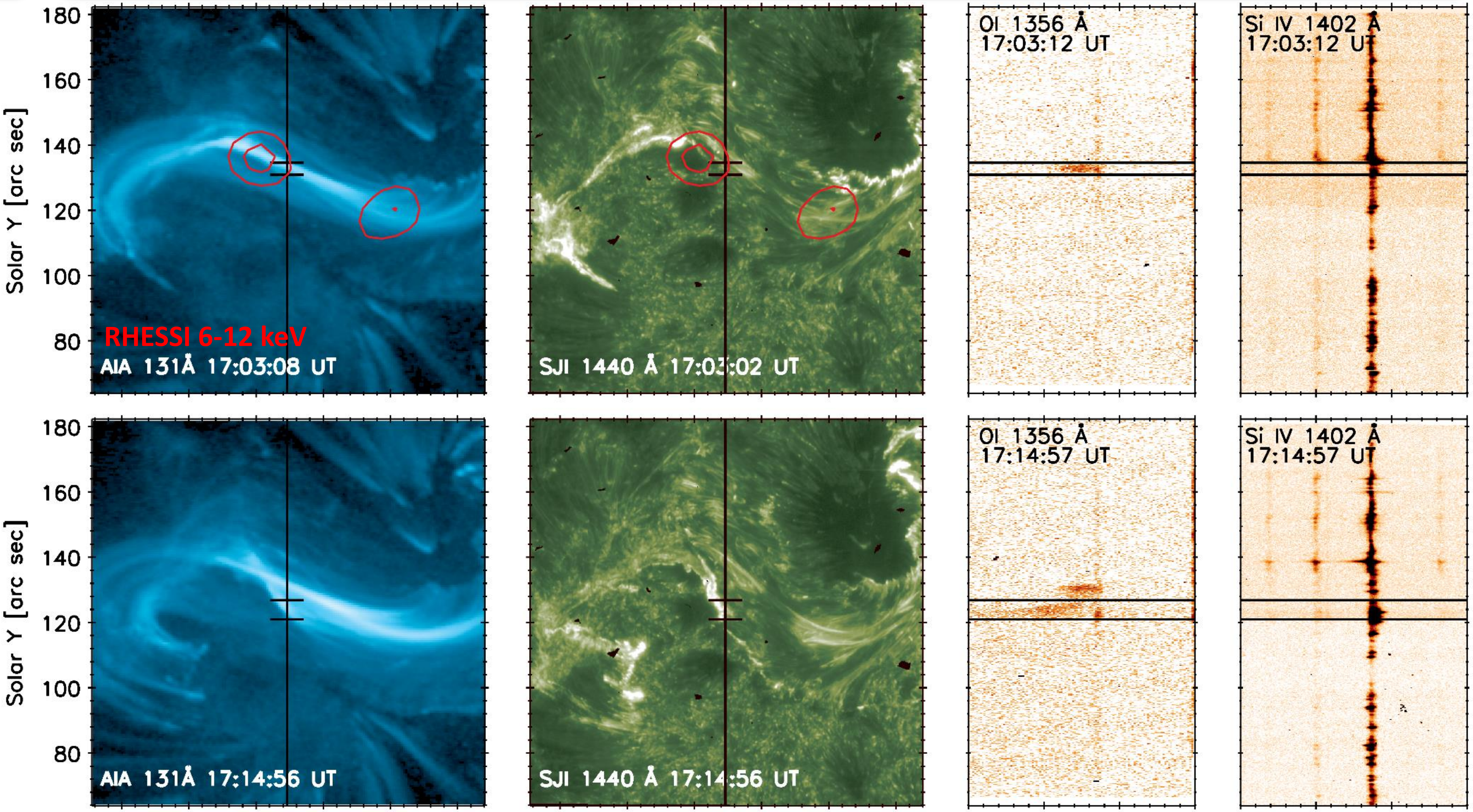

- Reported already by *Tian et al. (2015)* and *Graham & Cauzzi (2015)*
- However, both these papers consider impulsive phase only
- Evaporation in fact starts much sooner: in the "precursor" phase

Chromospheric Evaporation

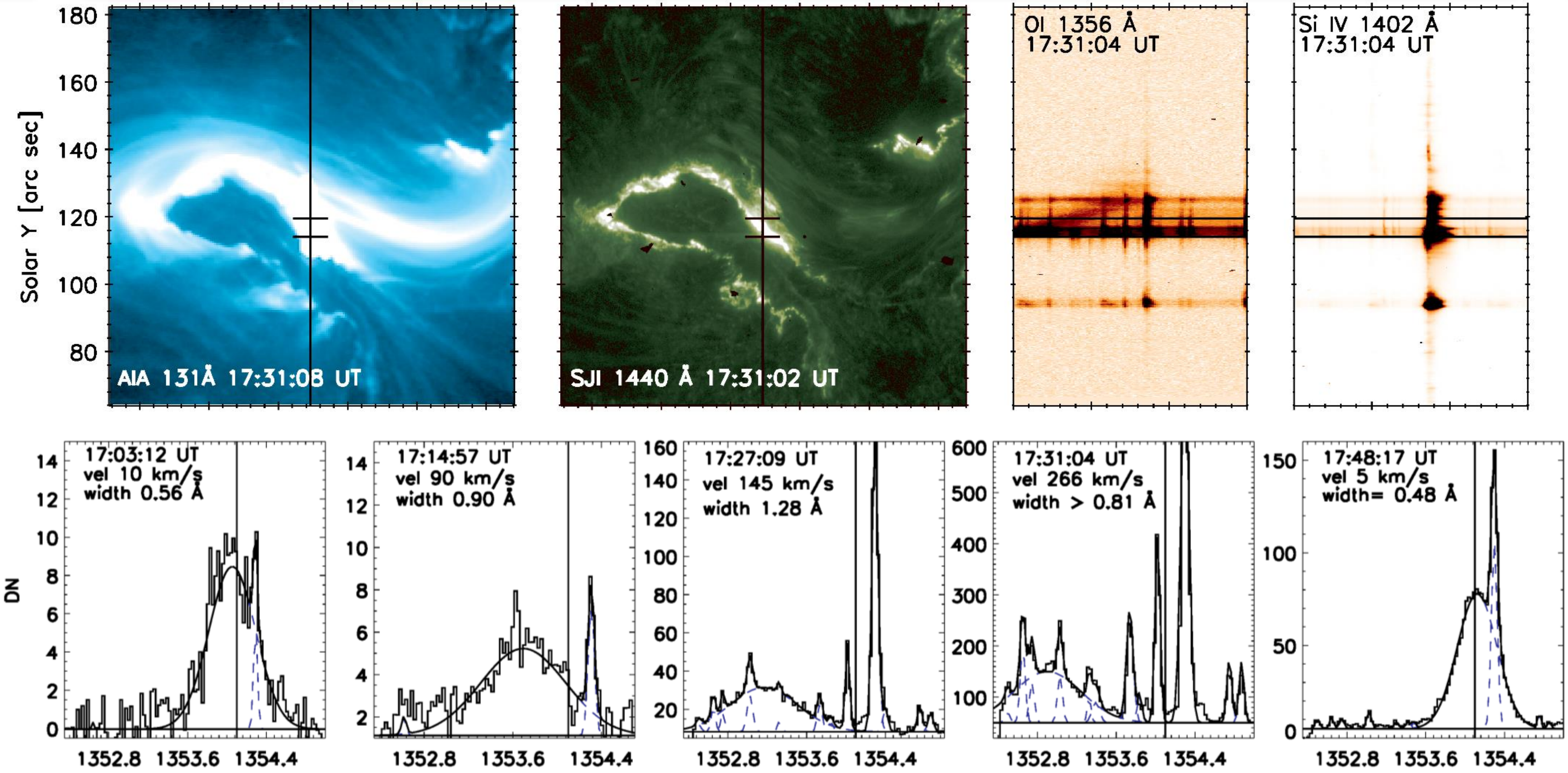

- Slipping reconnection: IRIS slit @ loop-top at 17:03, but footpoint at 17:14 UT
- Strongly blue-shifted in the ribbon edge
- Less blue-shifted in the trailing ribbon brightenings (flare loop footpoints)
- Thermalizes during the gradual phase

Tether-cutting Reconnection

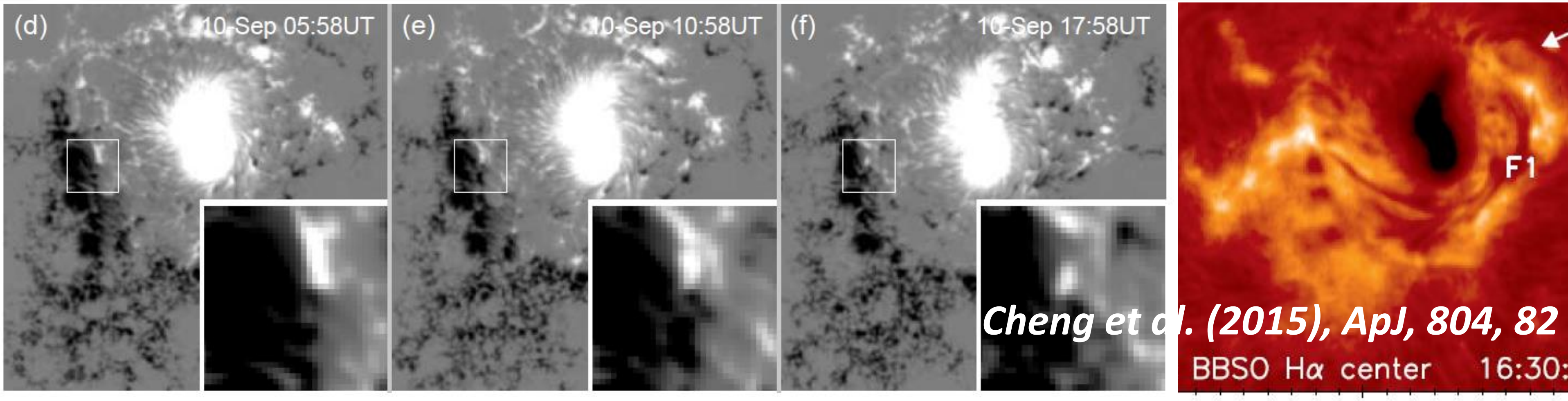

Cheng et al. (2015), ApJ, 804, 82

- **2D: Tether-cutting adds to the filament/flux-rope**
- **Allows for explanation of the observed Doppler velocities**

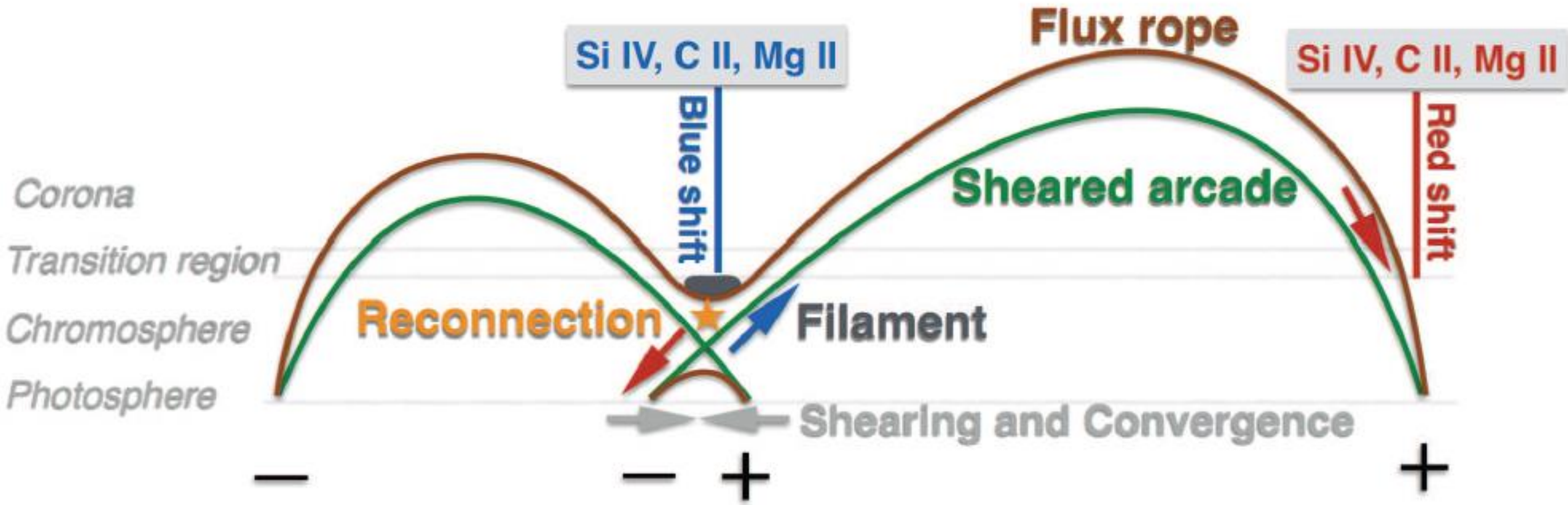

Slipping Reco. & Tether-Cutting

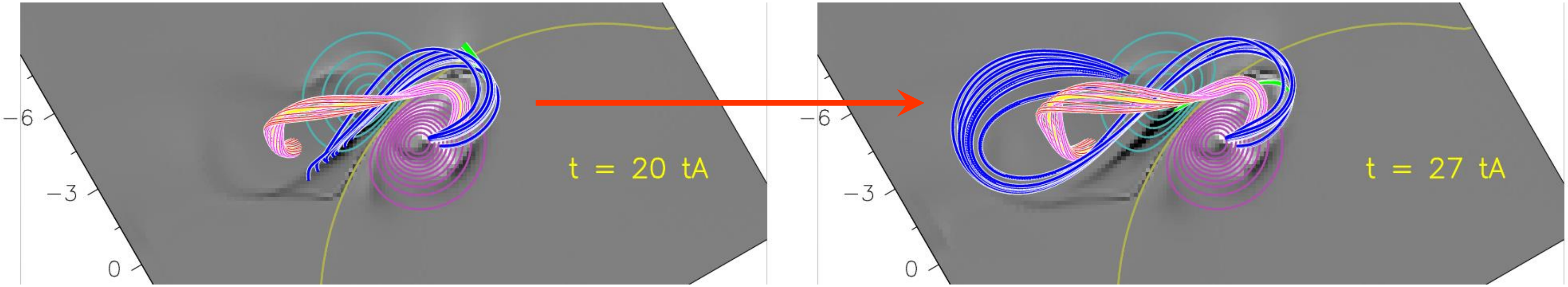

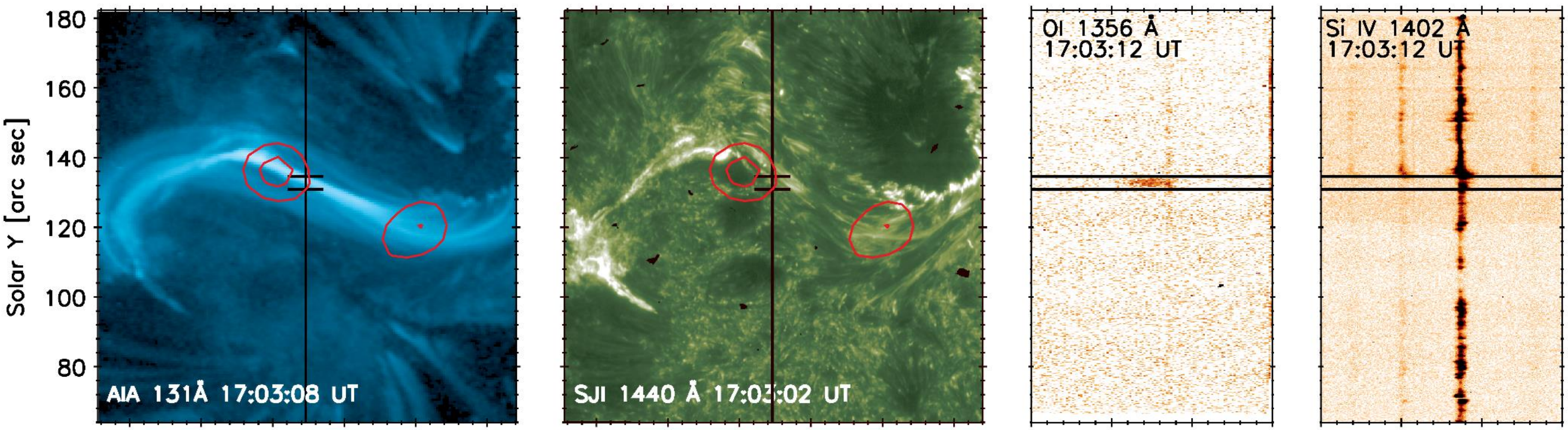

- Slipping reconnection **is the tether-cutting mechanism**
- Detection of the slipping reconnection during the early flare phase: **precursors are signatures of the flare itself**, progressing from early phase towards impulsive phase

3D: Global Evolution

Aulanier & Dudík (2018), subm. to A&A

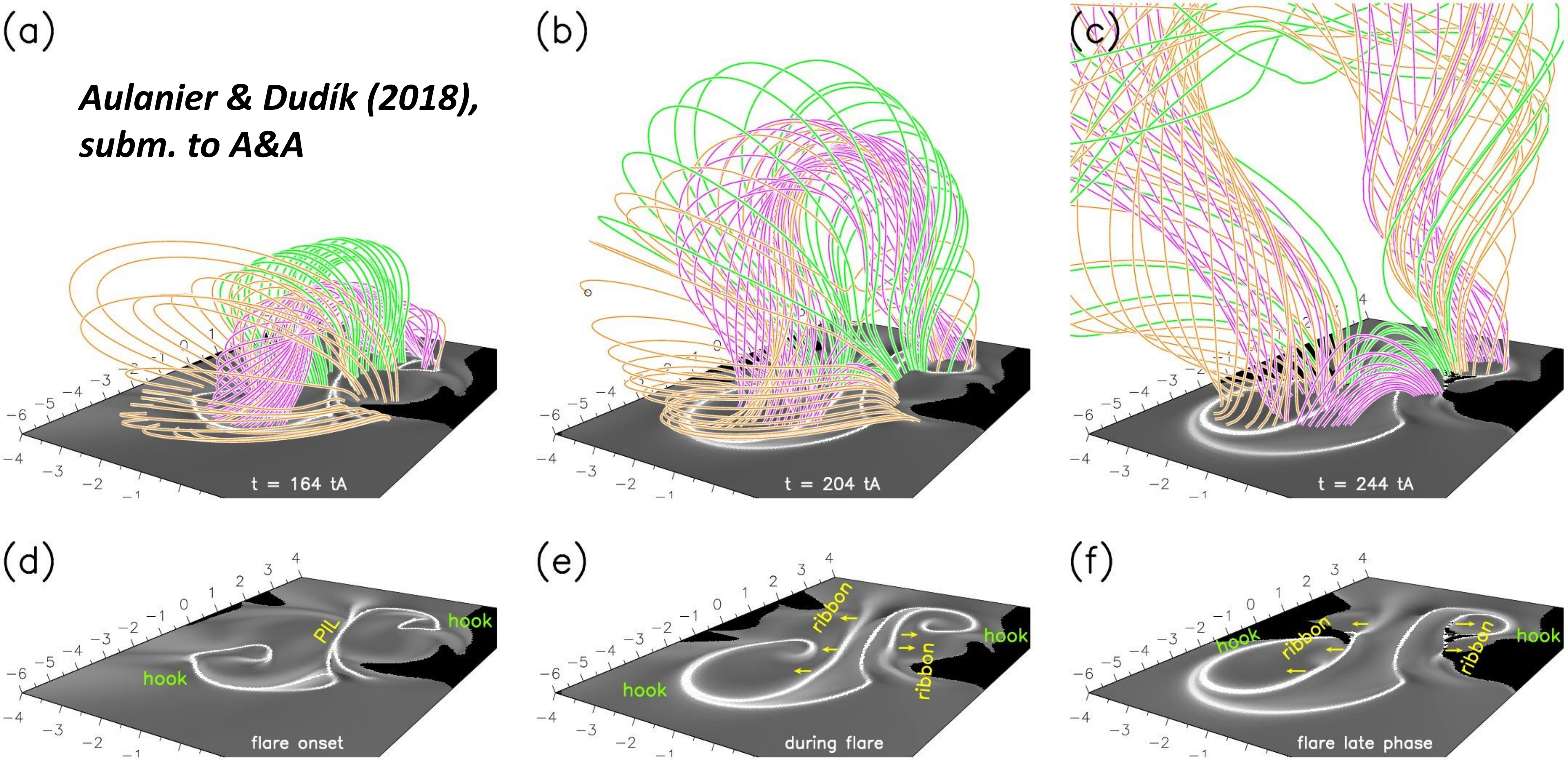

- Double-J ribbons: Ribbons spread away from PIL, ribbon hooks encircling the flux rope
- Flux rope and overlying arcades
- But: Coronal arcades → flux rope, and both flux rope & its envelope → flare loops

QSL Evolution

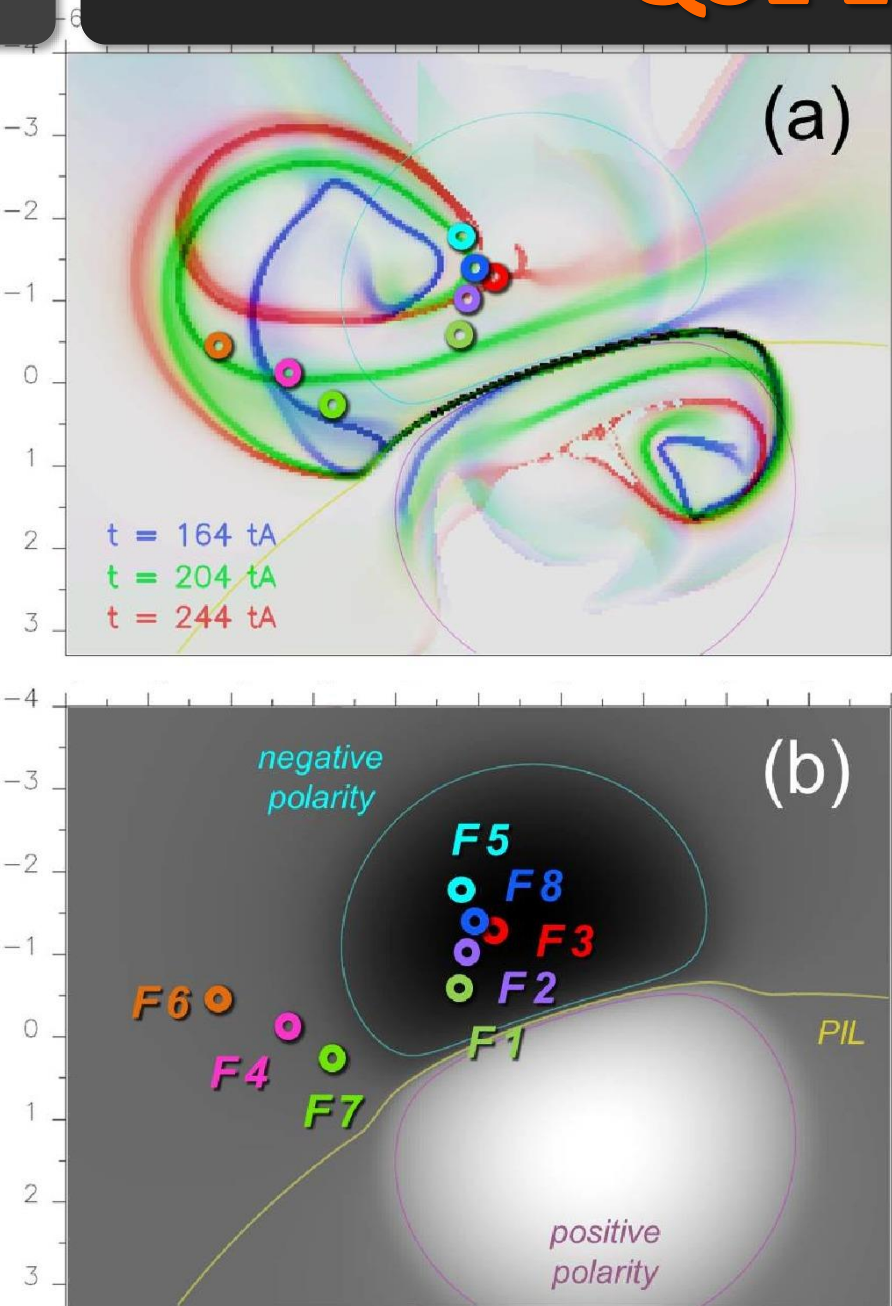

- Double-J ribbons:
  Ribbons spread away from PIL,
- Hooks also evolve in time
- Thus, a point outside the hook can become a part of the FR, and vice versa

QSL: start – early – impulsive

- F1: out (A) – out (A) – ins. ribbon (FL)
- F2: out (A) – out (A) – ins. hook (FR)

- F3: out (A) – out (A) – ins. hook (FR)
- F4: in (FR) – in (FR) – ins. ribbon (FL)
- F5: out (A) – at hook – ins. hook (FR)
- F6: out (A) – in (FR) – ins. hook (FL)
- F7: in (FR) – out (FL) – out (FL)

QSL Evolution

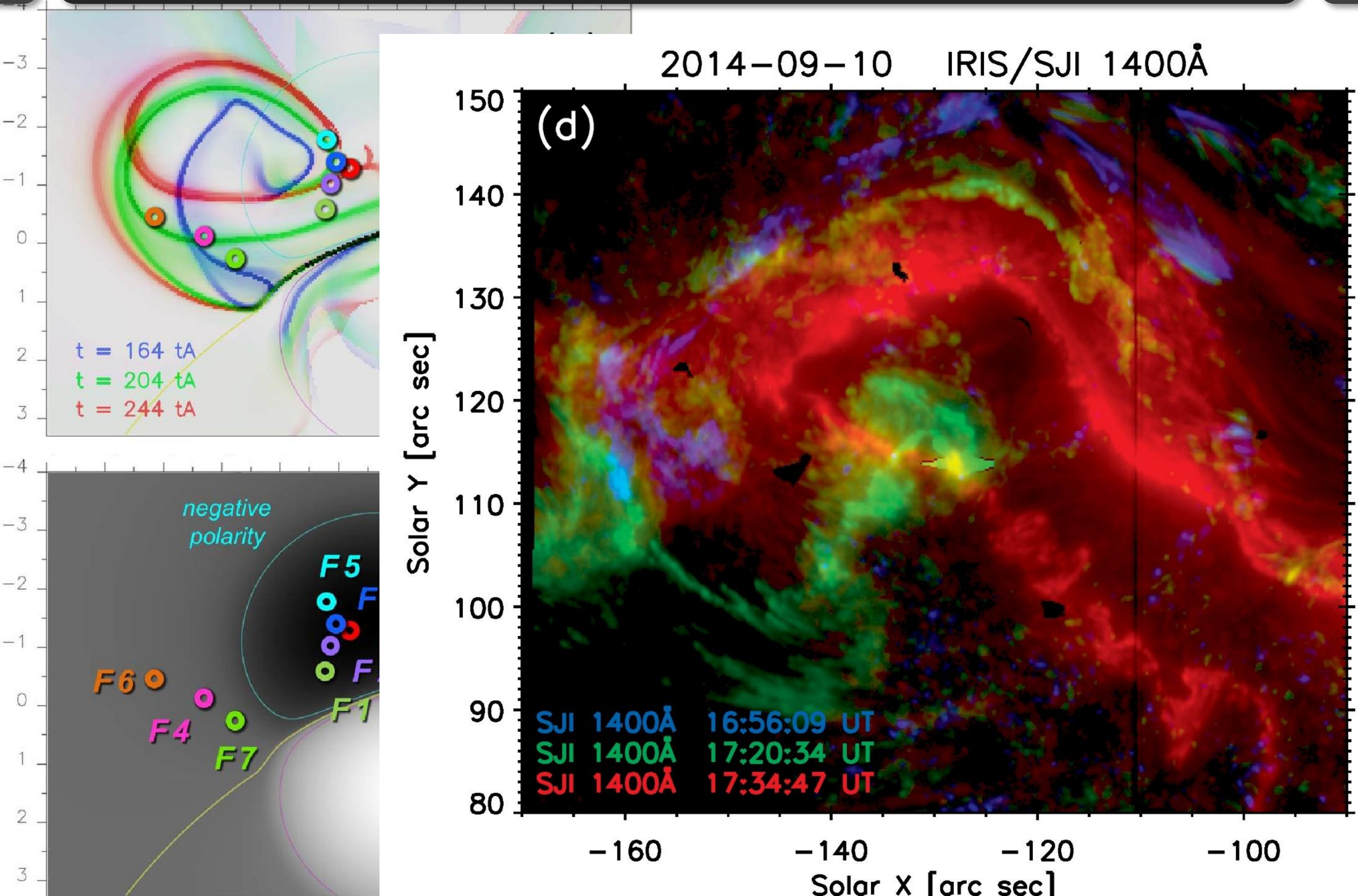

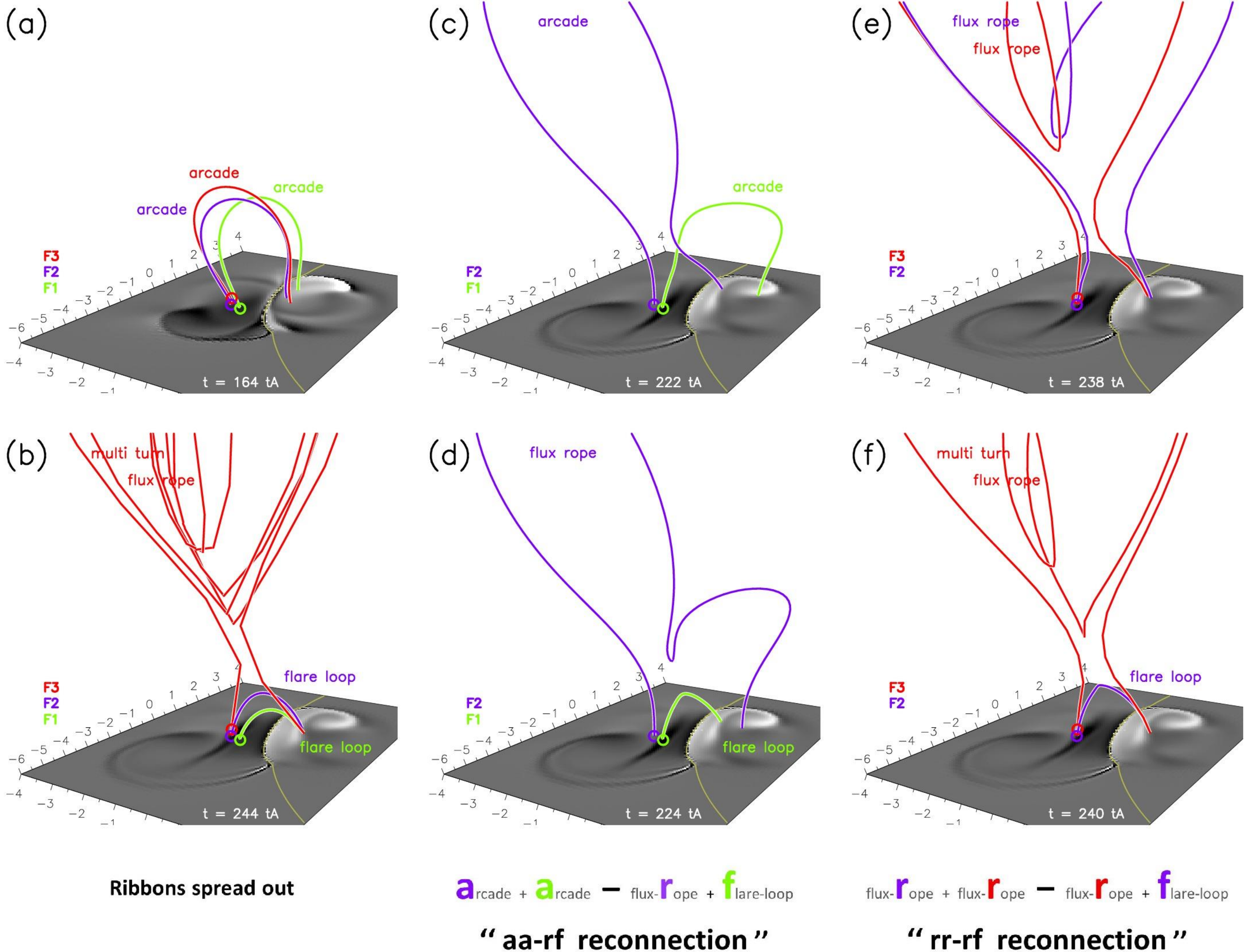
(a)
arcade
arcade
arcade
F3
F2
F1
t = 164 tA
(b)
multi turn
flux rope
flare loop
flare loop
F3
F2
F1
t = 244 tA
(c)
arcade
arcade
F2
F1
t = 222 tA
(d)
flux rope
flare loop
F2
F1
t = 224 tA
(e)
flux rope
flux rope
F3
F2
t = 238 tA
(f)
multi turn
flux rope
flare loop
F3
F2
t = 240 tA
Ribbons spread out
arcade + arcade – flux-rope + flare-loop
" aa-rf reconnection "
flux-rope + flux-rope – flux-rope + flare-loop
" rr-rf reconnection "

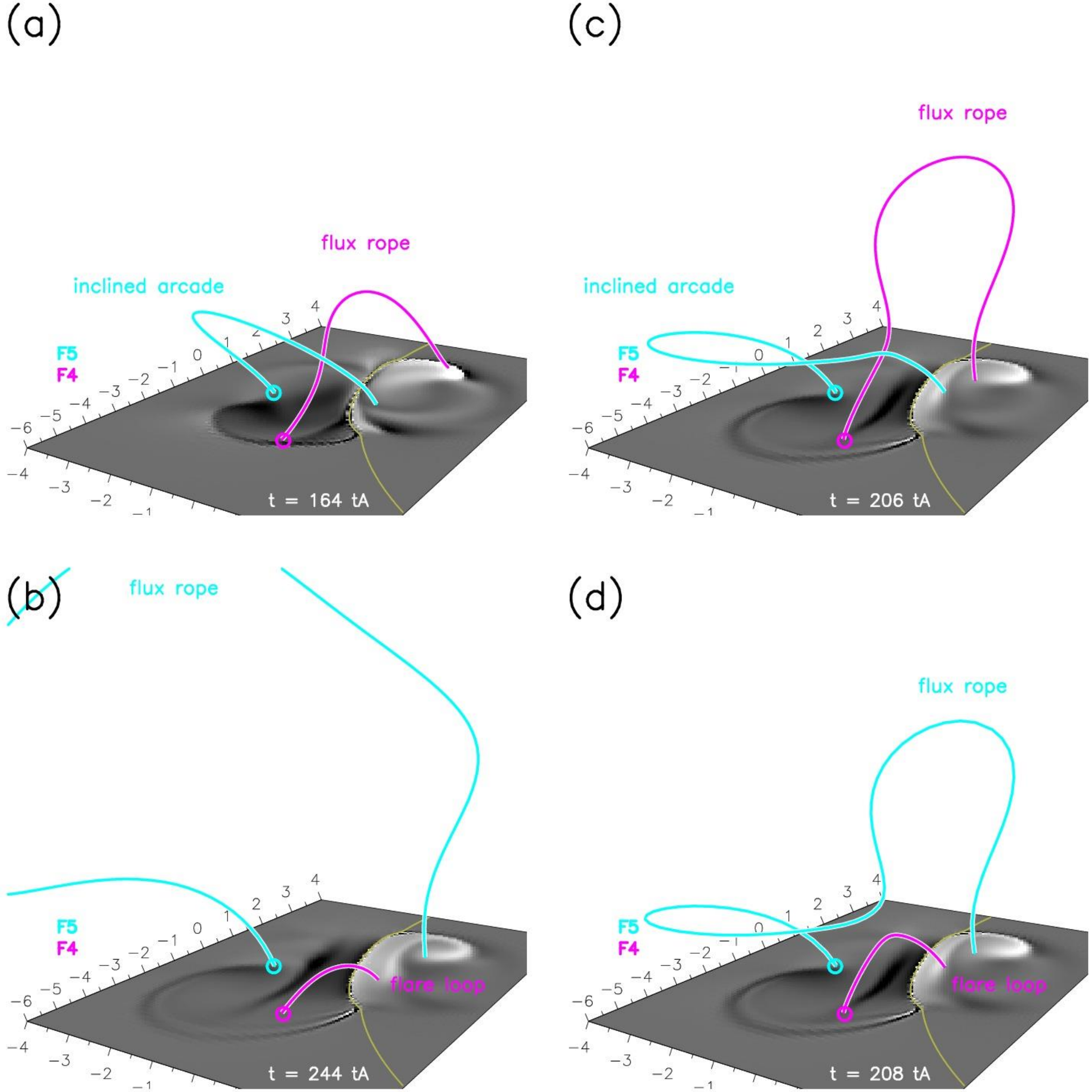

Ribbon swipes hook's surface

while

Hook moves out

arcade + flux-**r**ope – flux-**r**ope + **f**lare-loop

“ ar-rf reconnection ”

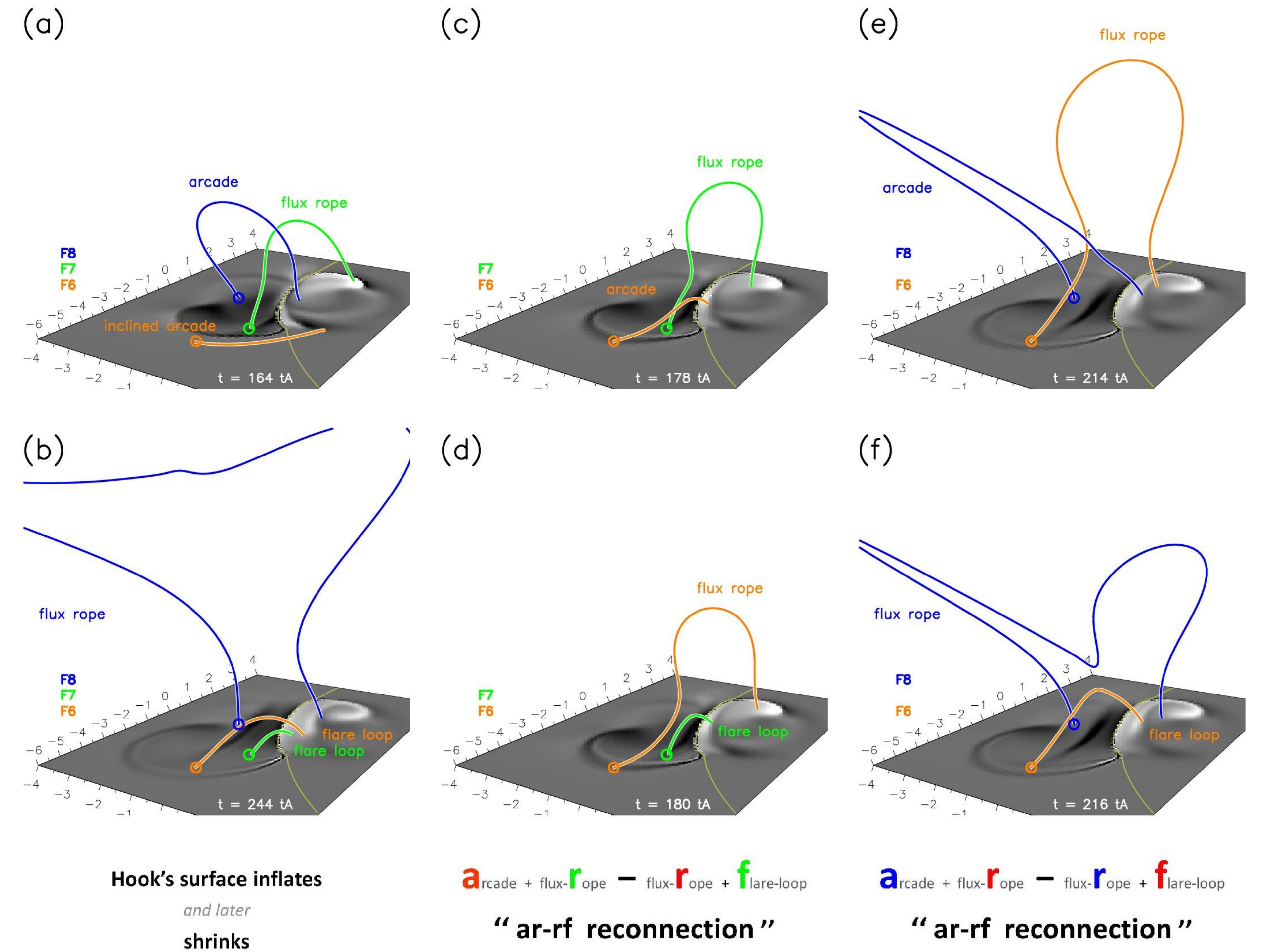

(a)
arcade
flux rope
F8
F7
F6
inclined arcade
t = 164 tA
(c)
flux rope
F7
F6
arcade
t = 178 tA
(e)
flux rope
arcade
F8
F6
t = 214 tA
(b)
flux rope
F8
F7
F6
flare loop
flare loop
t = 244 tA
(d)
flux rope
F7
F6
flare loop
t = 180 tA
(f)
flux rope
F8
F6
flare loop
t = 216 tA
Hook's surface inflates
and later
shrinks
arcade + flux-rope – flux-rope + flare-loop
" ar-rf reconnection "
arcade + flux-rope – flux-rope + flare-loop
" ar-rf reconnection "

Summary

- **Flare sometimes DO look like the 2D model**
  especially when observed on limb

- **Do not be fooled! Flares are intrinsically 3D:**
  Reconnection either at the true 3D null-point
  or slipping reconnection in quasi-separatrix layers
  Twisted structures present and erupting

- **Plasma dynamics very important:**
  EUV late phase due to difference in cooling timescales
  Chromospheric evaporation
  DEM analysis shows strong temperature structure

- **New types of 3D reconnection:**
  ar-rf, rr-rf, in addition to aa-rf

A Recent Example of a 2D-ish Flare

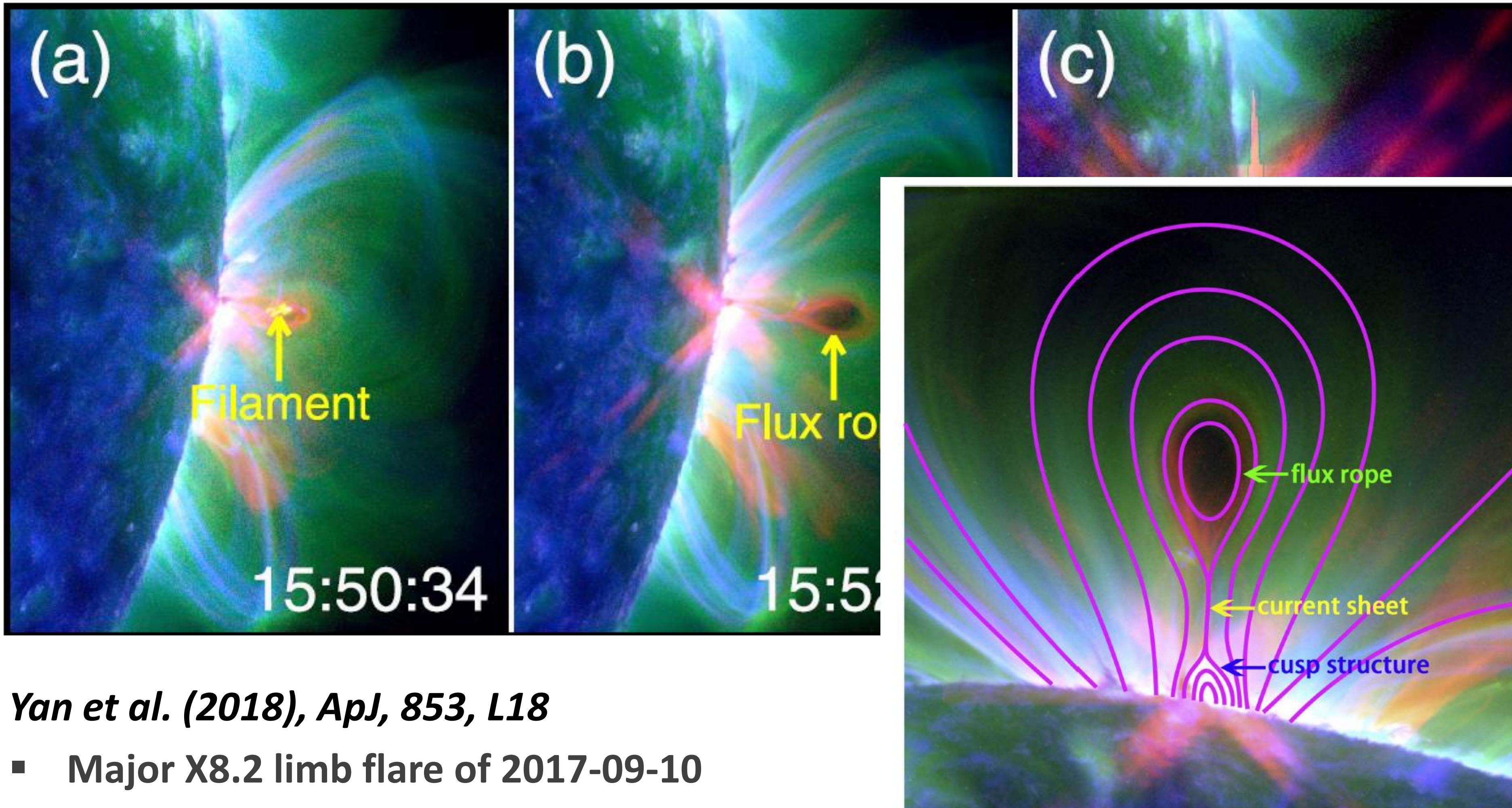

Yan et al. (2018), ApJ, 853, L18

- **Major X8.2 limb flare of 2017-09-10**
- **Observations of an erupting filament / hot flux rope**
- **After eruption: Long, protruding "current sheet" structure**
- **Properties of the current sheet in *Warren et al. (2018, ApJ, 854, 122)***

Movie courtesy of Francesco P. Zuccarello

Zuccarello et al. (2016), 821, 23